DEPARTMENT OF PHYSICS
UNIVERSITY OF JYVÄSKYLÄ
RESEARCH REPORT No. 14/2011

# INCREASING THE DRYING EFFICIENCY OF CYLINDER DRYING

**BY**
**JANNE KERÄNEN**

Academic Dissertation
for the Degree of
Doctor of Philosophy

To be presented, by permission of the
Faculty of Mathematics and Science
of the University of Jyväskylä,
for public examination in Auditorium FYS-1 of the
University of Jyväskylä on 19 December 2011
at 12 o'clock

Jyväskylä, Finland
December 2011

# PREFACE

I want to thank especially Dr. Oleg Timofeev for the excellent help and guidance throughout the years. Lic. Phil. Risto Talja has helped me in getting to think of the paper business. Lic. Phil. Harri Kiiskinen cannot be forgotten for his help in analytical thinking and in tutoring me at the beginning of my 'paper years' and Professor Jussi Timonen for his tolerance with my long project that should have been finished a long time ago. Many thanks also to the great co-workers at VTT who have made this Thesis possible; working with wonderful people is a pleasure.
Thanks belong also to Dr. Nenad Milosavljevic, for having the possibility to use the experimental device.
And my most sincere thanks go to my wife, Pauliina, who has loved me through these years, and to my two sons, Oskari and Eemeli, for giving me further perspective in life.
For the financial support, I want to thank two good organisations, Metso Paper and VTT, and people working there, whose continuing collaboration made this work possible.

Kuopio, December, 2011

Janne Keränen

# ABSTRACT

Keränen, Janne
Increasing the drying efficiency of cylinder drying
Jyväskylä: University of Jyväskylä, 2011
JYFL Research report 14 / 2011, Department of Physics, University of Jyväskylä
ISBN 978-951-39-4589-3 (paper copy)
ISBN 978-951-39-4590-9 (pdf)
ISSN 0075-465X

This PhD Thesis concentrates on paper drying: first on the drying rate in a cylinder covered with fabric, enhanced using hot air impingement through the fabric, and its potential effects on paper quality, and second, on the heat transfer rate from hot steam to paper through the cylinder shell.
Cylinder drying is a drying method where a heated surface in contact with paper causes water removal from the latter by evaporation. Impingement through the fabric of hot air has been suggested to cause increase in the water removal and drying of paper.
Increase in the drying rate by impingement of hot air was confirmed by laboratory tests and by simulations. In laboratory tests the increase in the drying rate was found to be accompanied by improvements in paper quality. The reason for the unexpectedly high increase in the case of combined cylinder-impingement drying of the drying rate was traced down to decrease in the temperature of paper. The thereby increased temperature gradient between paper and cylinder surface caused an increase in the heat flux from the cylinder. A simulation model for the system showed similar increase in the drying rate of paper. Simulations could also be extended to a paper machine scale. Use of the simulation model required further work on the experimental transport of moisture in the thickness direction of paper, with successful results.
The potential of impingement drying for improving paper quality was demonstrated, especially for prevention of shrinkage of paper during drying. Shrinkage prevention has a positive influence on the tensile properties of paper. Shrinkage prevention still needs verification in a larger scale, however.

Keywords: paper drying, moisture gradient, simulation, cylinder drying, impingement drying, heat transfer, cylinder shell

Author's address

Janne T. Keränen
VTT
Kuopio
Finland
Janne.Keranen@vtt.fi

Supervisors

Professor Jussi Timonen
Department of Physics
University of Jyväskylä
Finland

Dr. Oleg Timofeev
VTT
Jyväskylä
Finland

Dr. Jukka Ketoja
VTT
Espoo
Finland

Dr. Jussi Maunuksela
Department of Physics
University of Jyväskylä
Finland

Reviewers

Professor Jouni Paltakari
Department of Forest Products Technology
Aalto University
Finland

Dr. Kari Luostarinen
Metso Paper
Jyväskylä
Finland

Opponent

Docent Markku Karlsson
Process Design & Systems Engineering laboratory
Åbo Akademi
Finland

# LIST OF PUBLICATIONS

A. I. Experimental research on the combined contact-impingement drying of paper on the dryer cylinder
Timofeev, Oleg; Keränen, Janne; Milosavljevic, Nenad; Talja, Risto
13th International Drying Symposium. Beijing, (2002)

A. II. Impingement drying in papermaking
Talja, Risto; Timofeev, Oleg; Keränen, Janne; Manninen, Jussi
12th International Drying Symposium, Noordwijkerhout, (2000)

A. III. Simulated combined air-cylinder drying process
Keränen, Janne; Timofeev, Oleg; Talja, Risto
3rd Nordic Drying Conference, Karlstad, (2005)

A. IV. Moisture and temperature measurement of paper in the thickness direction
Keränen, Janne; Paaso, Janne; Timofeev, Oleg and Kiiskinen, Harri
Appita Journal, Vol 62 (2009), pp. 308-313

A.V. Some insight on paper structure and properties with different drying characteristics
Keränen, Janne; Myllys, Markko; Kiiskinen, Harri
Appita Journal, Vol 62 (2009), pp. 146-151

A.VI. Paper curl induced by drying
Timofeev, Oleg; Keränen, Janne; Kiiskinen, Harri
Pulp and Paper Canada. Vol. 103 (2002), pp. 25 - 28

A. VII. Analysis of the cylinder dryer with improved heat transfer rate
Timofeev, Oleg; Milosavljevic, Nenad; Keränen, Janne; Kiiskinen, Harri
16th International Drying Symposium, Hyderabad, (2008)

# AUTHOR'S CONTRIBUTION

The author of this Thesis made a major contribution to the design, testing and operation of the experimental set-up (Combo) described in this Thesis and related publications. The author collected most of the experimental data presented in this Thesis and the related articles. The author also performed the simulations and related analyses reported in article A. III., has written articles A.III-A.V. and participated in the writing of all the remaining articles.

# CONTENTS

# 1. INTRODUCTION TO PAPERMAKING AND DRYING OF PAPER

## 1.1. Background

Papermaking is essentially a large water removal process, where efficient water removal plays an important role.

The manufacturing process of paper is constantly under development, but the basic principles and raw materials have remained similar to what they were about fifty years ago. The basic manufacturing process has remained the same from the beginning of the 2nd century A.D. when paper manufacturing began in China: the fibres are pulped and formed to sheets, then pressed and dried. Papers produced this way were and are still used to carry information. Now all this is done in a paper manufacturing process, but still pulp is made, formed and dried before information can be stored and transported on paper.

Use of pure water is essential for papermaking since the mechanism of fibre bonding relies on hydrogen bonds [1]. Without water, other bonding agents are needed. However, some approaches towards a dry manufacturing processes have been made [2], and there is also clear indication that in developed countries paper as an information carrier is being replaced by electric means[3]. These means will become more widely used in the future, but the permanent information, or at least information considered to be unchanged, is still mainly stored and carried using paper. For other paper products, such as paperboards, the scope of use ranges from information carriage to protection of materials during their transport and storage.

## 1.2. The main objectives of the work

In the beginning of the work, the main objective was to discover more efficient drying method(s) than the ones in use today. An additional objective was to increase the control of paper properties during drying.

## 1.3. Research questions and hypothesis

The main research questions were then the following.

1. Analysis of methods that are expected to be efficient in paper (or board) drying.
2. Applicability of such methods at existing production sites.
3. How to control quality of the final product under drying.
4. Construction of experimental facilities needed for the above tasks.
5. Implementation of measurements needed to improve our understanding of the drying process.

The main hypothesis was that drying can be improved by combining methods that already exist. Such methods are efficient, reliable and economic. These topics are discussed further in Sections 1.7 and 1.8.

The first research task was then construction of an experimental system for the analysis of the drying process, which combined more than one drying method. To this end a small-scale test equipment was designed and constructed to keep the research costs reasonable. Laboratory work was then supported by drying simulations. Real-scale or pilot-scale operations were not targeted during the work. Laboratory-scale studies provided also a possibility to analyze the process with novel measurement methods.

## 1.4. Outline of the Thesis

In the following Chapter 2 effects of drying on paper properties are discussed.

In Chapter 3 the used drying model and discussion of the related equations that govern the drying process is reviewed. The important phenomena for which modelling is needed include heat transfer to paper, transport of water and water vapour in paper and removal of water vapour through paper surface.

In Chapter 4 results of the experiments and simulations related to high evaporation rates in drying through fabric is presented. The central issue here is paper temperature that can be lowered using impingement drying on a cylinder. Enhancement now of heat transfer from steam to paper is also

discussed. Some paper quality aspects are also discussed, mainly from a dimensional stability point of view. Finally, in Chapter 5, some conclusions are drawn on the topics covered in this Thesis.

## 1.5. Papermaking trends

Traditionally the consumption of paper and board has followed the gross national income/gross domestic product. However, it has been shown in References [4, 5] that the behaviour of growth of consumption does no longer follow the growth of gross domestic product or gross national income. Papermaking trends show that in developed countries use of paper is decreasing (see e.g. the recent FAO statistics [6]). This trend was already forecasted in a global bottom-up pulp and paper industry model [7, 8] and in demand estimations of wood [9]. However, a globally modest increase in the consumption of paper and board is expected, and in developing countries papermaking remains a growing business for some time to come.

The competitiveness of paper and board industry, like that of any other industry, requires strict cost control that will play a major role in the development of paper manufacturing processes in the future. To facilitate quality demands, new innovations are needed [10, 11]. Energy consumption in the drying of paper is always an aspect of papermaking, which needs to be considered carefully, though in many cases the number of practical solutions is limited by the available energy sources [12, 13].

The typical energy consumption rate of a paper machine dryer section is about 50 MW of power. It can be easily estimated that for 400 000 tonne of paper per year, the machine has a specific energy consumption of 4 GJ/tonne of paper [14]. The cost of drying energy is about 22-44 €/tonne of paper, assuming that 10% of the energy is electricity and 90% thermal energy (steam) [15, 16]. Typically, the price of steam production is 5-10 €/GJ and that of electricity is 60-120 €/MWh. Comparing the cost of drying with the other major costs of papermaking, *i.e.*, the cost of kraft sw-pulp (450 €/t, [17]) or mechanical pulp (approximately 100€/t), it is evident that the cost of drying energy is quite significant.

Papermaking process

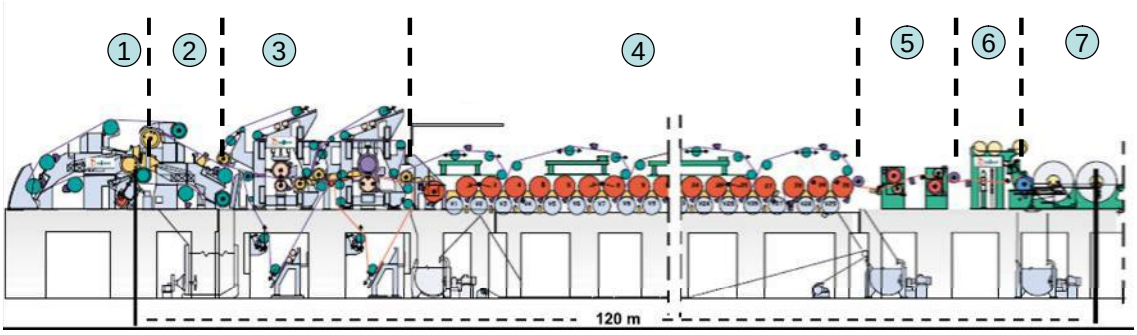


*Figure 1. A modern printing paper machine: 1 headbox, 2 forming section, 3 press section, 4 dryer section, 5 calandering, 6 winding and 7 roll storage. The length of the dryer section of the whole machine length is in this case 55%. [14]*

Papermaking process refers in general to water removal from and between fibres, fillers and fines. There are several stages in the process, where water is removed using pressure difference. In the paper machine (Figure 1) water removal from the paper web starts as filtration immediately at the wet end after the headbox (1). Water removal is then intensified with suctions (2), and this is followed by wet pressing (3). After wet pressing the dry content of the web is in the range 43-52% [14, 18]. After this stage the part of the paper machine, which most concerns this work, *i.e.*, the dryer section, is reached (4).

The removal of water from paper by drying requires control of heat and mass transfer. There are usually three stages in water removal from the paper web by drying: heating up, constant rate of drying and falling rate of drying [12, 19]. These last two stages are illustrated in Figure 2, in which the drying rate is given by the derivative of the kinetic curve. Typically drying lasts until a desired dry content has been reached. Energy needed to evaporate water is the physical constrain of drying, which cannot be altered. During drying the evaporated vapour needs to be carried away from the paper web.

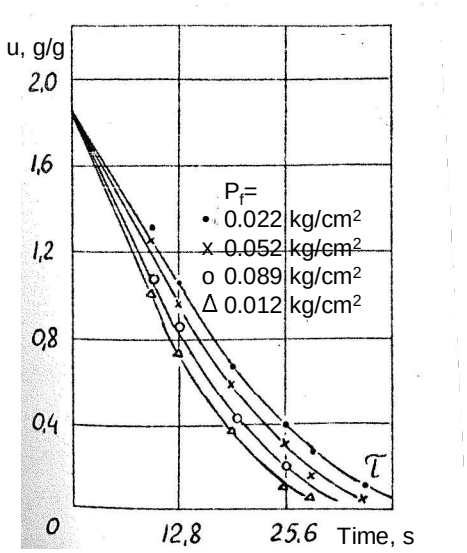


*Figure 2. Moisture ratio in a paper web as a function of time, often called as the kinetic curve. Different curves follow from varying the drying conditions on a cylinder (T=120°C) using different pressures induced by the paper machine fabric on paper [20].*

Traditionally paper is dried with steam-heated cylinders, and this cylinder drying is still widely used without competing methods, although it can be substituted by impingement drying. The latter is a drying method that uses hot air as the drying medium and gives flexibility to the use of primary fuel [21].
In a two-tier configuration the steam-heated cylinders are located on both sides of paper, and in each fabric group two fabrics are needed to support the paper web. In this configuration there is a location between the fabric changes where paper is free from support creating a possibility for web breaks. This configuration is still used in older and slower machines and in some board machines. As the production speed increases the web break handling becomes increasingly important. In order to eliminate the free draw, a one-tier or single-tier configuration was introduced [22, 23, 24]. In this single-tier configuration the fabric always supports the paper web from the top side and there is no need for a lower fabric. In rebuilds of existing machines, the lower cylinders were turned off because the fabric was now covering them, and the possibility to bring heat thus significantly reduced. This configuration change made possible a speed increase, but the length of the dryer section was increased. To increase the speed of this configuration, the lower cylinders were replaced by Vac-rolls. Vac-rolls have a vacuum inside that prevents the web from fluttering under the roll. However, there is still need for a shorter and faster dryer section. The demand for shortening the dryer section comes from limitations in the space available [25].

## 1.6. Requirements for new technology

Drying of paper has to meet some basic requirements: capacity, reliability, quality and economy [14]. The capacity requirement is given by the machinery available and it is hard to change after the installation. Reliability of the dryer has to be good, and it has to provide good operating and production efficiency. Therefore, the potential of new drying solutions needs to be studied carefully before making any installation in the production scale. The quality of paper has to be within certain limits, and the dryer section should not give rise to additional defects. Quality studies usually need larger-scale equipment in the semi-pilot scale. An uneven moisture profile in the cross direction after drying of the web is an example of a defect difficult to study in the laboratory scale.

On the other hand, the demands on energy efficiency have to be met. This means that, because drying uses a considerable amount of energy, energy has to be inexpensive and its losses must be minimized and recovery maximized [26]. The heat carried by air is thus recovered using heat exchangers [27, 28].

Combining impingement drying with existing cylinder drying is expected to provide enhancement of the drying capacity (see Figure 1), but limitations are typically set by the limited space inside the paper mill. An increase in the drying capacity would now be achieved by an expected lowering of paper temperature and an increasing mass (water) flux. A decrease in paper temperature would cause an increased heat flux from the cylinder due to the higher temperature difference between paper and the cylinder surface. The effect of cooling of paper on the drying rate was first reported by Paltakari *et al.* [29] on a pilot-scale paper machine.

Cylinder drying is the most widely used drying technology. Impingement drying is still an emerging technology, although it was invented already in the 1950s [30, 31]. Other methods developed during the last 100 years for paper drying, which have similarities to the method studied in this work, are the Condebelt drying, impulse drying and Papridryer process [32, 33, 34, 35, 36, 37]. Development of new drying methods takes time [31, 38] and an effective use is needed of the available equipment [22, 23, 24]. A comprehensive review of the drying technologies employed today has been given by M. Karlsson [38].

Drying could be used as a quality improving or sustaining component, and via better quality it could create savings in the material costs. On the other hand, all increases in the drying capacity lead to increased production.

In modelling the goal is typically to obtain the drying capacity of the dryer section. Experimental work is used to get necessary background information, and then to quantify properties that cannot be measured. Such work is an

iterative process. Experiments also give background information of the mass balance. Laboratory scale measurements are used to estimate effects on a mill scale by numerical simulations. Figure 3 illustrates this.

In this work the emphasis is on impingement drying through a fabric (COMBO). Paper properties are not considered, unless they are influenced by the drying method. As an example, shrinkage reduction improves the tensile properties of paper. Shrinkage is affected by the drying characteristics, but at the same time many other properties are as well affected [39, 40, 41].

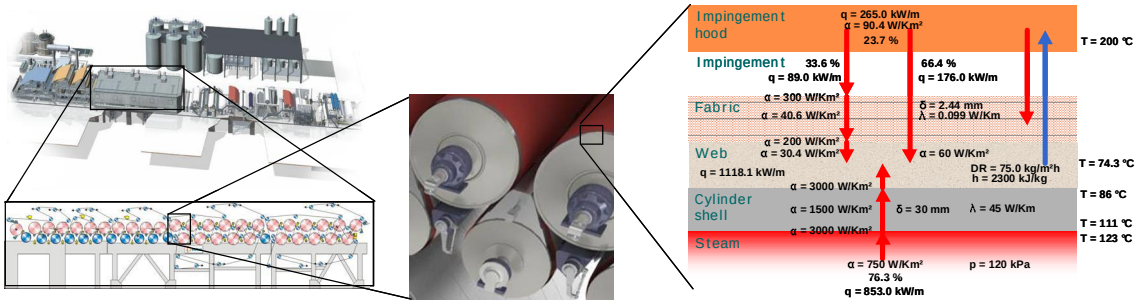


*Figure 3. Extrapolation from small scale to mill scale is possible using laboratory measurements together with simulations.*

## 1.7. Shorter dryer section via better understanding of fundamentals

This Thesis concentrates on the findings made experimentally using a small-scale laboratory dryer, which are then later utilized in simulations. Simulations are done to display effects of drying on a paper machine scale. These experimental findings were complemented by paper quality measurements. The goal of the Thesis was to study the possibilities to shorten the dryer section, and to explain the physical reasons for decreased paper temperature in a combined cylinder-impingement drying in comparison with cylinder drying. Decreased temperature was found to arise from an increased mass transfer rate [42, 43, 44, 45, 46, 47].

In order to control the drying process of paper understanding of several factors is needed. The most important ones of these are described in the schematic map of Figure 4 that illustrates the complexity of paper drying. In Figure 3 a list (the rightmost panel) of the paper properties that influence heat and mass transfer during drying is presented.


*Figure 4. Schematic map of drying factors*

A small static drying test rig was constructed during this work. The experimental data obtained were used to improve the accuracy of the simulations. The simulation model was based on a model reported earlier in [48, 49, 50, 51, 52, 53], which in a physical sense compares successfully with other drying models [54, 55]. Recent developments in the laboratory scale methods allowed us to couple experimental information about moisture in the thickness direction with the model [56, 57]. Moisture measurements have been done very early, dating back to 1956 (Dreshfield [58]), but not accurately in the thickness direction until very recently [58, 59, 60, 61, 62].

Mass transfer in paper includes migration of water and water vapour in the porous structure of paper, because water is present in both liquid and gaseous phase. Evaporation takes place at surfaces during drying. The movement of liquid and gaseous water inside paper is caused by capillary forces and pressure differences. Porosity and permeability of the network are important in this phenomenon. Vapour movement in the gas phase becomes more important with increasing dryness. Heat transfer in paper includes both conduction and convection, but radiation heat transfer is considered to be small due to low temperature differences. An important factor in this study is the information gained about heat transfer coefficients [63]. It has been found earlier that permeability of the fabric influences the drying rate more than the contact area, but the most important effect arises from the fabric tension [20, 64].
Energy consumption and drying rates in impingement drying and impingement drying through a fabric, have been studied earlier in Refs. [12, 13, 21, 28, 65, 66, 67, 68].

# 2. PAPER PROPERTIES AND DRYING

Feed stock and process variables influence paper properties, but only the influence of drying variables during the drying process are considered more closely in this work. Some aspects of fibre properties were chosen for closer consideration due to their direct impact on the porosity of paper. Typically, porosity is controlled by furnish and beating, and it is important in the drying of paper. This can eventually lead to a link between paper properties, like curl and cockle, and paper structure [69]. Fine paper is used in most analyses here. During drying, many paper properties change. For example, brightness and tensile properties are improved, while porosity is changed only little [14]. Examples of fibre length and fibre width distributions are shown in publication A.V [70]. These too influence the properties of paper [71]. Hemicelluloses influence the tensile properties: if they are removed there is a clear decrease in the tensile strength of paper [72, 73], and also in its recycling ability [72].

## 2.1. Effect of fibres on the drying rate

Network density is determined by the flexibility of fibres. Flexibility follows from the material properties of wood, and these are thus needed for estimating the porosity [70]. The wood material is composed of lignin, hemicelluloses and cellulose, and their typical densities are given in Table 1. Different types of wood have different fibre wall densities that vary in the range 1450 – 1530 $kg/m^3$. More details of such properties are given in Appendix IX.

The higher average density of cell wall in hardwoods causes the average bulk density of paper to decrease, if the basis weight of paper is kept constant. This indicates that porosity using hardwoods is higher than in the case of softwoods. Difference between the fibre lengths of hardwoods and softwoods is also a reason for different tensile properties of pulp, paper and board. Softwoods have

longer fibres than hardwoods, as well as lower fibre wall density, which are illustrated in Figure 5 that shows data given in Appendix IX.

The cell wall density is sensitive to changes in cellulose density. If cellulose density is assumed to be 1600 kg/m$^3$, then the density of cell wall as given in Appendix IX is between 1496 - 1600 kg/m$^3$. The density of fibre wall varies inside the tree: it e.g. increases in the xylem from the surface towards the core. In pine this increase can be 20% [74].

*Table 1. Densities of raw materials in the cell wall of wood fibres [74].*

| Density, kg/m$^3$ | Softwood | Hardwood |
|---|---|---|
| Lignin | 1347 | 1366 |
| Hemicelluloses | 1666 | 1457 |
| Cellulose | 1500 | 1500 |

The selection of raw materials and beating level will significantly influence the drying characteristics and other papermaking properties [69]. Increasing the level of beating is used to increase fibrillation and the fines content of the pulp [75]. Corte [76] showed that increasing the beating level decreased the average pore radius in paper, and thus decreased the permeability and porosity. He found that the distribution of pore radii can be approximated by a logarithmic Gauss distribution [77].

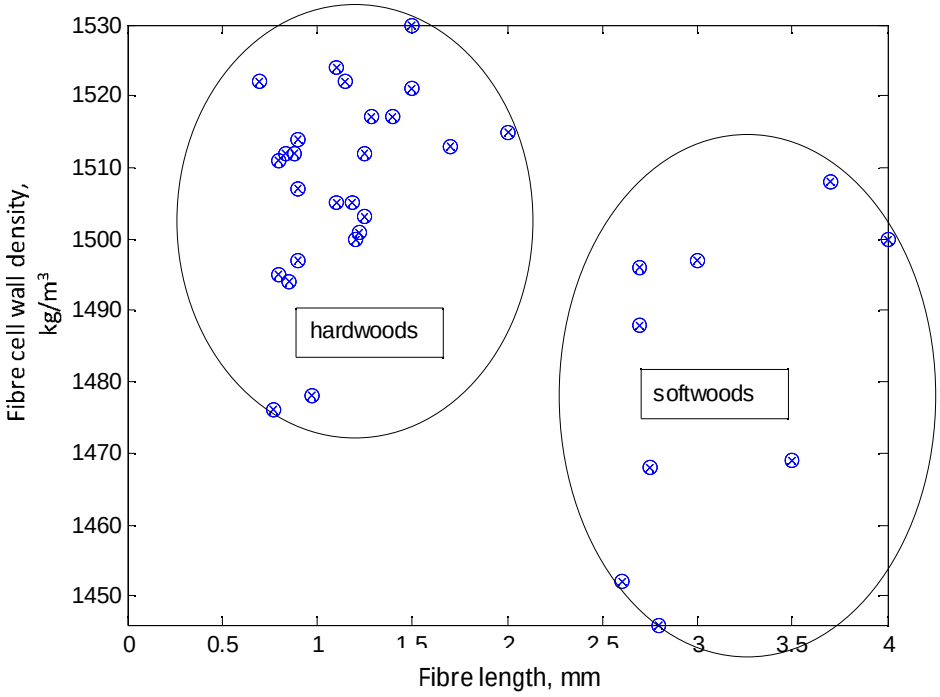


*Figure 5. Hardwood / softwood differences at the fibre level.*

A typical method to increase paper strength is beating [75]. Beating affects the strength of fibres itself, interfibre bonding and fibre resistance to slippage [78]. These effects can be seen in the bonding of fibres, structure of fibres, flocculation and tensile strength [38]. Specific surface area is a material property which measures total surface area per unit mass.

Braaten [79] has suggested that the specific surface area, SSA ($m^2/g$, total surface area per fibre / fibre weight), is given by $4/3t$, where t is the fibre wall thickness (m). With the fibre properties given in Appendix IX, the SSA varies between 0.16-0.6 $m^2/g$ for unrefined fibres (determined for those fibres which had the cell wall thicknesses available), but beating by 1 MWh/t reduced the measured fibre wall thickness by about 10% [80], leading to an increased SSA. Fines have typically a much greater SSA, 5-20 times that of fibres depending on the process conditions [81].

## 2.2. Shrinkage of fibres and the network during drying

During drying, the fibre network shrinks and this shrinkage changes its elastic modulus. An increasing shrinkage usually leads to a decreasing elastic modulus and vice versa, although a slight increase was found in both these quantities for lowering the drying temperature reported in Ref. [70].

The shrinkage upon drying of fibre network arises from changes that happen then in the morphology and structure of fibres. They have been described by Nanko [82, 83] and later by Weise [84] (Table 2).

*Table 2. Network shrinkage upon drying at different dryness levels.*

| Initial dryness | Final dryness | Shrinkage behaviour of fibres |
|---|---|---|
| < 50-55% | 50-55% | Dry solids content of web increases without changes in fibre morphology. |
| 50-55% | 60-65% | Removal of water starts from the lumen. Fibres begin to shrink at the contact areas between fibres, but no changes appear at the web surface. |
| 60-65% | 70-75% | Longitudinal wrinkles appear at fibre surfaces. Shrinkage and collapse of fibres continues as water is removed from fibre walls. |
| 70-75% | 80-85% | Transverse shrinking appears in the non-bonded regions, and shrinkage and collapse of fibres continues. Macroscopic shrinkage of the web increases and speeds up depending on the solids content. |
| 80-85% | up to 90% | Transverse shrinking of fibres appears mostly at fibre-fibre bonds. |

Upon drying the dry solids content of the web first increases without change in fibre morphology, for solids contents of about 50-55%. There after removal of

water begins from the lumen. Fibres begin to shrink at contact areas between fibres, but no changes appear at the web surface. This behaviour is prevalent in the dryness range 50-55% -> 60-65%. There after longitudinal wrinkles appear at fibre surfaces. Shrinkage and collapse of fibres continues as water is increasingly removed from fibre walls in the dryness range 60-65% -> 70-75%. Beyond that range transverse shrinking appears in the non-bonded regions, and earlier shrinkage and collapse continues. Macroscopic web shrinkage increases and speeds up depending on the solids content, in the range 70-75% -> 80-85%. Transverse shrinkage of fibres happens mostly at fibre-fibre bonds, up to 90% solids content. The dryness ranges above are only qualitative as many variables in the papermaking process influence their exact values. Bonding here mainly refers to bonding by hydrogen bonds, but naturally some bonding is due to chemical bonding resulting e.g. from acid-base interactions, and to entanglement of polymer chains. In a macroscopic scale, it is often difficult to determine the effect that dominates at certain solids content.

Upon drying many paper properties change, such that shrinkage, curl and cockle, e.g., appear at a macroscopic level, and many studies have been done on these phenomena [41, 45, 82, 85, 86, 87, 88, 89, 90, 91, 92, 93, 94, 95, 96, 97, 98, 99, 100]. The quality change of paper in drying has been studied extensively [34, 35, 65, 81, 101, 102, 103, 104, 105]. Maloney *et al.* [106] found that upon drying pore sizes in the fibre walls are decreased. Park *et al.* [105] measured changes in these pore sizes for varying drying rate, and reported that drying dynamics can be affected considerably, and that these effects mainly appear in large pores. The decrease in pore sizes begins at a moisture ratio of about one, and it stops when the moisture ratio is above 0.3 [105]. On the dryer section the moisture ratio of paper is typically below one, meaning that its solids content is above 50%.

Combined effects of moisture and temperature can cause irreversible changes in fibre walls [104]. They are sometimes explained by glass transitions[1] or softening of a chemical component [107, 108, 109].

The O-H-bonding formed between fibres during drying changes the viscoelastic behaviour of paper, which has been studied extensively [13, 69, 110, 111, 112, 113, 114, 115, 116, 117, 118, 119]. In chemical pulp the drying induced irreversible difference means that never-dried pulp produces better bonding at a certain refining energy level [120, 121]. Studies of irreversible effects on the mechanical properties of fibre networks (mainly tensile stress – strain dependence and creep) have concentrated on effects of cyclic[2] relative humidity conditions [122, 123, 124, 125]. Activation of segments plays an important role

[1] Below the glass-transition temperature, poled amorphous polymers, like lignins, are thermodynamically metastable

[2] Cyclic humidity accelerates the creep rate of paper, accelerated creep can also be called as mechano-sorptive creep

in cyclic conditions, and bonds play an important role in the strength behaviour of paper. Changes induced by drying appear at the micro fibril level as well [126]. Due to water removal the balance between water, fibre and air in wet fibre networks is changed. Changing porosity indicates that the pore volume increases as fibres shrink upon moisture removal. Mechanical furnish with stiff fibres produces more porous structures than chemical pulp, and beating decreases porosity and fibre thickness as fibre flexibility increases together with collapse of lumen [81]. Fines that appear in different pulps change also the drying characteristics of paper, as their properties differ considerably from those of normal fibre properties.

Restrained drying prevents the unconstrained contraction of bonded segments (parts of fibres between two bonds with other fibres) of fibres, leading to stretching in free segments. The loose segments between two bonds become tense during restrained drying and the structure of the restrained part of fibre network becomes more “loose” as free drying leads to a denser network of fibres with smaller porosity [82]. In free drying the shrinkage of the free segments contracts the sheet, but because longitudinal contraction of the segments is small, the overall contraction as also the shrinkage of the sheet remains small.

Typically a dense network having more bonds than a bulky structure displays higher shrinkage, but also a lower drying shrinkage with a density below the range 500-600 $kg/m^3$ for a mechanical pulp has been reported [127]. A network with more bonds is stronger also in the z-direction [128]. Shrinkage prevention leads to a considerable improvement in strength and stiffness [114, 129], some aspects of which behaviour have also been confirmed in this work [70].

Shrinkage prevention can improve the tensile properties of paper. Fibre orientation, a property that is set before drying, influences paper properties in the both CD and MD directions. Analysis of fibre orientation and flocculation are not included in this work. It is clear that they both affect the drying behaviour. Measurements show that shrinkage develops fastest when free water has been removed from paper, and its moisture ratio is below 0.6 g/g. Drying with shrinkage has been modelled [192], but such a model includes many structural and transport parameters that are quite hard to determine accurately. During drying CD shrinkage profiles are formed in paper [130]. Formation of such CD profiles can be prevented using vacuum that improves the contact between paper and fabric, and thus increases the friction forces and decreases shrinkage [130, 131]. Shrinkage prevention also changes the hygroexpansion of paper [132], which is correlated with its stress-strain behaviour [133].

In uniaxial restraint, the free direction transverse shrinkage of fibres is 17-32% (under restraint direction transverse shrinkage it is 1.1-1.8%), while free

direction longitudinal shrinkage is about 5-7% (under restraint direction longitudinal shrinkage it is 15-22%) [82]. Effects of shrinkage and drying on the optical properties are not discussed here, though it is clear that such effects exist as there are changes in the paper structure.

Htun *et al*. noted that "If a sheet of paper is allowed to dry under restraint, it will attain a higher elastic modulus and mechanical strength than a sheet which has been allowed to dry freely. This has been verified by Setterholm et al., Schultz, Gates and Kenworthy and many others." [134]. There are also other factors that influence the change in the tensile properties upon drying, e.g., faster drying leads to a better tensile index. If sheets of paper (handsheets) are dried between fabrics, with similar shrinkages, the drying rate (using impingement through fabric) affects their tensile index (unpublished).

Drying stress has been found to increase rapidly after 80% dryness (bleached kraft pulp). It is evident that the parameters that control paper properties during drying include drying temperature and drying time. Stresses introduced during drying are irreversible, and they depend on the drying conditions [134].

## 2.3. Curl and cockle caused by drying

Curl in paper is caused by its asymmetric moisture profile in the z-direction during drying. Such an asymmetry arises from asymmetric heating of the paper web. Earlier, when two-tier configurations were used in the drying section, moisture gradients in the thickness direction were at least symmetrical. As discussed above, higher production speeds led to needs to support better the paper web, and the solution was to use single-tier configurations. Today the drying section typically has heated cylinders only on one side of the paper, which leads to a difference in moisture content between paper surfaces. Such a gradient causes uneven shrinkage which appears as curl of paper. Curl, an out-of-plane deviation [135] in paper, is also an important factor in paper quality when effects of drying are considered. Cockling of paper appears often with curl.

Curl can be in the CD or MD direction in machine made papers. An MD-axis curl (*i.e.* a CD curl) means that curl happens around an axis that is parallel to the machine direction. A large MD curl prevents a CD curl and vice versa. A twisted curl can also exist (direction of curl axis between CD and MD).

Examples of curl and cockle are shown in Figure 6. Cockling usually arises from unevenness in the basis weight (formation). Both of these phenomena are considered as indicators of poor quality.

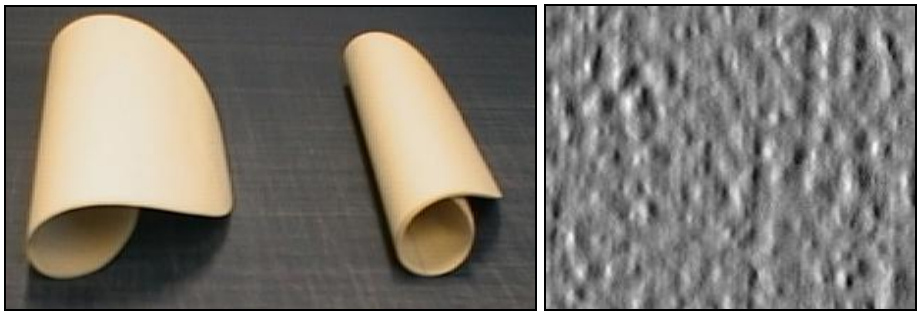

*Figure 6. Curl (left) and cocking (right) of paper which both appears as a result of unevenness of drying.*

Curl is affected by process conditions, especially the temperatures of the last heated cylinders in the drying section. Curl direction, either towards the top or bottom side, is mainly towards the side that has been dried last [86]. Moreover, changes in the ambient moisture conditions can lead to curl due to unevenness in anisotropy[3]. The network density and filler content also affect the curl. By controlling the stresses and shrinkage during drying, the quality of paper can be improved [130].

Quality control and product engineering using drying has been proposed earlier by Stenström [136]. Reduced temperature at the beginning of drying reduces the delamination tendency of multi-ply linerboard [66], which clearly improves its quality. The improvements achieved by a combined cylinder-impingement drying are somewhat similar to those of Condebelt technology: A considerable amount of new drying capacity, new ways to control the quality of paper (paperboard) and a possibility to use furnishes of lower quality or reduced basis weight [137].

[3] Anisotropy is the strength of orientation in the fibre network, *i.e.* the higher anisotropy is, the more fibres are aligned in the same direction (in a given layer of paper).

# 3. MODELLING AND MEASUREMENTS OF IMPINGEMENT AND CYLINDER DRYING

The modelling approach to impingement through fabric involves description of the temperature and moisture fields in paper during its drying, especially in the thickness direction.

In this chapter a short description of the drying model (the 'VTT model') originally made for newsprint is given. Also, methods and devices used for drying rate tests are described. A more detailed description of the model can be found in Refs [48, 49, 50, 51, 53]. Other drying models also exist [55, 138, 139, 140, 141, 142, 143, 144, 145]. A comparison of the models is done in Ref. [54]. The 'VTT model' includes an empirical equation for the falling drying rate at the end of drying, which was originally determined for drying curves of thin papers. The paper web is divided into a certain number of layers, and the temperature and moisture of each layer determines then the dominant transfer mechanism which can be controlled by either water or vapour. In this work basis weights less than 150 $g/m^2$ are considered, but with some adjustments also board grades of higher basis weight could be considered.

## 3.1. Drying model

Paper drying is controlled by the energy and mass balance under the imposed boundary conditions. All phases of different material components (solid, liquid, vapour and inert gas, subscripts from 1 to 4, respectively, in the following) are treated as continua, meaning that the density of each phase of each material changes continuously through the paper web. Once these densities are found, it is possible to determine the moisture content u(x,t) and temperature T(x,t) inside the paper in the thickness direction (x), as a function of time (t). The model includes various heat and mass transfer coefficients which depend on the moisture, temperature and structure of the paper. In order to model the

drying knowledge of what the properties of water are in a hygroscopic material like paper is needed. The gist of the model is that it includes water transport, water vapour transport, heat transfer by evaporation condensation of water and by conduction.

### 3.1.1. Mass Balance

The mass balance of liquid and gaseous water in paper denoted by subscripts 2 and 3, respectively, is [48, 49] given by

$$\frac{\partial \rho_2}{\partial t} + \frac{\partial}{\partial x}(\rho_2 \omega_2) = I_2 \ , \qquad \frac{\partial \rho_3}{\partial t} + \frac{\partial}{\partial x}(\rho_3 \omega_3) = I_3 , \qquad (1)$$

where $I_2$ and $I_3$ are the strengths of the mass sources (or sinks) of the corresponding phases, and it is assumed that $I_2$=-$I_3$ during (no net loss) evaporation at the boundary surface between the phases. Here $\rho_i$ is the partial density of phase *i* and $\omega_i$ its speed.

In Eq. (1), it is assumed that in the convection term had $\frac{\partial}{\partial x}(\rho_3 \omega_3)$ >> $\frac{\partial \rho_3}{\partial t}$ and $\frac{\partial \rho_3}{\partial t} << \frac{\partial \rho_2}{\partial t}$ so that $\frac{\partial \rho_3}{\partial t}$ can be assumed to be zero in the paper due to the small temperature gradient (though it is not small in the cylinder). With these assumptions, from Eq. (1) can be obtained the mass equilibrium of water at the boundary surface between the liquid and vapour phases [48, 49],

$$-\frac{\partial}{\partial x}(\rho_3 \omega_3 + \rho_2 \omega_2) = \frac{\partial \rho_2}{\partial t} . \qquad (2)$$

Mass equilibrium of water and vapour flows in the paper surface defines that, for a one-dimensional homogeneous, laminar flow (in the length and time scales used) without significant temperature gradients, where water ($p_2$) and gas pressure ($p_3$) and gravity are important, $\rho_2\omega_2$ and $\rho_3\omega_3$ are given by [48, 49]

$$\rho_2 \omega_2 = \frac{\rho_2 k_2}{\eta_2}\left(\frac{\partial}{\partial x} p_2\right) \qquad (3)$$

$$\rho_3 \omega_3 = \varepsilon_b \frac{M_3}{RT} \cdot D_{34} \frac{\partial p_3}{\partial x} , \qquad (4)$$

where $\varepsilon_b$ is the effective diffusion resistance coefficient, $M_3$ the molar mass of water and $\eta_2$ the dynamic viscosity of water. Derivation of Eq. (4) was first done by Lampinen and is reported in Ref. [48].

In order to solve Eqs. (3) and (4), several variables need to be measured such as hydraulic resistance ($\rho m = \alpha$), effective diffusion resistance coefficient ($\varepsilon_b$), diffusion coefficient of water vapour in dry air ($D_{34}$), and permeability ($k_2$). However, in practise this approach is not feasible and, thus, they are determined indirectly using simulations.

Hydraulic resistance

During water removal from paper, flowing fluid meets resistances. The resistance of flow (frictional force due to interaction) when different phases (vapour, moist air, liquid) flow against each other is given by $\rho m$, which is linearly dependent on the velocity difference between the constituents and depends also on the dynamic viscosities of the constituents [48, 49]:

$$\rho m_3 = -\eta_3 \phi_\beta \alpha_{34} (v_3 - v_4) - \frac{\rho_3}{\rho_\beta} \eta_\beta \alpha_{\beta 1} (v_3 - v_1) - \frac{\rho_3}{\rho_\beta} \eta_\beta \alpha_{\beta 2} (v_3 - v_2), \quad (5)$$

where $\eta_j$ is the dynamic viscosity, $\phi_j$ the volume fraction of constituent, $\nu$ the kinematic viscosity of constituent, $\alpha$ the hydraulic resistance between phases *i* and *j* and $m_i$ the mass of phase *i* and *j* (subscripts *i* and *j* 1=solid phase, 2=liquid phase, 3=water vapour, 4=dry air, $\beta$=humid air). In a stationary state and for $\phi_\beta$=1 (only humid air present), an equation analogous to Fick's law[4] is obtained. Then a relation between $D_{34}$ (diffusion coefficient) and $\alpha_{34}$ (hydraulic resistance) can be found such that [48]

$$\eta_3 \alpha_{34} = \frac{\rho_3 \rho_4}{M_3 M_4} \frac{M_\beta}{\rho_\beta} \frac{RT}{D_{34}} , \quad (6)$$

where $M_4$ and $M_\beta$ are the molar masses of dry and humid air, respectively, R is the universal gas constant and $T$ the temperature .
The hydraulic resistance ($\rho m$) is a measure of the frictional force due to the interactions of the mentioned constituents with each other. It assumes isotropic resistances, and can only be used in one dimension. Since $D_{34}$ is inversely dependent on hydraulic resistance, the diffusion coefficient can also be called the conductivity of water vapour through dry air.

Without the inertial forces, Eq. (5) can be written as

$$\rho m_3 = -\eta_3 \phi_\beta \alpha_{34} (v_3 - v_4) - \frac{\rho_3}{\rho_\beta} \eta_\beta v_3 (\alpha_{\beta 1} - \alpha_{\beta 2}) . \quad (7)$$

Replacement of water by air at the surfaces is a rather slow process. Thus, it can considered that $v_4$ is negligible in Eq. (7). [48, 49].

[4] Note: Fick's law is analogous to Fourier's law and it can be expressed in the form

$$N_A'' = -D_{AB} \frac{\partial C_A}{\partial y}$$

Here $D_{AB}$ is property of a binary mixture known as the binary diffusion coefficient, $N_A''$ is the flux and $C_A$ the concentration of substance *A*.

Effective diffusion resistance coefficient (gas, air and vapour)

The effective diffusion resistance coefficient $\varepsilon_b$ in Eq. (4) using Eq. (6) and applying both $k_\beta \equiv \phi_\beta^2 / (\alpha_{\beta 1} + \alpha_{\beta 2})$ and the ideal gas law together with the relation $p_4 = p_\beta - p_3$, can be expressed in the form

$$\varepsilon_b = \frac{\phi_\beta}{1 + \frac{p_\beta}{p_\beta - p_3} \frac{M_3}{RT} D_{34} \nu_\beta \frac{\phi_\beta}{k_\beta}} \quad . \tag{8}$$

Here $\phi_\beta$ describes the relative area through which the mixture can diffuse, has always a value less than unity, and thus the maximum value of $\varepsilon_b$ is one. Measurement of the total permeability gives information enough to determine the diffusion resistance coefficient, and thus there is no need for a separate measurement of the effective diffusion resistance coefficient. [48, 49].

Porosity and diffusion resistance

Diffusion resistance of a porous structure changes during its drying. It can be estimated by measuring the porosity:

$$\varepsilon_p \cdot \psi_t = \frac{D_{eff}}{D} \tag{9}$$

Here $\psi_t$ is called the tortuosity and $\varepsilon_p$ is the void fraction. Tortuosity is the relative path length in diffusion through the network. For paper like planar structures the tortuosity can be defined e.g. as $\psi_t$ =path length / thickness. Tortuosity is equal to one when the path is a straight line through the sample. An example of the temperature and moisture dependence of the effective diffusion resistance coefficient is shown in Figure 7. At high temperatures, the effective diffusion coefficient increases with moisture ratio below 0.3, but typically it decreases through the temperature range 0-100 °C.

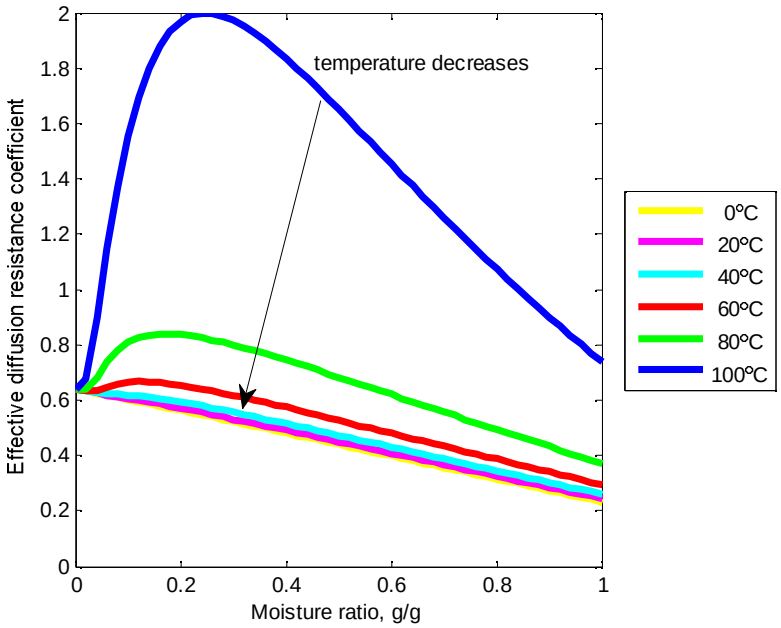


*Figure 7. Effective diffusion resistance coefficient as a function of moisture ratio for the temperature range 0°C to 100°C and for the moisture ratio range 0 to 1. [49]*

The current of fluid flow in the fibre network can be described using Darcy's law:

$$\frac{\dot{m}_{ev}}{A} = \rho_2 \frac{K}{\mu} \frac{dp_c}{dy}, \tag{10}$$

where $\frac{\dot{m}_{ev}}{A}$ is evaporation per surface area, $\rho_2$ is water density (1000 kg/m$^3$ for T=4°C), $K$ is permeability, $\mu$ is water viscosity and $\frac{dp_c}{dy}$ is capillary-pressure gradient. Now capillary pressure is proportional to water concentration [14] and moisture gradient becomes the driving force. The current of vapour flow can then be expressed in the form

$$\frac{\dot{m}_{ev}}{A} = \frac{D_{eff}}{R \cdot T} \frac{p_{tot}}{p_{tot} - p_v} \frac{dp_v}{dy} \tag{11}$$

where $D_{eff}$ is effective diffusivity of vapour in air, $p_{tot}$ the total pressure and $p_v$ the vapour pressure.

Thermal conductivity

Thermal conductivity is the sum of actual conduction in the gas phase ($\lambda_g$) and conduction via evaporation and condensation of water ($\lambda_d$ Stephan diffusion) such that the latter contribution is given by

$$\lambda_d = \frac{D_v \Delta h_v}{R \cdot T} \frac{p_{tot}}{p_{tot} - p_v} \frac{dp_v}{dy}, \tag{12}$$

where $\Delta h_v$ is the vaporisation enthalpy of bound water.

Thermal conductivity values in paper are typically found to be in the range 0.05-0.7 W/(m°C) when the moisture ratio is below one and temperature is 100°C [14, 146, 147].

The apparent thermal conductivity is given by

$$\lambda_{app} = \lambda + l \cdot \varepsilon_b \cdot \frac{M_3}{RT} \cdot D_{34} \cdot \frac{\partial p_3}{\partial T}, \tag{13}$$

where $\lambda_{app} = \lambda$ for dry paper (no vapour flow). Then also:

$$\lambda(T, u = 0) = \phi_1 \lambda_1 + \phi_\beta \lambda_\beta, \tag{14}$$

where $\lambda_\beta$ is thermal conductivity of humid air and *u* the moisture ratio. For dry newsprint $\lambda_1$=0.11 W/mK.

The apparent thermal conductivity $\lambda_a$ is shown for newsprint in Figure 8.

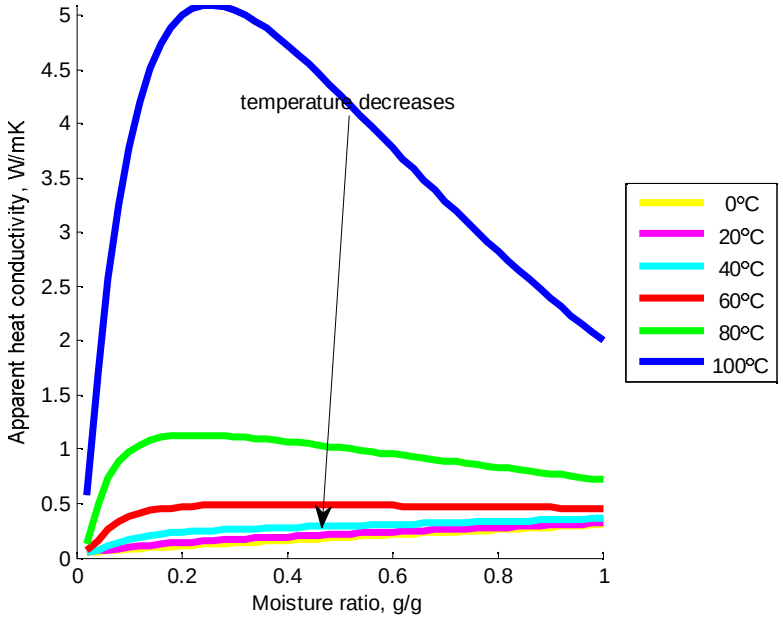


*Figure 8. Apparent thermal conductivity as a function of moisture ratio for varying temperature of newsprint [49].*

Permeablity of paper for air

The permeablity of paper can be described using the empirical equation determined by Lampinen [48]:

$$k_\beta = \frac{B_1}{T} \cdot \left[ e^{\left(-B_2 \cdot T \cdot u^{1.378}\right)} - e^{B_2 \cdot T \cdot u_0^{B_3}} \right], \tag{15}$$

where $B_1$=7.988·10$^{-12}$ m$^2$, $B_2$=-2.601·10$^{-3}$ 1/K, $B_3$=1.378 and $u_0$=1.581 for newsprint of 45 g/m$^2$. The permeability of paper for moist air ($k_\beta$) is shown in Figure 9. When the moisture ratio increases the permeability decreases. The temperature has a similar, but smaller, effect: when the temperature increases at a fixed moisture ratio the permeability decreases.

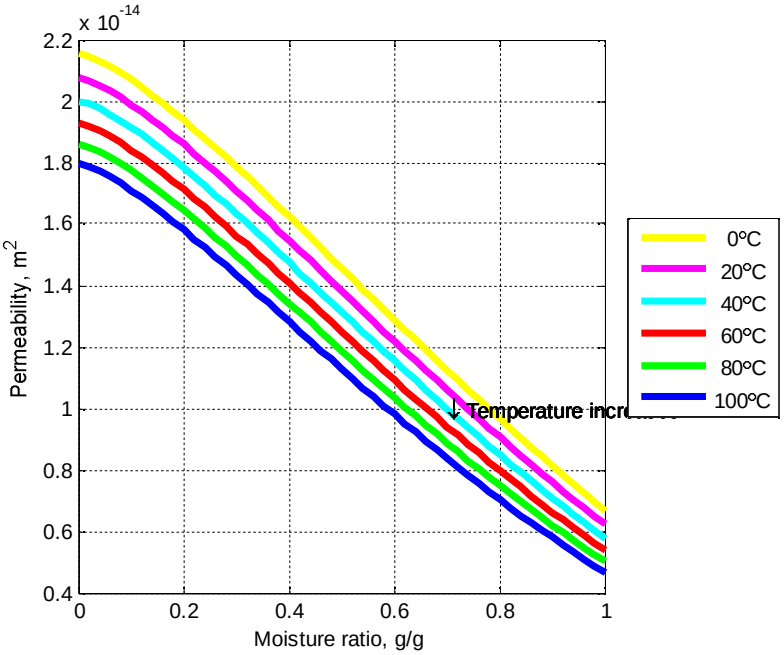


*Figure 9. The permeability of paper for moist air as a function of moisture for different temperatures [48].*

The maximal air permeability of paper is reached, for $u_0$=0 in the second term on the right hand side of Eq. (15) :

$$k_{\beta,\max} = \frac{B_1}{T} \cdot \left(1 - e^{B_2 \cdot T \cdot u_0^{B_3}}\right). \tag{16}$$

Permeability of paper for water

When determining the permeability of paper for water, $k_2$, an auxiliary parameter can be utilized

$$s = \frac{\phi_2}{1-\phi_1}, \tag{17}$$

where $\phi_1$ is the solid volume fraction and $\phi_2$ the volume fraction of water in paper. In practice it is convenient to use the moisture ratio in paper, $u$, as a directly observable parameter, and this ratio is simply given by $u = \frac{\rho_2 \phi_2}{\phi_1}$, with $\rho_{1(2)}$ the solid (water) density. Parameter $s$ is thus given by the moisture ratio such that

$$s = \frac{\rho_1 \cdot u}{\rho_2 (1-\phi_1)}. \tag{18}$$

In practical situations the prefactor in the above relation, $\frac{\rho_1}{\rho_2(1-\phi_1)}$ can typically be assumed to remain constant. In terms of parameter s the permeability $k_2$ has been shown [48] to take the form

$$k_2 = A_{k_2} \frac{k_{\beta,\max} s^3}{1 - \frac{k_{\beta,\max}}{k_\beta}(1-s)^3}, \qquad (19)$$

where $A_{k_2}$ is a constant (depending on paper type, such as newsprint). In Figure 10 this permeability for $A_{k_2} = 1$ and varying temperature as a function of *u* is shown. It is evident that $k_2$ vanishes for vanishing moisture ratio, and that varying temperature decreases the permeability but only slightly, especially at small moisture ratios.

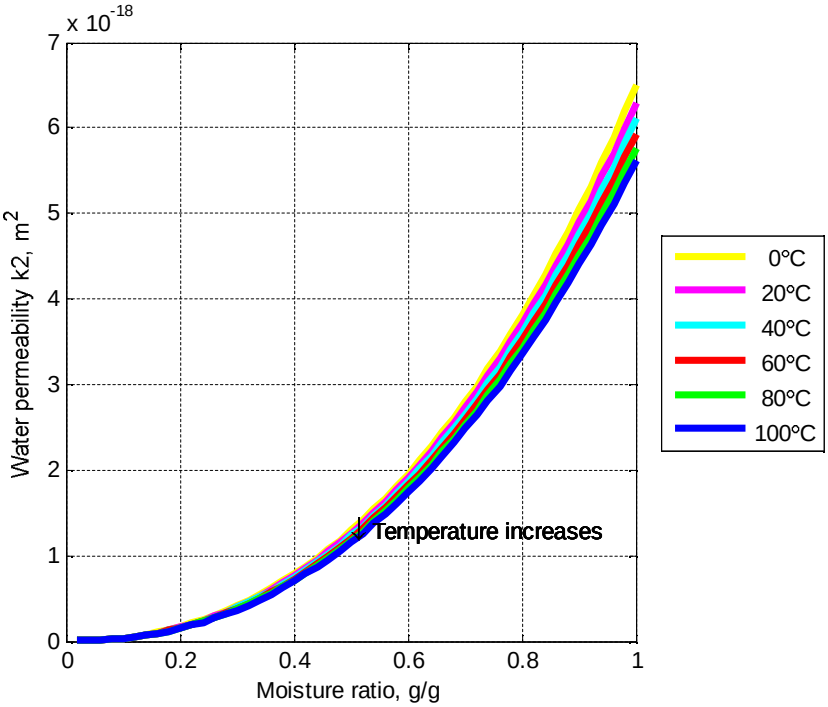


*Figure 10. The permeability of paper for water, $k_2$, as a function of moisture ratio for varying temperature [48].*

Saturated vapour pressure

Another useful equation is Antoine's equation [148] which expresses the pressure of saturated vapour ( $p$ ) for free water (pressure-temperature relation) in the form

$$\log p = A - \frac{B}{T + C} \quad \text{(a)} \qquad \text{or} \qquad T = \frac{B}{\log p - A} - C \quad \text{(b)}, \qquad (20)$$

where $p$ is given in units of kPa, and $A$, $B$ and $C$ are fitted parameters ($A$=10.18, $B$=1723.64 and $C$=-40.074 [193]); $T$ is the temperature. When the pressure and temperature values are known during a phase change, then the enthalpy of vaporization can be determined from a plot of ln $p$ vs. $\frac{1}{T}$. Vapour pressure is plotted in Figure 11. Equation (20) is valid for a large volume of free water (at least about $10^4$ times the separation between molecules), meaning that

the free distance between molecules is about nanometres for liquids and tens of nanometres for gases at normal conditions [49].

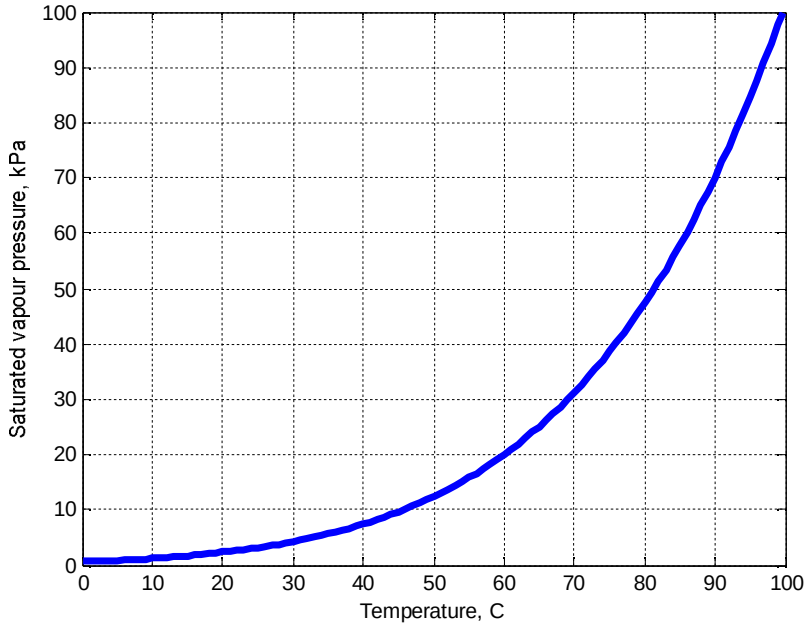


*Figure 11. Partial vapour pressure as a function of temperature as given by Antoine's equation. This equation is also used in the drying model for the pressure of saturated vapour.*

It is obvious that in the beginning the partial pressure of drying vapour is the same as that for water at the same temperature. Increase in the partial vapour pressure shows that the drying temperature has quite an impact on the drying characteristics of paper. However, at the end of drying the partial vapour pressure in the web surface is lower due to diffusion resistance that controls vapour transport to the surface. Diffusion resistance arises from the structure of the web (e.g. thickness) and the hygroscopic nature of fibres. The hygroscopicity of fibres is affected by both temperature and moisture in the paper.

### Adsorption and desorption

Fibres are hygroscopic. This means that part of the moisture is bound to fibres, and the properties of bound water differ from those of free water. On a macroscopic level this is seen as adsorption and desorption of water, which can be measured. An example of such a study is shown next. In this study measured results were fitted by the Soininen model which is one of the models compared in Ref. [60]. Soininen defines the isotherm such that

$$\varphi = 1 - e^{-(A+B\cdot T)u^{C+D\cdot T}}, \qquad (21)$$

where $T$ is temperature in °C, $u$ is moisture ratio (g/g) and $A$, $B$, $C$ and $D$ are fitting parameters.

### 3.1.2. Energy balance

Evaporation from the web

Evaporation of water happens to moist air. The evaporation rate from the web to air is usually given by Stefan's equation [14],

$$\frac{\dot{m}_{ev}}{A} = \frac{\beta \cdot p_{tot}}{R \cdot T} \ln\left( \frac{p_{tot} - p_{va}}{p_{tot} - p_{vp0}} \right) \qquad \text{[48, 49]} \qquad (22)$$

Here $\beta$ is the mass transfer coefficient, $p_{tot}$ is total pressure, [149], $p_{vp0}$ is the partial pressure of vapour on the web surface and $p_{va}$ the partial pressure of vapour in the surrounding air.

If the air flow around the drying web is turbulent, $\left( \frac{p_{va}}{p_{tot}} \right)^2, \left( \frac{p_{vo0}}{p_{tot}} \right)^2 << 1$, and the right hand side of Eq. (22) can be approximated by

$$\frac{\beta}{R_v \cdot T}\left( p_{vp0} - p_{va} \right), \qquad (23)$$

as reported by Berg [150]. The energy needed for evaporation is obtained by multiplying the evaporation rate with sorption heat *h*. Other energy balances are similarly obtained from mass balances.

### 3.1.3. Cylinder drying and conduction

In cylinder drying conduction is the dominant heat transfer mechanism. It involves in this case some specific features that need to be taken into account. One of them is that the removal of moisture from the paper cannot happen such that it is transferred to the cylinder. Evaporation of water takes place either after the cylinder, or while in contact with the cylinder through the other surface of the paper. During evaporation water must flow through the paper and therefore its structure plays an important role in the drying characteristics. Paper properties that affect the drying rate are the density, basis weight, and fines and filler content, just to mention a few.

The drying rate in cylinder drying is typically 20-40 kg/m$^2$h, which corresponds to a heat flux of 12.5 – 25 kW/m$^2$. In an over 10 m wide machine with more than 40 cylinders, each cylinder having more than 18 m$^2$ of drying surface, over 18 MW of drying power is needed for evaporation alone. Increasing the number of cylinders increases the heat flux from the paper. 50 MW of heating power is needed if there are more than 100 cylinders.

Heat transfer resistances between steam and paper

In the cylinder drying the overall heat transfer rate from steam to paper can be estimated [14] to be

$$q_p = \frac{1-a}{\phi_p}\frac{1}{\frac{1}{\alpha_s}+\frac{\delta_c}{\lambda_c}+\frac{1-a}{a_k\phi_p}}(T_s - T_p)A_k = \alpha_{s-p}(T_s - T_p)A_k\,, \qquad (24)$$

where $\alpha_{s-p}$ is the heat transfer coefficient from steam to paper, *a* the fraction of the heat flow from condensing steam to the air ($a = \frac{q_{air}}{q_{out}} \approx 0.05$), which is a loss term, $\phi_p$ the fraction of cylinder surface covered by the paper, $\alpha_s$ the heat transfer coefficient through the condensate layer (W/m$^2$ $^o$C), $\lambda_c$ the thermal conductivity of the cylinder shell (W/m$^o$C), $a_k$ the contact heat transfer coefficient from the cylinder to the web (W/m$^2$ $^o$C), $\delta_c$ the thickness of the cylinder shell (m), $T_s, T_p$ the temperatures of the inner (=$T_{c1}$) and outer surfaces of the cylinder ($^o$C), respectively, and $A_k = \phi_p A_{cy}$ ($A_{cy}$ is the total surface area of the cylinder) with $\phi_p$ the fraction of the cylinder surface covered by the paper.

For a cylinder with a diameter of d=1500 mm the heat transfer coefficient used was [151]

$$\alpha_{condensate} = \frac{685}{l_{condensate}} + \frac{10^6}{275 + 0.675 \cdot v^{2.79} + 0.0486 \cdot l_{condensate} \cdot v^{3.39}} \qquad (25)$$

where $l_{condensate}$ is the thickness of the condensate layer (mm) and $v$ is the web speed (m/s). This heat transfer coefficient from steam to cylinder has been found to be in the range 500-5000 W/m$^2$K [55].

The interface between the dryer and web surfaces creates an additional resistance to heat transfer. Due to the roughness of both surfaces, areas with direct fibre to cylinder contacts and with gas filled gaps both exist between them. The heat transfer coefficient across this interface is given by

$$\alpha_{contact} = \frac{q}{T_p - T_c}\,, \qquad (26)$$

where $T_p$ is the paper temperature on its surface facing the cylinder and $T_c$ is the surface temperature of the cylinder. The value of the contact heat transfer coefficient depends on many paper machine processes and paper related parameters. It cannot usually be predicted accurately. The most important factors that influence it include the moisture content of paper, thermal conductivity of paper, fabric tension, air or steam film accumulation between the web and the dryer surface, roughness and dirt on the dryer surface and smoothness of the paper surface. Contact heat transfer coefficients for dry paper have been reported in the range 900-1700 W/m$^2$K [55], and their values have been found to increase with increasing moisture. The effect of cylinder shell thickness on the overall contact heat transfer coefficient from cylinder to paper is shown in Figure 12.

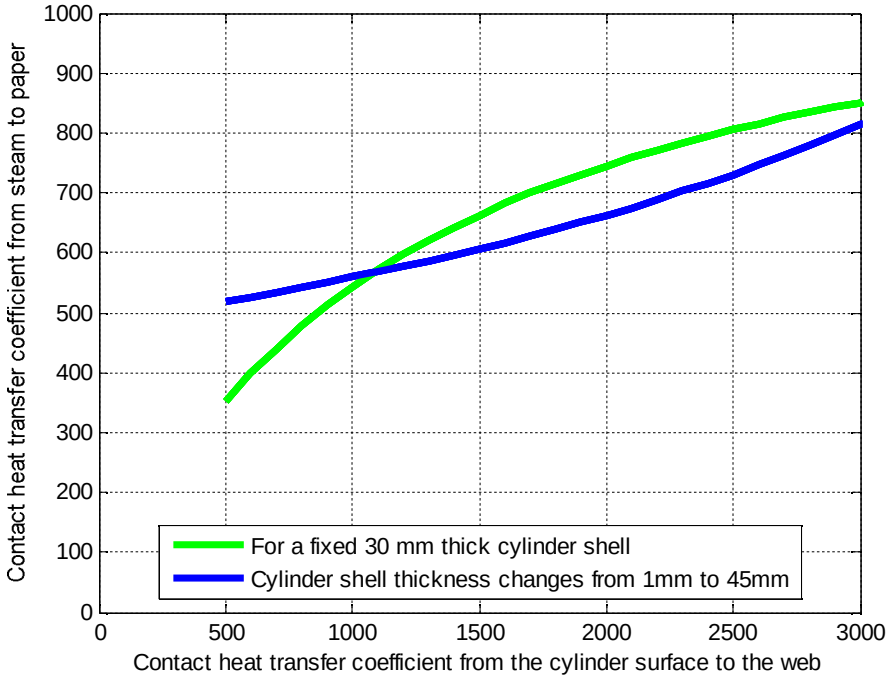


*Figure 12. Contact heat transfer coefficient from cylinder surface to the web as a function of the contact heat transfer coefficient from steam to paper. Contact heat transfer coefficient (green) and cylinder shell thicknesses are varied (blue). A contact heat transfer coefficient of 1500* W / m²K, *and shell thickness changes from 1* mm *to 45* mm *(blue). The fraction of the heat flow from condensing steam to the air (a = $q_{air}/q_{out}$ was 0.05, the fraction of dryer surface covered by the web was 0.6 and the thermal conductivity of the dryer shell was 45* W / mK.

When the area covered by cylinder surface increases, the overall heat transfer coefficient from steam to paper web also increases as the effect of losses on that coefficient is quite small. Factors that affect the heat transfer coefficient include effectiveness of condensate removal, pocket ventilation, fabric tension, geometry of the dryer and moisture content of the paper. The specific energy consumption in drying decreases with increasing humidity, as the need for supply air is reduced, but heat recovery becomes more effective [14].

Temperature and moisture development of paper in cylinder drying

The structure and properties of paper undergoe dramatic changes during drying. For example, in cylinder drying the temperature vs. moisture history is very different in different layers of paper. This is illustrated in Figure 13 [42]. At the same time changes appear in many paper properties.

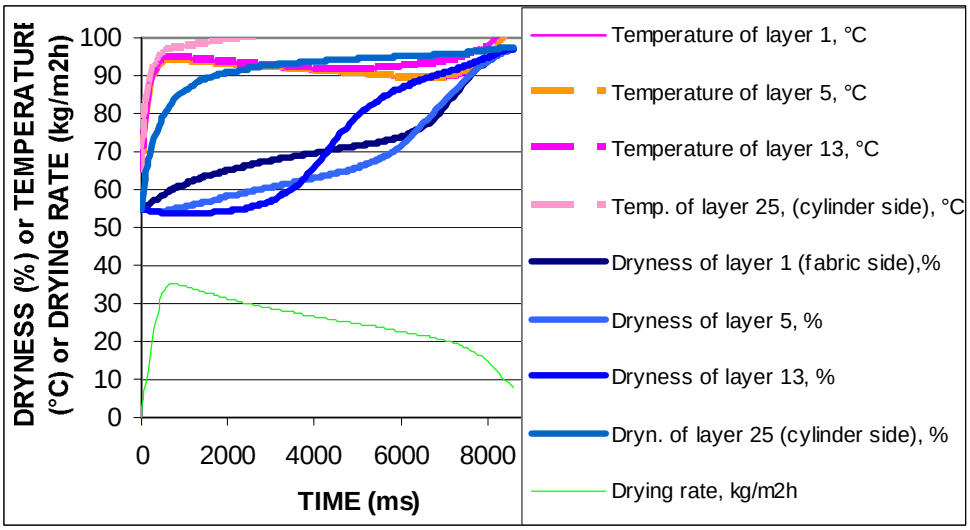


*Figure 13. Temperature and moisture history of different layers of paper during cylinder drying with a cylinder temperature of T=100°C. During simulation paper was divided into 25 layers. Layer 25 faces the cylinder and layer 1 faces the fabric. Note that layer 25 heats up and dries very fast, and moisture moves towards the fabric, while layer 1 only heats up first and dries later [42].*

Until very recently there have been no tools to control in a desired manner the development of paper properties during drying. The recently introduced impingement drying combined with cylinder drying has provided additional tools for this control.

### 3.1.4. Impingement drying and convection

Impingement drying is used to increase the convection (*i.e.* convective heat transfer). In this work it was used to improve drying under the fabric, and, as an interesting additional finding, a decrease in paper temperature was found. More importantly, the decrease of paper temperature leads to increased heat flux, drying rate, but also to some improvements in paper quality. These improvements are discussed later in this work. Impingement drying has been described before in many publications, but for clarity some short notations of it will be made also here. The most important process parameters in impingement drying are the air temperature, air jet velocity, air moisture content and nozzle geometry which includes factors like nozzle pattern and diameter, blow distance and angle and location of exhaust ports. Fabric porosity, machine speed, radiation and pressure difference inside the paper influence also the drying of paper as already mentioned above.

It is assumed that the velocity boundary layer, thermal boundary layer and concentration boundary layer can be considered as incompressible (density is constant), they have constant properties ($k, \mu$ etc.) and are non-reacting, there are negligible body forces and there is no energy generation.
Usually the boundary layer is also thin (in 1D) and there are non-zero velocity components only in planar directions. Pressure is also assumed to be constant

in the direction normal to the surface. The continuity equation and momentum equations can be written (constant pressure normal to the surface) in the form

$$u\frac{\partial T}{\partial x}+\upsilon\frac{\partial T}{\partial y}=\alpha\frac{\partial^2 T}{\partial y^2}+\frac{\nu}{c_p}\left(\frac{\partial u}{\partial y}\right)^2. \quad (27)$$

Note that the last term on the right hand side is what remains of the viscous dissipation. In most situations this term may be neglected relative to those that account for advection (the left hand side) and conduction (the first term on the right hand side). Only in sonic flows this term may not be neglected (or in fast pumped lubricating oils with viscous dissipation).
Now the continuity equation for material component $A$ takes the form [152]

$$u\frac{\partial C_A}{\partial x}+\upsilon\frac{\partial C_A}{\partial y}=D_{AB}\frac{\partial^2 C_A}{\partial y^2} \quad (28)$$

where $C_A$ is the concentration of component $A$.

Dimensionless numbers (Re, Pr, Nu, Sc, St) in impingement drying used in the model

Dimensionless numbers are used in engineering due to the fact that they give correlation with performance parameters, which in impingement drying relate to the drying rate, for example. The important dimensionless numbers in impingement drying are the Nusselt, Reynolds, Stanton and Prandtl number [152]. They can be defined in the following manner.

- Reynolds number is related to the velocity boundary layer,
  $$\mathrm{Re}_L \equiv \frac{vL}{\nu} \quad (29)$$
  with $v$ the air velocity, $L$ the chord of airfoil and $\nu$ the kinematic viscosity. If two systems have a similar geometry and similar Reynolds numbers, their flow patterns are also similar.
- Prandtl number is related to convection heat transfer, and measures the relative importance of momentum and thermal diffusivity,
  $$\mathrm{Pr} = c_p\mu/\lambda \quad (30)$$
  with $c_p$ the specific heat at constant pressure, $\mu$ the absolute viscosity of the fluid and $\lambda$ the thermal conductivity.

- Schmidt number is related to the concentration boundary layer and mass transfer,
  $$Sc \equiv \frac{\nu}{D_{AB}} \quad (31)$$
  with $\nu$ the kinematic viscosity and $D_{AB}$ the mass diffusion coefficient.
- Stanton number is related to forced-convection heat transfer,
  $$St = h/\rho c_p v \quad (32)$$

with $h$ the convective heat transfer coefficient, $\rho$ the mass density and $c_p$ the specific heat at constant pressure of air [153].

- Nusselt number is also related to forced convection, and relates the total heat transfer with the conduction heat transfer:
  $Nu = hL / \lambda$ (33)
  with $L$ a characteristic length and $\lambda$ the thermal conductivity of the gas. Nusselt number is also the product of the Stanton, Prandtl and Reynolds numbers.

Reynolds number can also be interpreted as the ratio of inertial forces to viscous forces in the velocity boundary layer. Thus inertial forces dominate for large Re and viscous forces for small Re. Likewise the PrandIt number provides a measure for the relative effectiveness of the momentum and energy transport by diffusion in the velocity and thermal boundary layers. Prandtl number of gases is near unity, and therefore the energy and momentum transfer are comparable. Growth of Pr results from growth of the velocity and thermal boundary layers. The Schmidt number provides a measure for the relative effectiveness of the momentum and mass transport by diffusion in the velocity and concentration boundary layers.

In impingement drying (convection) the Lewis number is as well of importance. Lewis number is found by dividing the Schmidt number by the Prandtl number. This is important for simultaneous heat and mass transfer by convection. This number measures the relative thickness of the thermal and concentration boundary layers. The Eckert number gives a measure for the kinetic energy of the flow compared to enthalpy difference across the thermal boundary layer. This is important in high speed air flows, like in impingement drying, for which viscous dissipation is significant. The Nusselt and Biot numbers are similar in form but their actual definitions and interpretations are different. Nusselt number is related to thermal conductivity of the fluid and Biot number to thermal conductivity of the solid. As Nusselt number represents heat transfer, Sherwood number ($Sh = kL / D_{AB}$) represents mass transfer. Boundary layer analogies that relate the Nu and Sh numbers are useful in convection analysis. A profound experimental work on this topic was carried out by Martin [154]. This work has been continued by others so as to extend the applicable temperature range [155, 156, 157, 158, 159, 160, 161].

Impingement nozzle geometry and mass diffusion coefficient

The geometry of nozzle arrangement is an important factor in the impingement drying rate, in which the most important geometric parameters are the diameter of impingement jet hole (D) divided by the distance from impingement (H) and the open area (fraction of the hole area of the total surface area, $A_r$).
Examples of an impinging jet and jet geometry are shown in Figure 14 and Figure 15. The former example is similar to flows measured in impingement drying [154, 162].

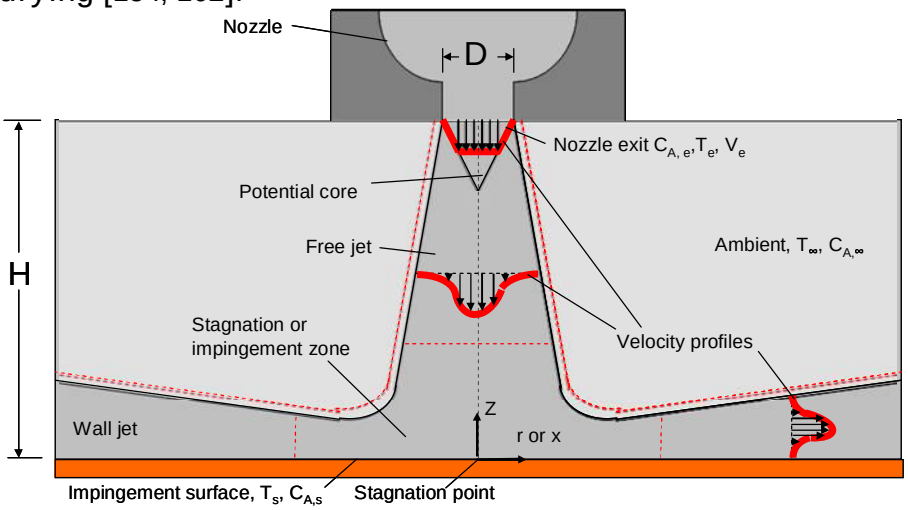


*Figure 14. An impinging jet [152].*

Local measurements of heat and mass transfer coefficients for an impinging flow from arrays of nozzles are similar to those for single nozzles and arrays of nozzles [154]. Single nozzles are not used in papermaking due to their limitations in getting even heat and mass transfer rates (*i.e.* they lead to an uneven drying profile) on a large flat surface.

Figure 15 shows some possible geometries and open areas for nozzles. Commercially, a hexagonal type geometry is often used due to the quality achieved with it. The alignment of impingement jets together with air circulation can then be arranged such that variation in the heat and mass transfer rates is lower than for a square type of geometry.

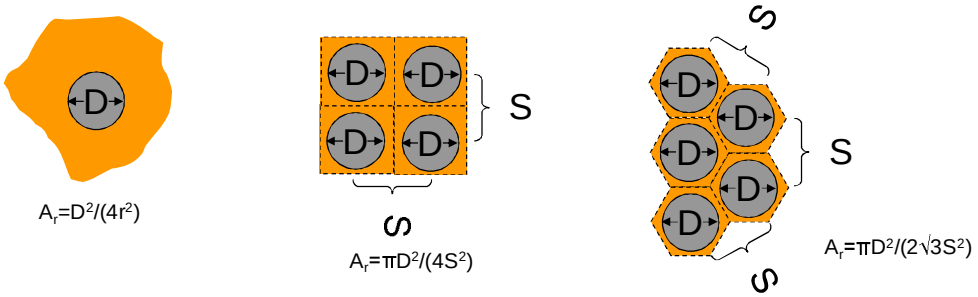


*Figure 15. Round nozzles with different geometries have different open areas $A_r$. [152]. D is the diameter of the nozzle and S the spacing between nozzles.*

The heat transfer coefficient from air to paper for a given impingement geometry could be determined in the experimental work of Ref. [154], where e.g. a correlation was found such that

$$\overline{\left(\frac{Nu}{\mathrm{Pr}^{0.42}}\right)} = K\left(\frac{H}{D}, A_a\right)\sqrt{A_a}\,\frac{\left(1-2.2\sqrt{A_a}\right)}{1+0.2\left[\left(\frac{H}{D}\right)-6\right]\sqrt{A_a}}\,\mathrm{Re}^{\frac{2}{3}} \quad . \tag{34}$$

This result is called the Martin equation in the following. $\overline{Nu}$ is the average value of *Nu* in Eq. (34). Here $A_a$ is the open area of nozzles, D the nozzle diameter, H the nozzle to paper distance and

$$K\left(\frac{H}{D}, A_a\right) = \left\{1+\left[\frac{\left(\frac{H}{D}\right)\sqrt{A_a}}{0.6}\right]^6\right\}^{-0.05} \quad . \tag{35}$$

The validity limits for Eqs. (34) and (35) are: $2000 \le \mathrm{Re} \le 100{,}000$, $0.004 \le A_a \le 0.04$ and $2 \le \mathrm{H/D} \le 12$ [154]. The lower limit is caused by transition from laminar to turbulent flow, and the consequent change in the Reynolds number. The optimal values for round nozzles have been found to be (H/D)=5.43 and f=0.0152, and for 5.0 mm diameter nozzles the optimal blow distance is 27.2 mm [154]. The heat transfer coefficient from air to paper using round nozzles with a triangular geometry is shown in Figure 16 for varying impingement jet temperature and velocity.

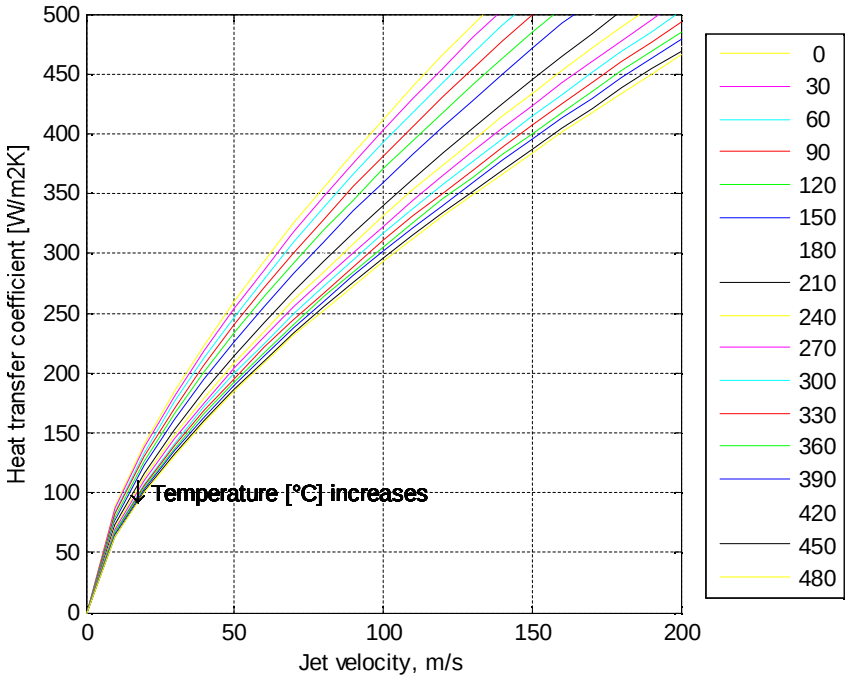


*Figure 16. Heat transfer coefficient as a function of jet velocity for varying temperature (°C) according to Martin [154]. Open area was 1.5%, H/D was 5 and D=5* mm. *At low velocities, below 30* m/s, *the behaviour displayed in the figure is not valid because Re is then below 2000.*

Studies show that values given by the Martin equation deviate from measured ones at high temperatures, having a difference by almost 20% (Figure 17) [155, 161].

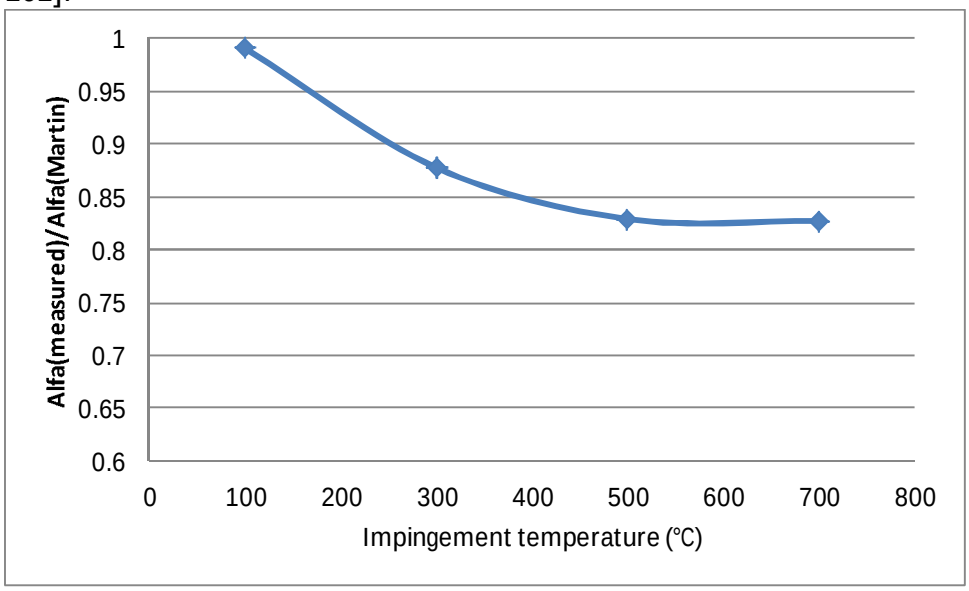


*Figure 17. The ratio of a measured convective heat transfer coefficient to that given by the Martin equation as a function of temperature [redrawn from 155].*

The mass diffusion coefficient in gas can be estimated for an ideal gas such that

$$D_{AB} \approx p^{-1} T^{3/2}. \tag{36}$$

This behaviour is assumed to be valid for binary mixtures of gases.
Now for example for water in air $D_{34}$ is given by

$$D_{34} \approx \frac{p_{\beta,atm}}{p_{\beta}} \cdot 9.9 \cdot 10^{-10} T^{1.81}. \tag{37}$$

In this work the impingement units had round nozzles with a triangular geometry, and therefore slot nozzles are not considered. Heikkilä [151] has found similar experimental correlations, also in high temperature, for slot nozzles as Martin has found for round nozzles.

Specific heat of air and water vapour

In paper machines measurement of air humidity is often a practical approach to estimate evaporation from the paper web. The evaporation rate from the web can be expressed in the form [14]

$$\frac{\dot{m}_{ev}}{A} = \frac{\alpha}{c_{da} + x_{p0} \cdot c_v} \left( x_{p0} - x_a \right), \tag{38}$$

where $A$ is the web area, $\alpha$ is the heat transfer coefficient, $c_{da}$ is the specific heat of dry air, $c_v$ is the specific heat of water vapour, $x_{p0}$ is the air humidity at the web surface and $x_a$ is that in the surrounding air. Specific heat curves determined in this work, shown in Figures 18 and 19 as a function of air

temperature and air humidity, respectively, reveal that, close to condensation, the driving force in evaporation is the difference in air moisture between the web surface and the surrounding air, but evaporation decreases rapidly if the condensation limit is reached ($c_v$ decreases in Figure 18 when temperature is increased from 0°C to 50°C, a relative humidity of 100% is reached and the specific heat of water vapour, $c_v$, increases also in Figure 19 beyond the moisture 0.3 kg / kg dry air).

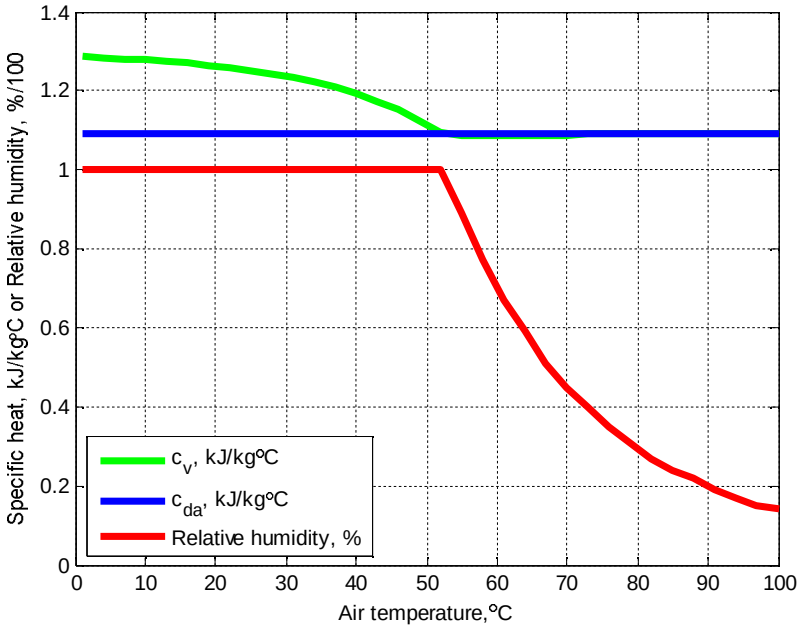


*Figure 18. Specific heat of water vapour and dry air are shown as a function of air temperature. Air moisture is 100* g / kg *dry air and air pressure is 1.013 bar.*

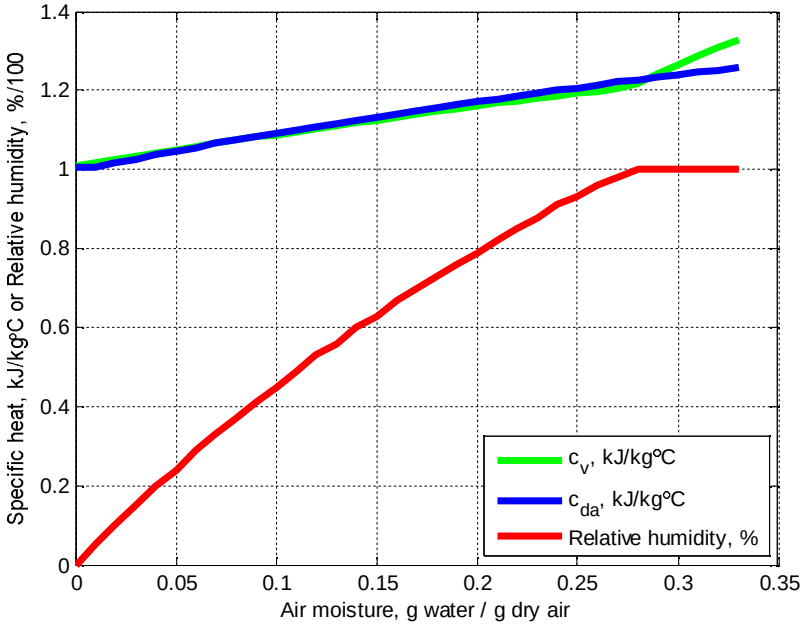


*Figure 19. Specific heat of dry air and water vapour are shown as a function of air moisture. The air temperature is 70°C and air pressure is 1.013 bar.*

## Thermal conductivity

Heat flux (heat current per unit area, q") is given by Fourier's law,

$$q'' = -\lambda \nabla T = -\lambda \left( \frac{\partial T}{\partial x} + \frac{\partial T}{\partial y} + \frac{\partial T}{\partial z} \right). \quad (39)$$

Thermal conductivity can thus be defined as

$$\lambda_x \equiv -\frac{q_x''}{(\partial T / \partial x)}, \quad (40)$$

and similarly in the other directions. Heat flux is dependent on paper properties and its moisture contents. The thermo-physical properties of paper can be divided into two distinct categories, transport and thermodynamic properties. Transport properties include diffusion coefficients and thermal conductivity (for heat transfer). Thermodynamic properties describe the equilibrium state of the system. Density ($\rho$) and specific heat ($c_p$) are commonly used in thermodynamic analysis. The product of the two, called the volumetric heat capacity, measures the ability of the material to store thermal energy. In porous paper thermal conductivity is given by those of fibres, water and air contained in the paper, *i.e.* it is given by

$$\lambda = \lambda_p \cdot \frac{\rho_p}{\rho_f} + \lambda_2 \cdot \frac{\rho_p}{\rho_w} \cdot u + \lambda_a \cdot \left[ 1 - \left( \frac{\rho_p}{\rho_f} + u \cdot \frac{\rho_p}{\rho_w} \right) \right], \quad (41)$$

where $\lambda_p$, $\lambda_2$ and $\lambda_a$ are the thermal conductivities of paper, water and air, $\rho_p$ and $\rho_w$ are corresponding densities and $u$ is the moisture ratio (g/g). It is relatively easy to notice that an increase in moisture content of paper increases its thermal conductivity (note that $\lambda_a$ is smaller than 1). This means that fibre materials are much better insulators when they are dry.

## Thermal diffusivity

Also the thermal diffusivity $\alpha$ ($m^2/s$) is an important transport property, and it is given by

$$\alpha = \lambda_p / (\rho_p c_p), \quad (42)$$

where $\rho_p$, $\lambda_p$ and $c_p$ are the density ($kg/m^3$), thermal conductivity ($W/mK$) and specific heat capacity ($J/kgK$) of paper.

Thermal diffusivity measures the ability of the material to conduct thermal energy relative to its ability to store thermal energy. A high value of thermal diffusivity indicates that changes in the surrounding will reflect quickly as a corresponding change in the material temperature.

Thermal diffusivity $\alpha$ is a complex function of the temperature and moisture of paper. Thermal diffusivity of dry paper is typically $1\text{-}16 \cdot 10^{-6}$ $m^2/s$ (see Eq. (42) and [146, 163]). Thermal diffusivity together with drying conditions determine how the temperature inside paper develops during drying.

Relative vapour pressure and sorption heat

Consider next the behaviour of water, which is very important in the energy and mass in paper.
The relative vapour pressure *p* in paper can empirically be expressed in the form [48]

$$\ln p = A_1 \cdot u^{A_2} e^{A_4 \cdot u} \cdot \left( \frac{T_{cr} - T}{A_5} \right)^{A_3} , \qquad (43)$$

where the constants are: $A_1$=-3.433, $A_2$=-1.3820, $A_3$=7.557, $A_4$=-3.372 and $A_5$=583.5 K [48]. This equation is plotted as a function of moisture ratio for a number of different temperatures in Figure 20. It is evident that increasing moisture ratio or temperature, the relative vapour pressure increases. Equation 43 has been found to work best for moisture ratio over 0.05. Here the relative vapour pressures were determined by weighing paper samples in equilibrium with different saturated salt-water solutions in a vessel.
The sorption heat (*r*, the difference of absorption heats) determined using calorimetric measurements can empirically be expressed in the form [48]

$$r = h - h_0 = A_6 \cdot u^{A_2} \cdot e^{A_4 \cdot u} \cdot T^2 \cdot \left( \frac{T_{cr} - T}{A_7} \right)^{A_3 - 1} , \qquad (44)$$

where r is the sorption heat for paper in the final part of drying, T is the temperature, $T_{cr}$ is the critical temperature of the vapour (distinction between gas and liquid phase of water disappears) and the constants are: $A_2$=-1.3820, $A_3$=7.557, $A_4$=-3.372, $A_6$=8.633·10$^{-3}$ kJ/kgK$^2$ and $A_7$=696.0 K [48].
Sorption heat for water absorbed in paper is plotted in Figure 21 as a function of moisture ratio for different temperatures, which shows that a decreasing moisture ratio increases the sorption heat, and an increasing temperature decreases it.

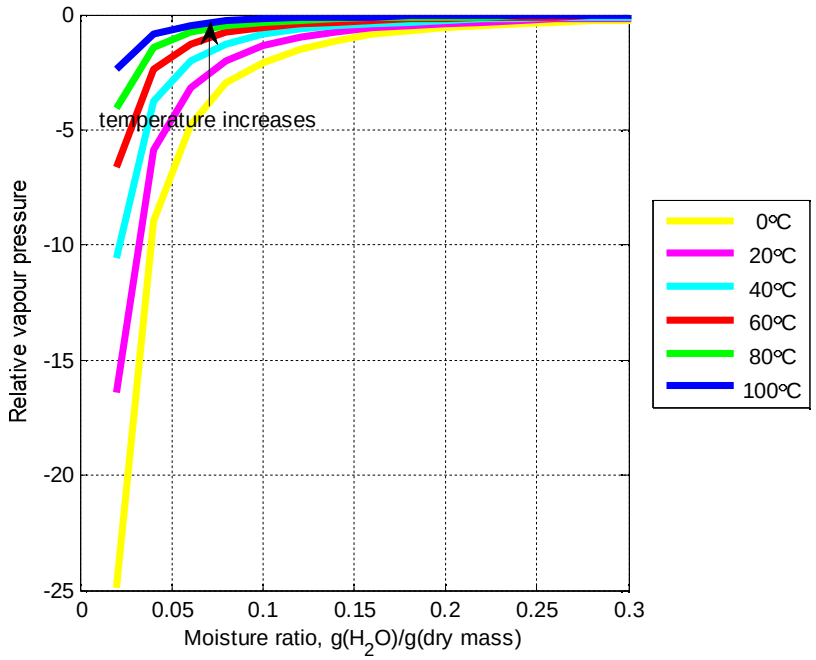


*Figure 20. Relative vapour pressure (ln p) as a function of moisture ratio for different temperatures [48].*

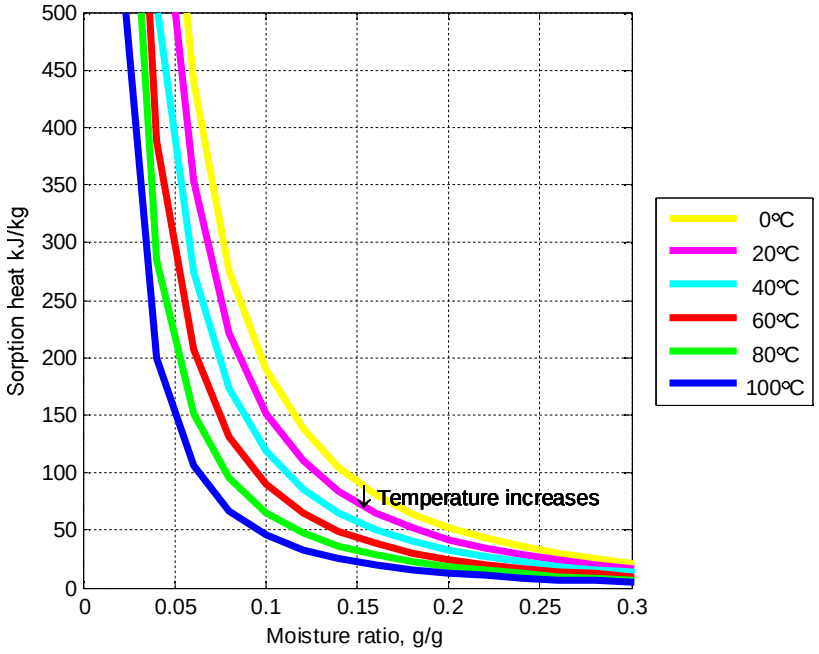


*Figure 21. Sorption heat as a function of moisture ratio for different temperatures [48].*

When the surface energy of the liquid is known, its pressure and also the capillary pressure can be calculated. It is given by [48, 49]

$$\mu_{2s} = \frac{RT}{M_3}\ln p - \left(T + \frac{T_{cr} - T}{A_3 + 1}\right)\cdot\left(\frac{r}{A_3}\cdot\frac{T_{cr} - T}{T^2}\cdot\frac{R\ln p}{M_3}\right), \qquad (45)$$

where $M_3$ is the molar mass of water.

### 3.1.5. Boundary conditions

When the processes relevant in impingement drying are described with numerical models, it is important to specify the boundary conditions imposed in each particular case considered. Here the main cases are described.
Paper in contact with heated cylinder: no water is allowed to move from paper to the cylinder.
Paper in contact with fabric: the temperature of air in paper is assumed to be the same as in the area on the other side of the fabric. The heat transfer coefficient through the fabric can be expressed in the form,

$$\alpha_f = \left( \frac{\kappa_f}{\kappa_f^{\max}} \right)^{\frac{\kappa_f^{\max} - \kappa_f}{\kappa_f^{\max}}} \cdot \alpha_{air}, \qquad (46)$$

where $\kappa_f^{\max}$ is the maximum permeability of the fabric, 25000 $m^3/m^2h$, and $\kappa_f$ is the permeability of the fabric ($m^3/m^2h$). This is a slightly different expression from the ones used before [53], but it eliminates the need to specify the thickness of the fabric. The heat transfer coefficient is shown in Figure 22 as a function of fabric permeability.

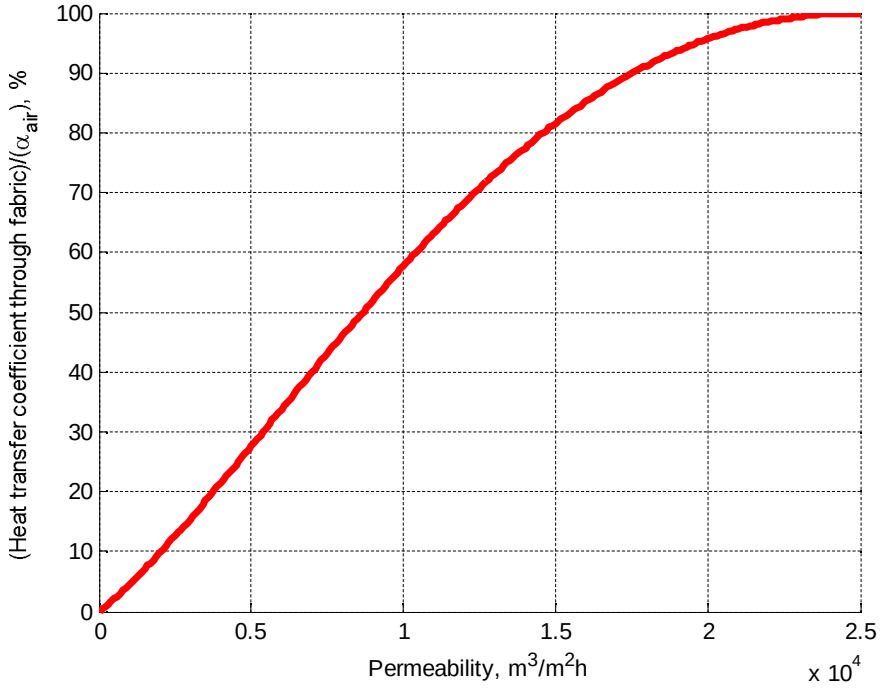


*Figure 22. Heat transfer coefficient as a function of permeability of the fabric. Note that the range of typical permeabilities is 1500-6000* $m^3/m^2h$.

The mass transfer coefficient of air can be expressed in the form

$$\beta_{air} = A \cdot \frac{\lambda}{L} \cdot \mathrm{Re}^{0.78} \cdot \frac{Le}{c_{pm}^{air}}, \qquad (47)$$

where Le is the Lewis number, Re the Reynolds number, $c_{pm}^{air}$ the molecular heat capacity of air (29.07 kJ/mol K), L the characteristic length of Le and $A$ = 0.01 a

fitted parameter [49]. The heat transfer coefficient (with dimension W/m·K) for free air can be expressed in the form

$$\alpha_{air} = A \cdot \frac{\lambda}{L} \cdot \mathrm{Re}^{0.78}. \quad (48)$$

These results are also valid in free draws when paper is in contact with free air. For impingement drying and float drying the Martin equation for the heat transfer coefficient is used with round and slot nozzles.

Boundary conditions are imposed on both sides of the paper, and, for example, in cylinder drying the boundary conditions are on one side those in contact with cylinder and on the other side those in contact with fabric. In a two-tier configuration there exists also a short distance with cylinder conditions on one side and free draw conditions on the other side. With impingement through a fabric there is a reduction in the heat transfer coefficient because the fabric must be included, and it should be verified that Eq. (40) can be used.

## 3.2. The numerical method of solution

The coupled heat and mass transfer in drying of paper is described here by nonlinear differential equations, in which the characteristics of the studied system depend on moisture and temperature. Solving these equations can be tedious, having the need first to separate variables so as to get linear equations and then to use boundary conditions for finding the needed parameter values. However, these equations can be solved by determining the coefficients shown earlier in sections 3.1.1 and 3.1.2 using finite-difference methods in one-dimensional (1D) geometries. There are analytical solutions for some equations, but these solutions are restricted to simple geometries and boundary conditions, and cannot thus be applied here.

In this work, the boundary conditions included complex time-dependent processes and, thus, finite-difference methods were used in solving the combined heat and mass transfer in the drying model. An explicit method called the *forward-difference approximation to the time derivative* was used. Since the resulting values were dependent on moisture and temperature, the required time step, *dt*, needed to be small compared to the timescale related to changes in temperature and moisture. Otherwise there may have arisen unrealistic and undesired oscillations due to the rate of temperature change being much larger than the rate of moisture change.

Selection of the time step depended on the magnitude of the spatial step *dx* and also on the values of some other parameters. They are not discussed here in detail, but a short note is made. An upper limit to the time step can be estimated assuming that simulation of effects in a “cubicle” of a given size *dx* was wanted, so $dx/(dt \cdot \textit{web speed}) \approx 1$ and this leads to a maximal time step of

$3.3 \cdot 10^{-5}$ s for 0.1 mm thick paper divided into ten layers of equal thickness, when the machine speed is 1800 m / min.

The mass balance equation

$$\rho_1 \frac{\partial u}{\partial t} = \frac{\partial}{\partial x}\left( \frac{k_2}{\nu_2} \frac{\partial p_2}{\partial x} + \varepsilon_b \cdot \frac{M_3}{RT} \cdot D_{34} \cdot \frac{\partial p_3}{\partial x} \right), \tag{49}$$

can thus be approximated by

$$\begin{aligned} \rho_1 \cdot \frac{u(i,n+1) - u(i,n)}{\Delta t} = {} & \frac{1}{(\Delta x)^2} \cdot \left\{ \frac{k_2(i+½,n)}{\nu_2(i+½,n)} \cdot [p_2(i+1,n) - p_2(i,n)] - \frac{k_2(i-½,n)}{\nu_2(i-½,n)} \cdot [p_2(i,n) - p_2(i-1,n)] \right\} + \\ & \frac{M_3}{R(\Delta x)^2} \left\{ \frac{\varepsilon_b(i+½,n)}{T(i+½,n)} \cdot D_{34}(i+½,n) \cdot [p_3(i+1,n) - p_3(i,n)] \right\} + \\ & \frac{M_3}{R(\Delta x)^2} \left\{ - \frac{\varepsilon_b(i-½,n)}{T(i-½,n)} \cdot D_{34}(i-½,n) \cdot [p_3(i,n) - p_3(i-1,n)] \right\}, \end{aligned} \tag{50}$$

where the spatially varying permeability coefficient $k_2$ for water is given by

$$k_2\left(i+\frac{1}{2},n\right) \equiv \left[ \frac{k_2(i+1,n) + k_2(i,n)}{2} \right], \; k_2\left(i-\frac{1}{2},n\right) \equiv \left[ \frac{k_2(i,n) + k_2(i-1,n)}{2} \right]. \tag{51}$$

Similar expressions apply also for the kinematic viscosity ($\nu_2$) of water, diffusion coefficient of vapour ($D_{34}$) and effective diffusion resistance ($\varepsilon_b$) in the air-vapour mixture. The explicit solution method was applied to the equations (4), (8), (13), (15), (19), (36) and (49) [96].

Similarly, the energy balance equation

$$\rho_1 \cdot c_p \cdot \frac{\partial T}{\partial t} = l \cdot \frac{\partial}{\partial x}\left( \varepsilon_b \cdot \frac{M_3}{RT} \cdot D_{34} \cdot \frac{\partial p_3}{\partial x} \right) + \frac{\partial}{\partial x}\left( \lambda \cdot \frac{\partial T}{\partial x} \right) \tag{52}$$

can be approximated by

$$\begin{aligned} \rho_1 \cdot c_p \cdot \frac{T(i,n+1) - T(i,n)}{\Delta t} = {} & l(i,n) \cdot \frac{M_3}{R(\Delta x)^2} \cdot \left\{ \frac{\varepsilon_b(i+½,n)}{T(i+½,n)} \cdot D_{34}(i+½,n) \cdot [p_3(i+1,n) - p_3(i,n)] \right\} + \\ & l(i,n) \cdot \frac{M_3}{R(\Delta x)^2} \cdot \left\{ - \frac{\varepsilon_b(i-½,n)}{T(i-½,n)} \cdot D_{34}(i-½,n) \cdot [p_3(i,n) - p_3(i-1,n)] \right\} + \\ & \frac{1}{(\Delta x)^2} \{ \lambda(i+½,n) \cdot [T(i+1,n) - T(i,n)] - \lambda(i-½,n) \cdot [T(i,n) - T(i-1,n)] \}, \end{aligned} \tag{53}$$

in which the thermal conductivity $\lambda$ of paper is evaluated (*i.e.* $\lambda\left(i+\frac{1}{2},n\right)$ and $\lambda\left(i-\frac{1}{2},n\right)$ with an expression similar to Eq. (51).

Now the information of moisture and temperature together with paper properties at the first timestep (*n=0*) needs to be given as the initial data. The first element of paper (*i=1,* paper bottomside) in the thickness direction can be, for example, in contact with a cylinder surface, and the $i^{th}$ (paper topside)

element in contact with a porous fabric. The mass of these edge elements is chosen to be a half of the mass of the internal elements.

## 3.3. Experimental methods

It is clear that simulations cannot be done without experiments and suitable devices are needed to make proper estimation of the properties of the drying process described in this work. Two types of devices were used for experiments that were done to determine the drying rate, temperature and moisture gradients inside the paper web. Results found by using these devices for the drying rate were consistent with those of simulations for similar boundary conditions. Experimental evaluation of the drying rate and heat transfer makes it possible to estimate the energy consumption on a mill scale [12, 160] using e.g. Balas-simulations [21, 63].

### 3.3.1. Drying rate measurements

A comparison of different drying methods is given in Ref. [43]. For this study a small-scale drying rig called the Combo system (Figure 23 and Figure 26) was built, which could be modified for different drying geometries and could utilize either a hot surface or hot air for drying. In the device the paper is placed on the cylinder surface (which is a curved brass plate with two K-type thermocouples for temperature control and a 1 kW heater) and the fabric is placed on top of the paper with fabric tension controlled using tensioned springs. Fabric tension was 1.5 kN/m whereas the typical fabric tension level in a modern paper machine is 3-4 kN/m, thus the tension used in these experiments does not prevent shrinkage totally. The paper is moved back and forth under the impingement hood. The impingement heating power is 45 kW.

A typical geometry for impingement through a fabric on a cylinder is shown in Figure 24. Four drying configurations were studied both experimentally and through simulations. These configurations are shown in Figure 34. The impingement hood temperature of the rig can be raised up to 350°C and the impingement air velocity up to 150 m/s. The cylinder surface temperature can be raised up to 160°C. Geometry of the impingement nozzle was quite typical of the commercial devices the open area was 1.5% and the distance from paper was 25 mm. In the configurations with a heated cylinder, paper samples were placed between a heated plate and a drying fabric. A piece of forming fabric with dimensions exceeding those of the paper was also placed between the plate and the sample so as to prevent wetting due to condensation when tests using a cold plate were performed. The impinging jet temperature was kept at 200°C and the air speed at 90 m/s. The heated plate was kept either at a temperature of 130°C or at room temperature. This surface temperature was higher than conventionally in paper making. The fabric used in the tests was a

commercial synthetic drying fabric with a permeability of 6,500 $m^3/m^2/h$. The paper used in the tests was fine paper with a basis weight of 60 $g/m^2$ (bone dry) [43].

Samples were dried from 50% solids content, typical of a sheet after wet pressing, to a final solids content of 95% The drying rate was determined per the actual contact area. The experiments performed consisted of a total of 2286 trial points in the set of parameters. The drying rate was measured at each point. In addition, in some of the experiments the curl and elastic properties were also determined.

*Figure 23. Combo system in the impingement drying mode.*

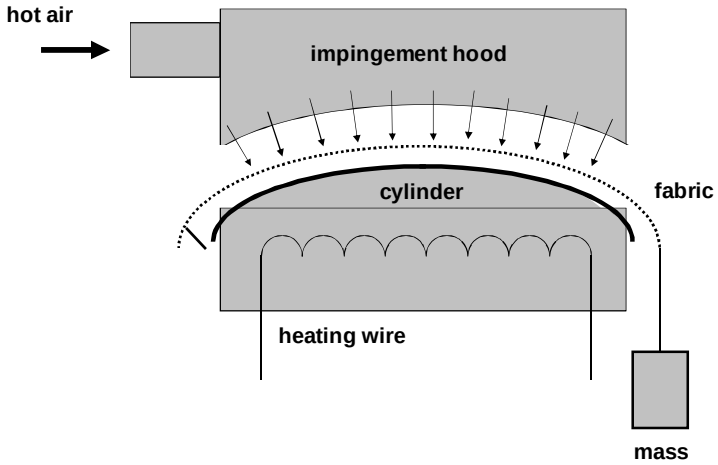


*Figure 24. A schematic view of impingement drying in a cylinder geometry of the Combo system.*

The experimental procedure was such that a paper sample was first placed on a hot metal plate (cylinder) which was then covered with a fabric. In Figure 24 the mass at the end of the fabric illustrates the tension created on the fabric using springs of known tension. Then the paper stressed over the hot plate was

moved into the impingement drying unit using a linear conveyor. The drying rate was determined by weighing the sample before and after drying. Due to manual handling between weighing of the sample before and after drying, adjustments to sample's dwell time on the cylinder were made in each test run of impingement drying.

Test runs with the Combo system were reproduced in Metso Research Center in Turku, Finland with an experimental setup (Figure 25) that could be used to study both a running web as well as sheet samples. In experiments sheet samples with two basis weights were used to measure the effect of basis weight on the drying rate (Figure 38), and the temperature change in the paper (Figure 35) and in the cylinder (Figure 37) during drying. The test rig consists of an air-heated Ø 400 mm cylinder enclosed in a hood, a motor with variable speed drive, a blow box for fabric heating, an impingement box under the cylinder and a system for adjusting the fabric tension. The fabric wrap angle was 270° and that of the impingement hood 180°. An impingement box was placed inside the cylinder for cylinder heating, instead of electrical or steam heating. The temperature of the cylinder was measured with three Pt100 temperature sensors embedded into the cylinder surface. The cylinder temperature was kept at 100 °C. An inverter-controlled gear motor was used for running the cylinder. The maximum available cylinder speed was 50 m/min. The fabric tension was adjusted by adding weight to the specially designed box. The dimensions of the investigated fabrics were 300 mm in width and 4270 mm in length. The fabric permeability was 5500 $m^3/h/m^2$. An impingement box was assembled below the cylinder at a distance of 25 mm from the fabric. Hot air at 200 °C temperature and 90 m/s velocity was blown through the fabric to the paper. Three different configurations of the dryer were tested, all representing contact drying; impingement drying through the fabric, in which the paper was insulated from the cylinder by an additional fabric between the paper sample and the cylinder, and combined drying, in which the paper was first dried only by contact drying, after which the combined drying was started in the impingement hood area. Handmade paper sheets with two basis weights (50 and 150 $g/m^2$) were used in the drying rate measurements. Drying rates for contact drying, impingement drying and combined drying were obtained by weighing samples before and after drying using a scale. Drying was repeated for five sheets under the same conditions, and the results were given as averages over these individual measurements.

*Figure 25. Experimental drying device in Metso Research Center in Turku, Finland.*

### 3.3.2. Temperature and moisture gradient measurements

To achieve proper boundary conditions for the control of temperature and moisture in the paper, simultaneous measurements of the evolution of these quantities during drying was needed. Moisture measurements have earlier been done in the thickness direction of paper [59, 61, 164, 165]. In this work a fast and simple measurement technique was realised. Figure 26 shows the related modification in the Combo system. Results for the modified Combo system are reported in [166] (see Appendix IV) and shown in Figure 41. Multilayered samples made of handmade sheets were used in these temperature measurements. The internal temperature of the sample during the drying process was measured by thin K-type thermocouples of 25.4 μm in diameter. Thermocouples were sandwiched between wet paper sheets after which the stack of wet sheets was pressed to obtain a homogeneous structure and to remove the extra water. Paper samples with a basis weight of 150 g/m$^2$, made of four handmade sheets and three thermocouples at different locations were used. The top and bottom layers of the stack were sheets with a basis weight of 15 g/m$^2$ and the two middle layers were sheets with a basis weight of 60 g/m$^2$. In the 50 g/m$^2$ sheets, 25 g/m$^2$ layers were used, and an example of such measurement is shown in Figure 35. The measured data were collected with a Hewlett Packard 34970 data acquisition logger and exported to PC files. The output data were analysed using MS Excel.

Moisture measurement system using a near-infrared spectral camera

The measurement of moisture with near-infrared spectroscopy is based on exciting vibrations of water molecules, and the absorption they thereby cause in the NIR spectral region. The spectral bands of water observed in the NIR spectral range are 970 nm, 1200 nm, 1440 nm, and 1940 nm. Determination of the amount of water is done by determining the area under the water absorption band after subtracting the baseline absorbance. The cellulose band can be used for normalisation of the transmission measurement at lower moisture levels. Laboratory calibration of the system was done by stacking handsheets and placing a thin PE-film between the layers. Locations of the wet layer(s) were changed during the calibration procedure. Fine paper furnish was used to make handsheet samples of 25 $g/m^2$ in the calibration phase and 69 $g/m^2$ (3x23 $g/m^2$) samples were used in the drying experiments (the same furnish) with a dry density of 430 $kg/m^3$ and an initial moisture of 28%. The furnish was a mixture of eucalyptus (75%) and pine (25%). The moisture level of each sample was determined by weighing it before and after drying. During the calibration phase, PE-films were used to prevent moisture movement from one paper layer to another, so that accurate information of the moisture in each layer was available. The sample stack was placed between glass plates during the measurement, so that any possible air between samples was removed. Calibration must be done separately for each furnish, as in all IR-based measurements. The RMS error was less than 2% in each layer of large area, and if the measured area was smaller, the RMS error was less than 1%. In these measurements the impingement distance was 50 mm. Samples with a size of 161 mm x 161 mm were dried from 28% solids content to dry (95% solids content). Temperature data from thermocouples were gathered using an Instrunet I100 data acquisition box, which had an accuracy of 0.6°C, and an Instrunet I230 Controller card. Data were gathered at a rate of 25 Hz using the InstruNet World (iW) software on a HP Compaq nc8000 (1.6 GHz) with 1 GB of ram and in the results presented here, filtering of the data was used. The filtering time was 1 s. Data was analysed using Matlab (R2006b) [56].

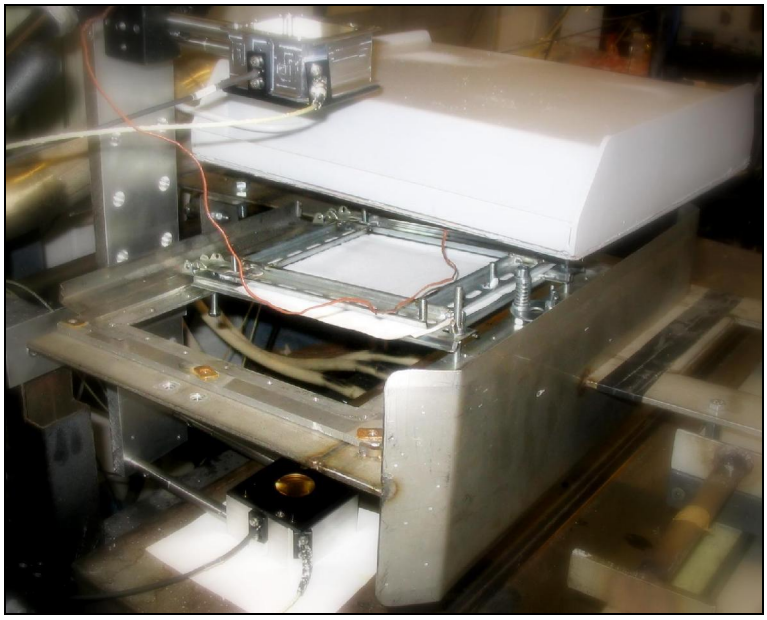

*Figure 26. Combo system in a moisture gradient measurement.*

The results given in Ref. [56] indicate that, during drying there exists a significant gradient in the z-directional moisture profile, with a variation in the moisture content of up to 25-35% across the thickness of the sheet, depending on the drying conditions. Moisture content variation of similar magnitude was observed in both measurements and in numerical simulations. Information of about the moisture gradient is needed to improve the existing drying models as well as to help to improve our understanding of the drying phenomena and their effects on the paper structure. Measured information of moisture gradients in paper during fast drying processes had not been available before these measurements.

### 3.3.3. Structural measurements with X-ray tomography

After drying, the structure of a set of samples was analysed by X-ray tomography. The X-Ray tomography device used to scan the samples was Skyscan 1172 (μ-CT), capable of measuring various structures from biomedical to geological materials and electronic components. With this device it is possible to acquire internal images in 3D of the sample without damaging its structure. The camera has 4000 by 2000 pixels and the minimum pixel size in the reconstructed images is 0.9 μm. The maximum acceleration voltage is 100 kV, and this was used in the measurements reported here. The spot size at X-rays is less than 5μm, and the used power is at most 4W. Images of stacks of samples were made in order to reduce the time needed for imaging.

The number of samples used in one stack was 8 and they were separated using papers between them in both end of narrow paper strip. Stacks were fixed using fast epoxy glue. Glue was also used to mount the stack on the acrylic holder that was used to place the samples in the imaging chamber of the X-ray device. Images gathered were reconstructed using the Nrecon-software (v.1.43)

on a PC-cluster. It consisted of four Intel XEON 3.2 GHz processors. The reconstruction time for one image was approximately one night. The pixel size was 1.04 µm for samples of 2 mm by 2 mm close to the maximum resolution available with this device. Visualisation and analyses of the 3D images were made using ImageJ (v.1.37 and Java 1.5.0_06).

### 3.3.4. Other measurements

Formation was analysed using a Fuji Formation scanner and surface topography using a profilometer. Formation was measured using ß-radiography, based on the decay of $^{14}C$. For these measurements the activity of the $^{14}C$-source was 1,18 GBq. The device used in this measurement was a Fujifilm Bas-1800 II Storage Phosphor Imaging System with a 100 µm pixel resolution. Formation maps were obtained from these measurements. The resolution in the x and y direction was 1/10 mm (the size of analysed paper was 100 mm by 100 mm). Surface deviations were also measured using an optical, non-contact profilometer (AltiSurf 500), with a measurement area of 10 mm by 10 mm. Data from the profilometer were filtered using a 2 mm filter, and 5% of the edges of the histogram were discarded. Values for Ra, Rsk and Rq were determined in this study. Ra is the average of the absolute values of the surface height deviations as measured from the best fitting plane. When calculating the Rq value, the amplitudes of peaks and valleys are squared. (Rq is the standard deviation of the height distribution.) Because Rq involves squared amplitudes, it is more sensitive to peaks and valleys. Rsk is a measure of the "skewness' or in other words the symmetry of peaks and valleys in the surface.

Fibre level analysis (Fibermaster analysis) was used to evaluate fibre level properties. Fibermaster measurements were made only once on reslushed sheets [70].

Curl was measured using the modified Xerox-curl method, where samples' edge displacement is transferred to an average curl radius. Averages of 10 samples were used in these measurements.

Other standard paper analyses were also made.

# 4. RESULTS AND DISCUSSION

The main findings reached at the laboratory level, which indicate the potential of increasing the drying rate, are shown in this section. The methods and devices used in this work were described in the previous section. Some aspects of paper properties are also discussed here, mainly from the drying point of view. This viewpoint was adopted as many paper properties develop during drying, and the whole field is too large to be covered thoroughly here.

## 4.1. Paper properties

### 4.1.1. Adsorption and desorption

Fits to experimental data were made using the Soininen model described (see Equation 21) and related results are shown in Figure 27. It is evident that adsorption-desorption curves can be fitted with this model, and the adsorption / desorption values obtained can be used to estimate the adsorption / desorption behaviour also for different filler contents. A result of such an analysis is shown in Table 3.

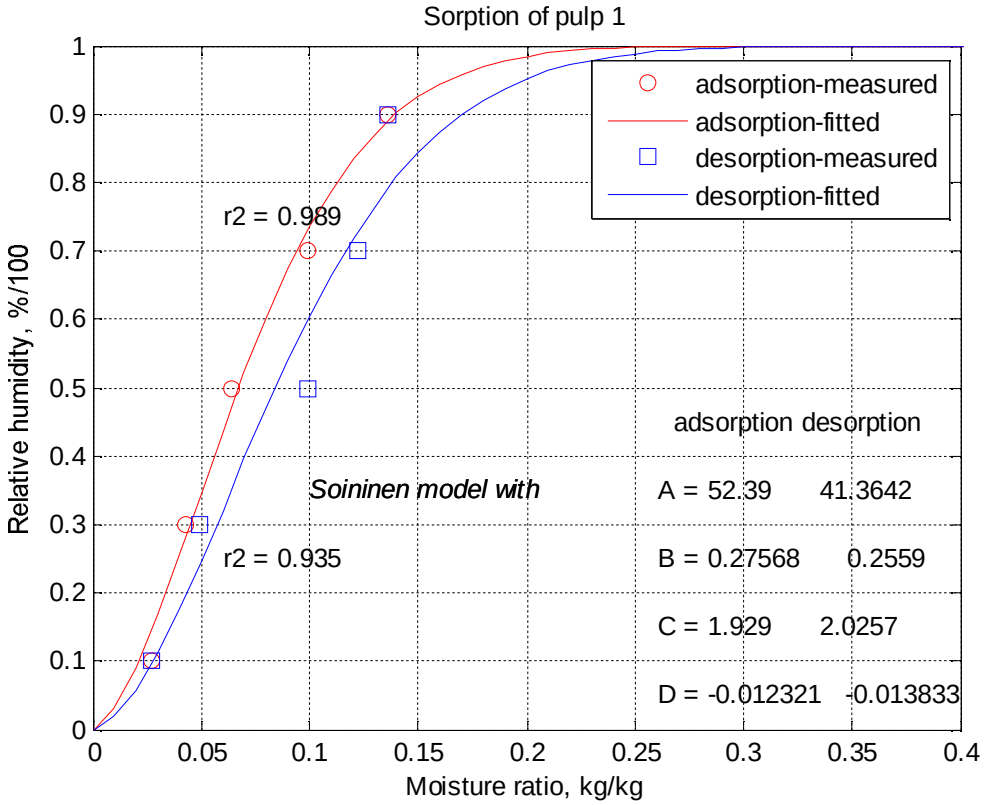


*Figure 27. Adsorption (a) and desorption (b) of water by fibre material and corresponding results (full curves) of the Soininen model fitted to the measured results. The temperature of the system was 23°C, and the paper was made of chemical birch pulp with a filler content of 10%(unpublished).*

The estimated effect of filler content using the measured data of Figure 27 is shown in Table 3. Here the filler was assumed to be inert to moisture. An increase in the filler content increases parameter A, meaning that a paper with higher filler content reaches lower moisture ratio under same relative humidity.

*Table 3. Effect of filler content on the fitted parameter values of the Soininen model (unpublished).*

| | Adsorption | | | | Desorption | | | |
|---|---|---|---|---|---|---|---|---|
| Filler content | A | B | C | D | A | B | C | D |
| 5 % | 52.4 | 0.276 | 1.93 | -0.0123 | 41.4 | 0.256 | 2.03 | -0.0138 |
| 10 % | 58.4 | 0.301 | 1.91 | -0.0111 | 47.9 | 0.213 | 2.02 | -0.0135 |
| 15 % | 66.0 | 0.290 | 1.89 | -0.0099 | 53.7 | 0.231 | 2.00 | -0.0122 |

### 4.1.2. Porosity of paper

Publication [70] focuses on the changes in the structure and quality of paper caused by varying drying conditions, *i.e.* contact drying, impingement drying or combination of these. The main interest was in the mechanical properties and detailed characterization of the structure of fine paper, and the methods used

included microtomography, high resolution formation measurements as well as several standard methods. It was found e.g. that, by changing the drying conditions such that paper was cooled during the drying process, its elastic properties and surface smoothness could be improved.

Paper is under these drying conditions considered as a mixture of three material phases: the solid, liquid and gas phase. The solid phase consists of fibres and fillers, water comprises the liquid phase and moist air forms the gas phase. The network structure changes when drying proceeds. Defining the porosity of the network as the total volume subtracted by the fraction filled by the solid phase it can be found that

$$\varepsilon_p = 1 - \left(1 - f_{filler}\right)\frac{\rho_{ds}}{\rho_f} + f_{filler}\frac{\rho_{ds}}{\rho_{filler}} - u\frac{\rho_{ds}}{\rho_w}, \tag{54}$$

where $\rho_{ds}$ is the density of paper, $\rho_f$ the constant fiber density of 1500 kg/m$^3$, $\rho_w$ the constant water density of 1000 kg/m$^3$, $f_{filler}$ the filler fraction (the density of PCC is assumed to be $\rho_{filler}$ =2710 kg/m$^3$) and $u$ is the moisture ratio. Figure 29 shows the effect of moisture on porosity for varying density of dry paper. Porosity varies in the interval 0.4-0.8 for dry paper densities of 300 - 900 kg/m$^3$. For a filler content of 10%, the porosity range is 0.5-0.83. It is evident that also the paper thickness must change during drying. For increasing moisture content the thickness is as well increased. In other words, in most cases, paper thickness decreases during drying. This result was also found by Gallay [37]. Density is the ratio of the basis weight and thickness of paper, and its inverse is the specific volume or bulk. The effective density is determined such that surface roughness effects are excluded from the volume. Volume is typically estimated by measuring the thickness and lateral dimensions of the sample.

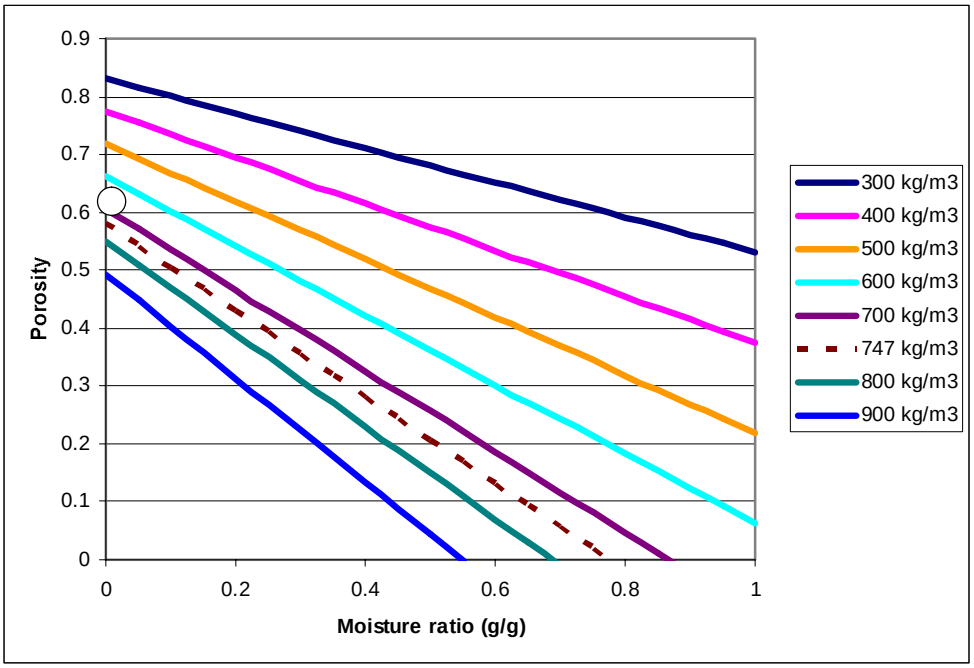


*Figure 28. Porosity as a function of moisture ratio for varying dry paper density. Dashed line shows the density for 10% PCC content in 77 g/m² paper with a thickness of 103 µm, and a porosity of 0.632 (shown by a circle). Difference between the dashed line and circle can be explained by the thickness measurement method (paper is compressed with a 100 kPa pressure during the measurement). For a porosity of 0.632 (0.05* g/g *moisture content), the thickness should be 128* µm.

Porosity was also determined experimentally for a fine paper of 77 g/m² basis weight, and the result is shown by a circle in Figure 28. The fibre wall density is probably a little higher than 1500 kg/m³, perhaps 1600-1650 kg/m³, because the bulk density of the sample was about 670-680 kg/m³, *i.e.* higher than Figure 28 suggests. This difference may have caused by the estimated effect of filler content and uncertainties in the thickness estimation, *i.e.* uncertainty in the density. Pore structure refers here to the void space between fibres, not in the cell wall. The fibre wall pores that are closed first during drying do not reopen when the fibres are treated again with water, while the pores that are closed during later stages of drying do reopen by adding water [168]. Also, it can be noted here that densities and porosities of coatings are in the range 1630-1710 kg/m³ and 25-30%, respectively [84], so for coated paper the measured (apparent) density of fibre wall is seemingly increased.

### 4.1.3. Drying and its effect on shrinkage and tensile properties

Let us consider macroscopic structural effects that occur during drying when the removal of water causes many properties to alter quite dramatically. The structure of the paper network can be illustrated by x-ray microtomography as described in publication [70]. A tomographic reconstruction of a paper sample is shown in Figure 29.

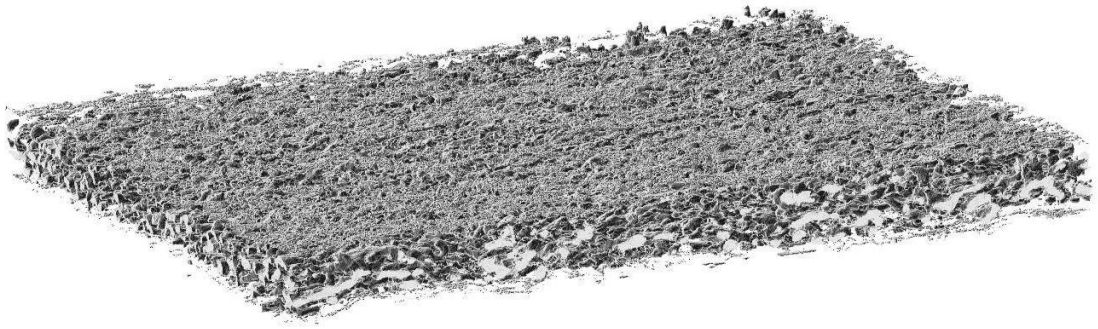

*Figure 29. A tomographic reconstruction of a paper sample based on x-ray microtomography. Sample size was 1x1 mm², and the voxel resolution was 1 µm [70].*

As discussed above, prevention of shrinkage can improve tensile properties of paper. The effect of shrinkage and drying on the optical properties are not discussed here, although it is clear that such effects exist.

Experimental results indicate [70] that the structural changes that appear in paper during drying are affected by the drying conditions. Contact drying with and without hot air impingement was investigated at different temperatures. The main focus was on relating mechanical properties to the detailed structure of the paper and the constituent fibres as measured by methods such as x-ray microtomography, high resolution formation measurements and standard paper analysis methods. When paper was dried under different drying conditions, with shrinkage prevented, significant differences were observed in the surface roughness and elastic properties (Table 4). The drying time also influenced the development of the tensile properties during drying, the faster was the drying the better was the tensile index obtained (Figure 30). This was shown (unpublished) by drying paper (handsheets) with similar shrinkages between fabrics for varying drying rate (using impingement through fabric). This result means that savings can be made in raw materials.

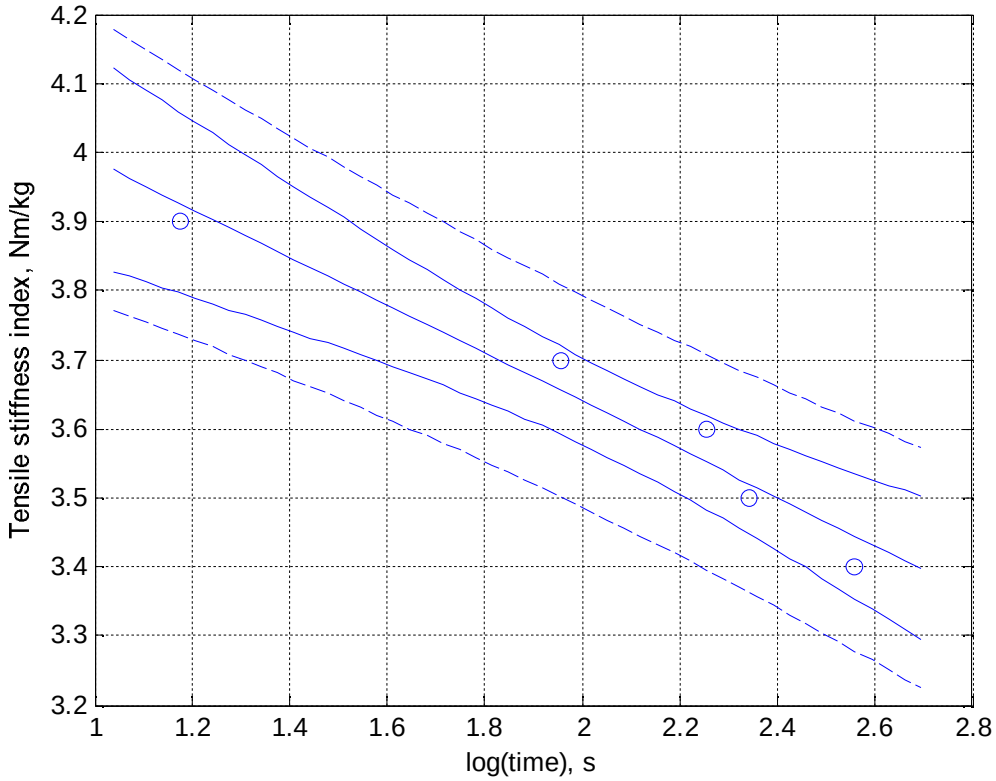


*Figure 30. Tensile stiffness index as a function logarithm of the drying time for samples of similar shrinkages during drying (95% confidence limits are also shown: solid lines are for changes only in the y-direction, dashed lines for confidence when changes appear in both directions).*

The possibility to control paper properties during drying arises through control of the drying temperature and drying time. Stresses introduced during drying are irreversible, and they depend on parameters that can be adjusted.

Measurements of porosity and fibre wall thickness have not indicated noticeable dependence of these quantities on the drying conditions. Changes that appear are rather related to properties like bonding of fibres. One of the practical results of this work is that the elastic properties and surface smoothness of paper can be improved by lowering the paper temperature during drying. Effects of drying conditions on various paper properties are shown in Table 4.

*Table 4. Properties of fine paper depending on the drying methods applied [70]. Applied drying methods were cylinder drying with cylinder temperature $T_c$=80°C and $T_c$=120°C and cylinder+ impingement drying with cylinder temperatures 80°C and 30°C, with impingement temperature of 20°C.*

| Sample | $T_C$=80°C+ $T_I$=20°C | $T_C$=30°C+ $T_I$=20°C | $T_C$=80°C | $T_C$=120°C |
|---|---|---|---|---|
| Porosity | 0.631 | 0.633 | 0.681 | 0.632 |
| Mean thickness | 77±11 | 77±10 | 78±11 | 82±11 |
| Min thickness | 0 | 0 | 0 | 0 |
| Max thickness | 150 | 145 | 125 | 167 |
| SCAN(mean) | 103±1 | 103±4 | 104±3 | 104±3 |
| Rq, BS | 11.4 | 10.6 | 8.1 | 8.4 |
| Ra, BS | 7.4 | 8.3 | 6.3 | 6.3 |
| Rsk, BS | 6.6 | 1.1 | 0.4 | 0.5 |
| Rq, TS | 10.1 | 10.6 | 7.6 | 7.8 |
| Ra, TS | 7.6 | 8.4 | 5.8 | 5.8 |
| Rsk, TS | 1.0 | 1.0 | 0.8 | 2.7 |
| Mean Rouhgness, Bendtsen, TS | 1143±120 | 1005±51 | 940±16 | 932 |
| Mean Rouhgness, Bendtsen, BS | 712±12 | 632±90 | 500±48 | 494±0 |
| Permeability, Bendtsen [ml/min] | 346 | 309.5 | 334 | 377.5 |
| Coarseness [µg/m] | 144 | 144 | 144 | 144 |
| Coverage [layers of fibers] | 12.7 | 12.7 | 12.7 | 12.7 |
| Simulated max. paper temperature during drying | 57±1 | 25±1 | 79±1 | 97±1 |
| Drying time | 35±1 | 120±1 | 120±1 | 30±1 |
| Tensile Strength X1 (N/m) | 2957±119 | 3036±128 | 2960±128 | 2911±81 |
| Tensile Index (Nm/g) | 37.0±1.5 | 38.0±1.6 | 37.0±1.6 | 36.4±1.0 |
| Energy to Break Z1 (J/m²) | 63.7±10.3 | 71.2±11.2 | 59.5±11.5 | 48.5±6.8 |
| Energy to Break Index Z2 (mJ/g) | 0.8±0.1 | 0.9±0.1 | 0.7±0.1 | 0.6±0.1 |
| Strain at Break % (mJ/g) | 3.1±0.4 | 3.4±0.4 | 2.9±0.5 | 2.5±0.3 |
| Modulus of Elasticity E (N/mm²) | 3294±212 | 3341±152 | 3293±314 | 3135±283 |
| Tensile stiffness index (Nm/kg) | 4.2±0.1 | 4.3±0.1 | 4.2±0.1 | 4.0±0.1 |
| Shrinkage, % | 1.4±0.1 | 1.4±0.1 | 1.2±0.1 | 1.1±0.1 |

### 4.1.4. Curl of paper

Theoretical aspects related to moisture gradients in the thickness direction of paper and the influence of such gradients on curl were discussed in publication [45] (see Figure 31). Curl was also modelled [42]. The edge displacement (or curl) was found to be the greater the faster was the drying, see Figure 32. Curl can be controlled by either controlling the drying conditions in one-sided drying or by combining different drying techniques. If conditions inside the paper are symmetrical during the drying process, the paper remains planar. These properties provide one possibility to improve and control the quality of paper by means of drying conditions. Such control is based on controlling the moisture and temperature profiles inside the paper during drying.

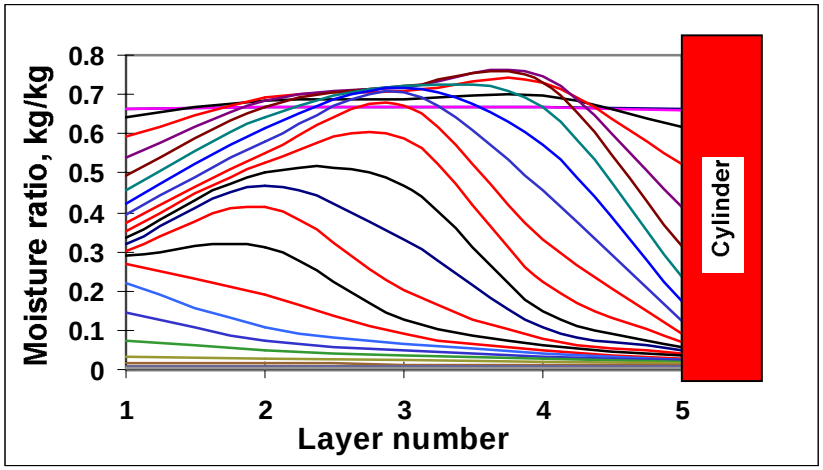


*Figure 31. Moisture gradients inside paper during cylinder drying [44].*

The main cause for formation of curl was found to be a moisture gradient inside the paper, shown in Figure 31 for the case of cylinder drying.

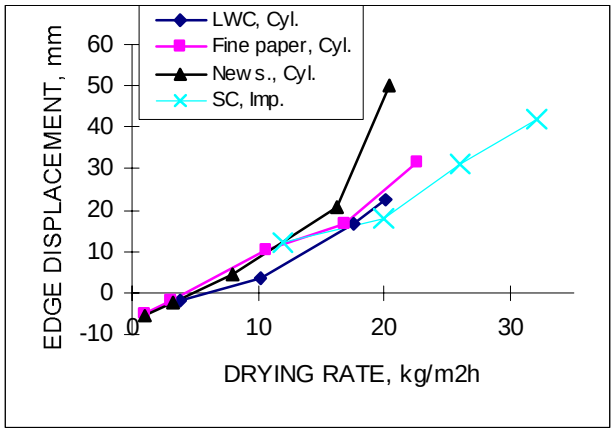


*Figure 32. Edge displacement (or curl) as a function of drying rate [170].*

An index was introduced to estimate the formation of curl during drying, based on the difference of moisture between the top and bottom surface layers. An example of the curl index as a function of surface temperature is shown in Figure 33.

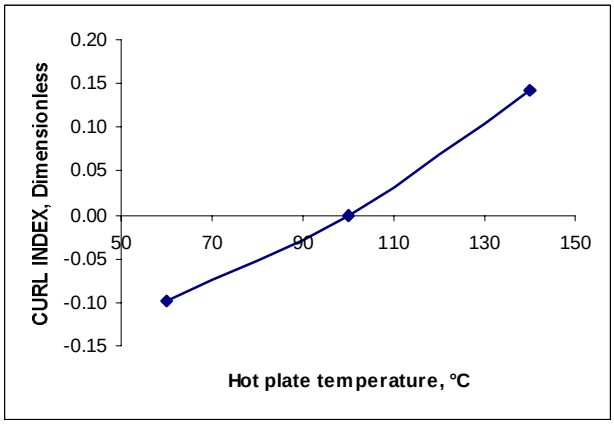


*Figure 33. Curl index as a function of surface temperature of the cylinder in a laboratory drying of paper.*

The analysis presented publication [45] showed that curl is determined by the symmetry of the moisture profile inside the paper, the drying method does not affect the curl as long as the symmetry of the drying rate remains the same. Paper curls towards the side that remains wet longer, and curl can vary depending on the paper grade for the same conditions because of differences in the paper structure. Curl can be controlled by either altering the drying conditions and/or combining different drying techniques, e.g., cylinder drying and impingement drying. If moisture gradients are controlled, shrinkage behaviour and drying stresses can be predicted, and the dryer section can be controlled so as to minimize the drying time and possible defects in paper quality.

Impingement intensifies drying, but it is also a tool for controlling paper properties, like curl, as discussed above. To this end four drying configurations were studied experimentally and through simulations. The drying geometries, drying rate and the related curls measured are shown in Figure 34 [43].

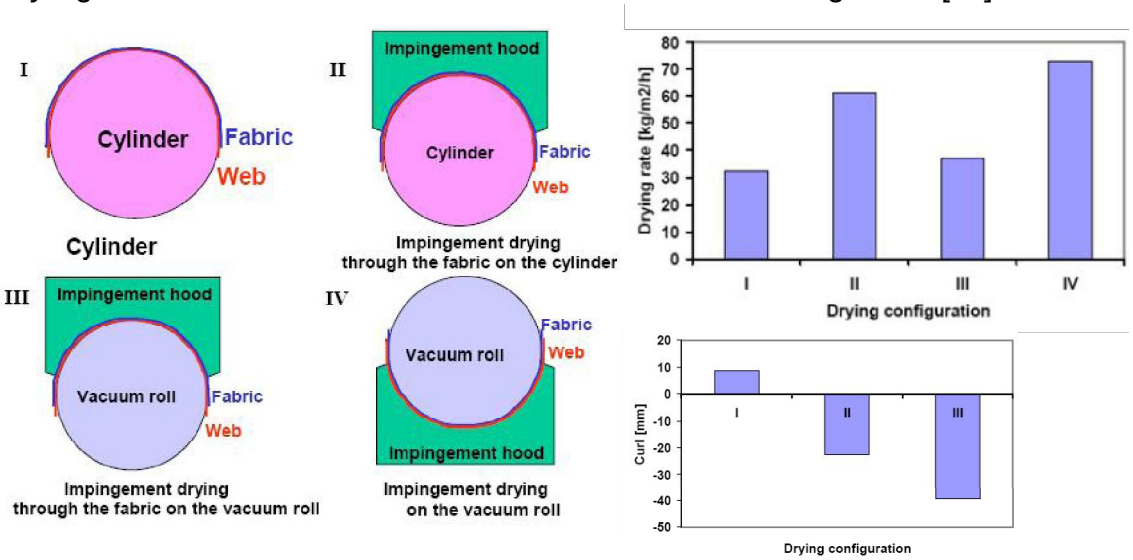


*Figure 34. Experimentally tested impingement-supported geometries. I:Conventional cylinder drying. II: Impingement drying through a fabric on the drying cylinder. III: Impingement drying through a fabric on the vacuum roll. IV: Impingement drying directly on paper on the vacuum roll.* $T_c$*=130°C,* $T_{imp}$*=200°C and* $v_{imp}$*=90* m/s.

The results of Figure 34 show the superiority of impingement drying with respect to the drying rate. Hot air impingement through a fabric on an unheated surface produced approximately the same drying rate as a conventional cylinder drying for given air speed and temperature. The barrier effect of the fabric was about 50 % compared to direct hot air impingement onto the web. The results also show that the combined effect caused by hot air impingent through the fabric and a heated surface will not reach the level one would expect by adding up the individual drying rates of these two systems. The barrier effect of the fabric seems to increase as the web temperature is increased. Impingement drying seems to produce a larger curl than cylinder drying. The

tests point out however that it is possible to control curl by bringing heat in a suitable way onto both sides of the web.

Impingement drying uses hot air as the drying medium. When the amount of impingement drying is increased, more and more hot air is required to replace steam. To this end biomass gasifying may present new opportunities. Low cost fuel compensates for the high investment costs associated with gasification. Increase in the drying rate can be found in wide ranges of impingement and cylinder temperatures [69, 119] as shown in Table 5.

*Table 5. Drying rates for different combinations of cylinder and impingement drying conditions [69, 119].*

| Drying method | Cylinder temperature (°C) | Impingement jet temperature (°C) | Impingement jet velocity (m/s) | Drying rate (kg/m²h) |
|---|---|---|---|---|
| cyl.(low) | 80 | | | 6.8 |
| cyl.(high) | 130 | | | 37.4 |
| imp.(low) | | 100 | 90 | 16.3 |
| imp.(high) | | 200 | 90 | 23.8 |
| cyl.&imp.(low) | 80 | 100 | 90 | 43.7 |
| cyl.&imp.(high) | 130 | 200 | 90 | 81.2 |

## 4.2. Combined drying

In publication [47] experiments performed with a dynamic laboratory-scale drying rig are described. Paper temperature distributions in the thickness direction and evaporation rates were determined. Three cases were compared: conventional cylinder drying, impingement through a fabric and combined cylinder-impingement drying.

### 4.2.1. Paper temperature

An interesting finding was that paper cools down when the impingement phase begins, as shown in Figure 35. Paper temperature drops down extremely fast as drying with impingement on a cylinder starts. This phenomenon was also observed when the temperature of the cylinder shell was measured (Figure 37). In combined drying paper will get dry quicker, and due to lack of moisture the temperature of paper increases faster at the end of drying than in impingement drying and cylinder drying separately, when the drying time is the same. Similar cooling of cylinder and web was also observed by Paltakari et. al. [29]. The increase of 15% found [29] was much less than the one reported in publication [42] due to the low cylinder temperature used in the latter experiments. The blow box geometries and direction of the airflow were also

different. Drying was also tested with air impingement perpendicular to the web [171], with an increase of 33% in the drying rate, but the cylinder temperature was lower than in the case of publication [42] The observed effects were also simulated numerically, and related results are shown in Figure 36. The simulation reveals that drying histories of layers are different from each other, centre of paper drying last. Thus, quality of paper may be different in different layers.

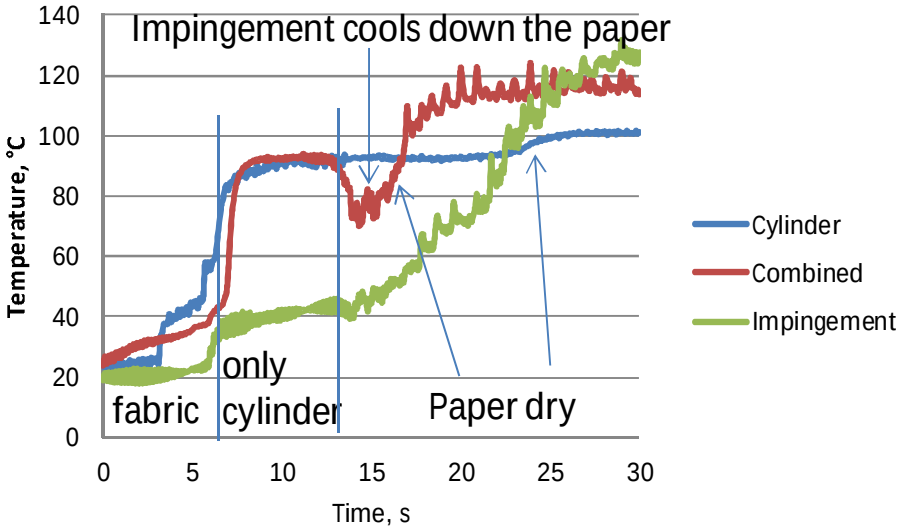


*Figure 35. Temperature measurements inside a paper of 50* g / m². *[42]*

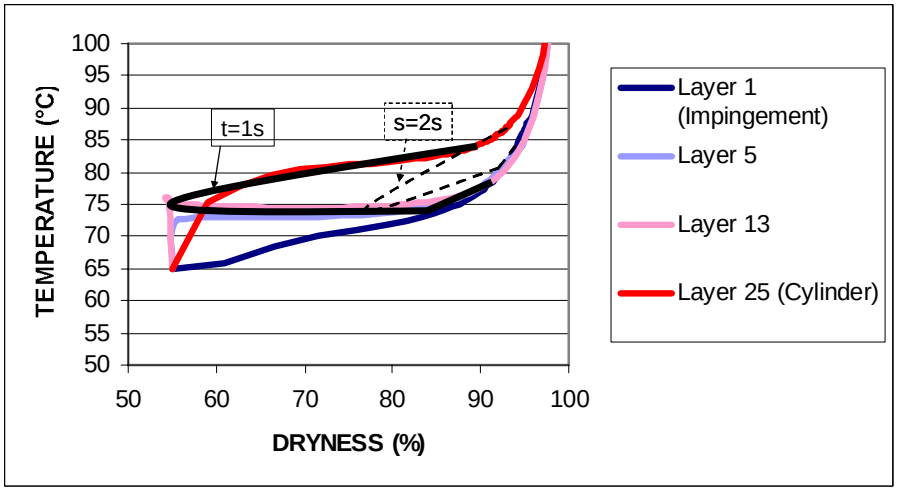


*Figure 36. Simulation of combined cylinder and impingement drying. Isochronous drying curves for 1* s *and 2* s *are also shown.*

### 4.2.2. Cylinder temperature

The cylinder cools also down extremely fast in the fast drying process (Figure 37). This clearly shows that more energy is obtained from the cylinder side of the paper due to an increased temperature difference between the paper and

the cylinder shell. This explains also why the drying process is so rapid, and provides direct evidence of the mechanism of increased heat transfer in combined drying. Publications [43, 47] are concerned with this part of the work.

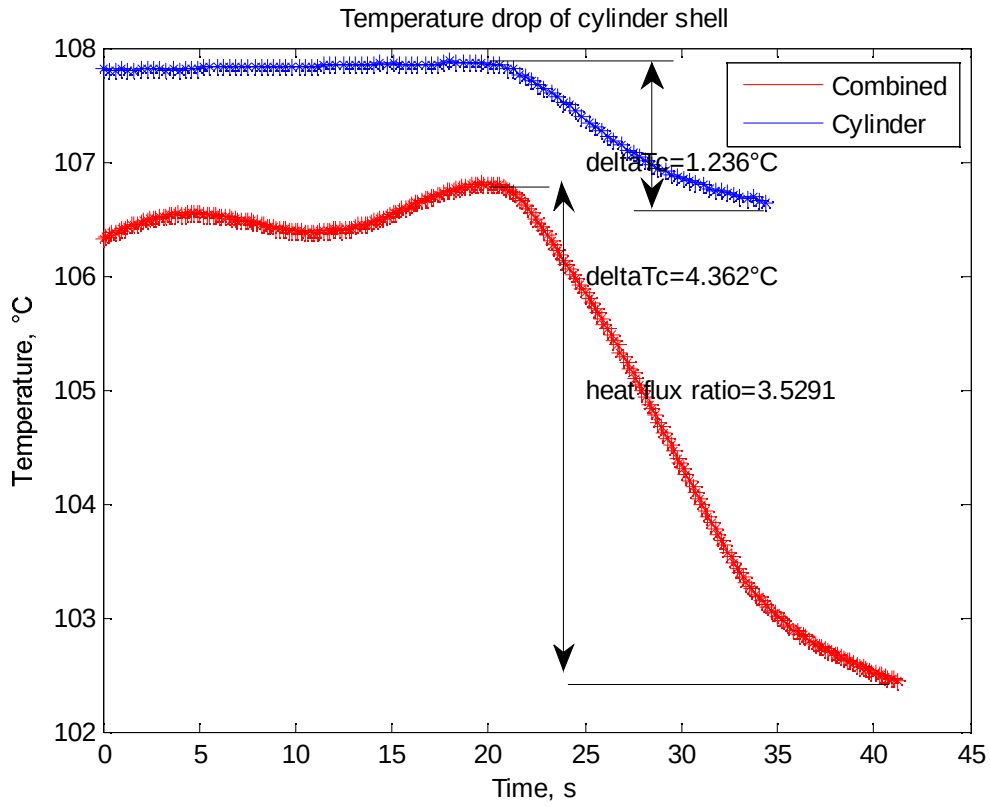


*Figure 37. Cooling effect of the cylinder [47]. DeltaTc is the change in surface temperature of the cylinder in one drying cycle of paper. Heat flux ratio is the temperature change ratio of combined drying to cylinder drying.*

### 4.2.3. Drying rate

An important finding of this work was that a combined drying provides the highest drying rate, higher than the sum of the individual drying rates of the cylinder and impingement drying (see Figure 38). A significant number of experiments were done before a proper understanding of this phenomenon emerged.

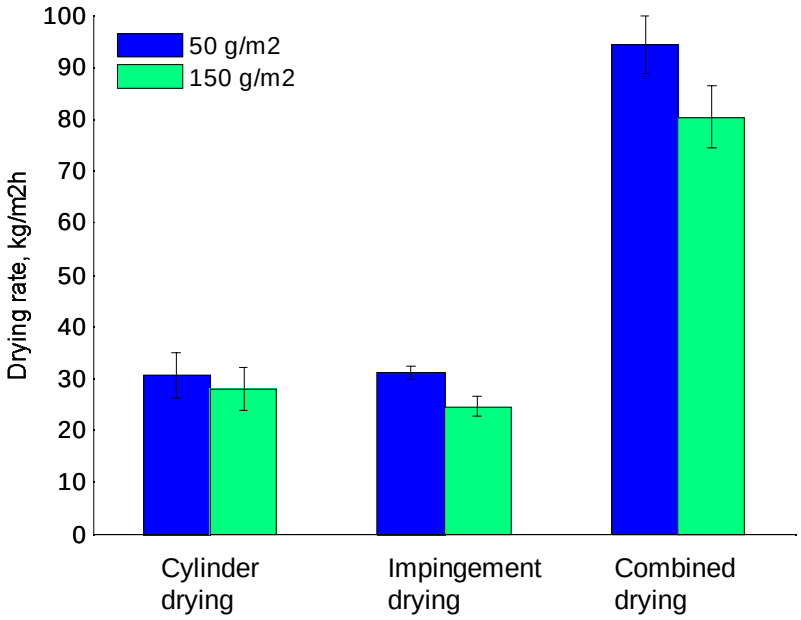


*Figure 38. Drying rate results for two basis weights. Cylinder temperature was 100°C, impingement temperature was 200°C and the impingement velocity was 90 m/s (publication [47]).*

The paper temperature decreased more in the impingement drying than in the conventional cylinder drying. This implies that the heat transferred from the cylinder was utilised better in the former case. Computer simulations were used to confirm the experimental results. To some extent Wedel et al. [172] have reached similar conclusions.

Increase in the drying rate was greater for lower basis weights due to smaller thermal insulation. This effect is illustrated in the next section.

### 4.2.4. Heat transfer to paper

Simulations and experimental work were done to evaluate the heat transfer from the cylinder to paper, which arises from a temperature difference between the two surfaces. There are few factors that limit the transfer of heat from steam to paper: a condensate layer inside the cylinder surface, heat resistance of the dryer shell, contact heat transfer coefficient and heat transport in the web. The surface related to heat transfer on the cylinder side is equal to the total cylinder surface, but on the paper side the area is that covered by the paper web on the cylinder.
Expressed in a simple form the heat flux is thus given by

$$q'' = \alpha_{c-p}\left(T_c - T_{p0}\right), \tag{55}$$

where $\alpha_{c-p}$ is the contact heat transfer coefficient and $T_{p0}$ is the temperature of the web surface in contact with the hot cylinder surface. Experimentally, temperature of paper during drying is measured using thermocouples inserted inside the paper. The recorded temperature is not exactly the paper surface temperature, but it is very close to it. Air temperature can also be measured close to the paper surface. Drying rate measurements give then the basis for determination of heat transfer coefficients, when heat transfer to air is also included. Heat transfer from air to the paper web can be expressed in the form

$$q'' = \alpha_{a-p}\left(T_a - T_{p0}\right), \tag{56}$$

where $\alpha_{a-p}$ is the convective heat transfer coefficient, $T_a$ is the air temperature and $T_{p0}$ is the temperature of the web surface. The radiative heat transfer can be expressed as the Beer-Lambert-Bouguer law [173]

$$q''_{abs} = q''_{rad}\left(1 - e^{-C_\alpha \cdot \delta}\right), \tag{57}$$

where $q''_{rad}$ is the flux of infrared radiation exposed onto the web, $\delta$ is the web thickness and $C_\alpha$ is the absorptivity of infrared radiation in paper per unit thickness.

Evaporation and convection take place simultaneously and affect each other, because vapour is flowing through a laminar boundary film. This effect is usually taken care of by using the Ackermann correction [153]:

$$q''_0 = \alpha_{a-p}\left(T_a - T_{p0}\right)\frac{E}{e^E - 1}, \tag{58}$$

where $E$ under cylinder drying conditions is [14] given by

$$E = \frac{\dot{m}_{ev}}{A}\frac{c_v}{\alpha}\frac{T_1 - T_{p0}}{T_a - T_{p0}}. \tag{59}$$

Here $c_v$ is the specific heat of water vapour and $T_1$ is determined by the heat balance [14],

$$T_1 \approx T_a - \frac{\alpha(T_a - T_{p0})}{\frac{\dot{m}_a}{A}c_a}, \tag{60}$$

where $\frac{\dot{m}_a}{A}$ is the impinged mass flow per unit area and $c_a$ is the specific heat of impinging air.

The total heat flow is then ($q''_{tot} = q''_{cond} + q''_{conv} + q''_{rad}$) given by

$$q''_{tot} = \alpha_{c-p}\left(T_c - T_{p0}\right) + \alpha_{a-p}\left(T_a - T_{p0}\right)\frac{E}{e^E - 1} + \frac{\dot{m}_{ev}}{A} c_v \left(T_1 - T_{p0}\right) + \varepsilon A \sigma \left(T_s^4 - T_{sur}^4\right)\left(1 - e^{-C_\alpha \cdot \delta}\right). \quad (61)$$

The proportions of the different heat transfer components can be estimated by assuming, e.g., that the paper temperature is $T_{p0}$ =80°C, air temperature is $T_a$ =150°C and cylinder temperature is $T_c$ =100°C, where

$$\begin{aligned} q''_{tot} &= 2000\text{W/m}^2\text{*(100°C-80°C)} + \\ &\quad 300\text{W/m}^2\text{°C*(150°C-80°C)*0.999} + \\ &\quad 0.0083\text{kg/m}^2\text{s*1.09kJ/kg°C*(137.5°C - 80°C)} + 860\text{W/m}^2 \\ &= 40000\text{W/m}^2 + 21795\text{W/m}^2 + 860\text{W/m}^2 \\ &= 62655\text{W/m}^2. \end{aligned} \quad (62)$$

This means that the radiation heat transfer is about 1% of the total heat transfer, about 34% is due to convection and about 65% is due to conduction. This simple calculation reveals that steam is the major source of energy, even though additional energy is acquired from the hot air during impingement.
The heat flux to paper divided between the different heat transfer mechanisms is given in Figure 39 as a function of paper temperature.

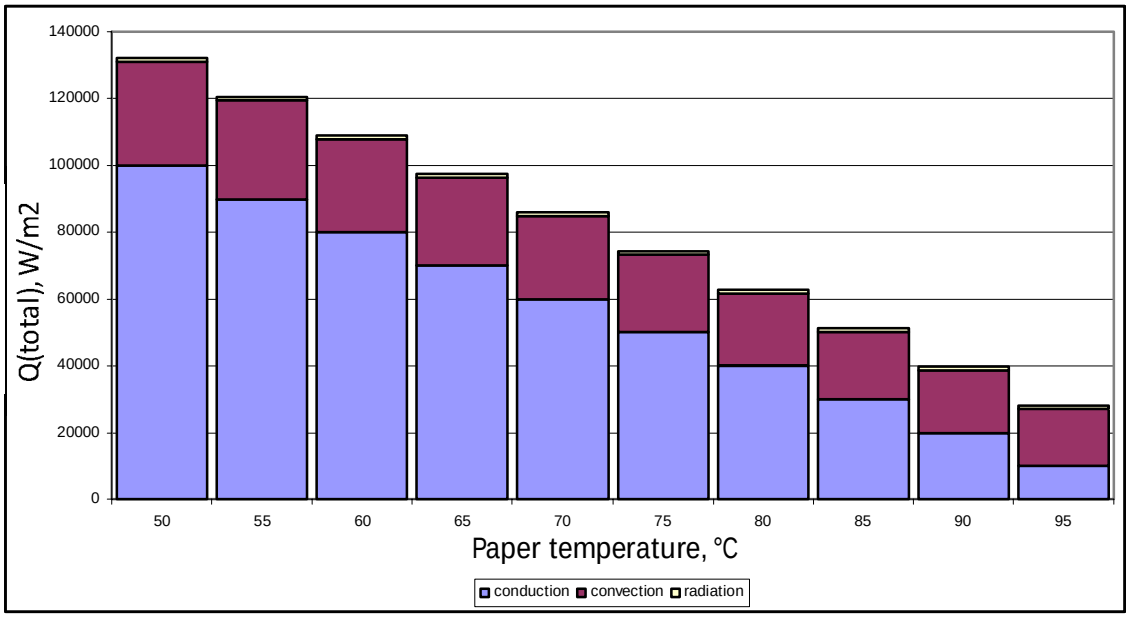


*Figure 39. Heat flux into paper as a function of paper temperature, divided into contributions from the different heat transfer mechanisms.*

Typically the paper temperature during cylinder drying is 90-92 °C, but in experiments it was observed to decrease even down to 70 °C in some cases. Increase in the heat flux was 50% when the paper temperature was decreased from 90 °C to 80 °C.

Solution to achieve the increased heat transfer rate with decreasing paper temperature was given in publication [174]. The main result is also presented in

Figure 40. In this figure the steam and paper temperatures were considered as constant at 120 °C and 80 °C, respectively, while the thermal conductivity of the cylinder shell was 50 W/m/K. For the basic case (total heat flux from steam to paper was 2000 W/m²K and 35 mm thick cylinder shell) the surface temperature of the cylinder on the side in contact with paper was 99 °C and the temperature difference across the shell was 11 °C. For a steam condensate the heat transfer was 15000 W/m²K for the same shell thickness, while the temperature on the paper side was 103.5 °C which is 4.5 degrees higher than in the basic case. The biggest increase in the heat transfer could be obtained in the third case (total heat flux from steam to paper was 15000 W/m²K for a cylinder shell thickness of 10 mm). The temperature of the cylinder surface in contact with paper was increased up to 112°C. It is evident that intensification of heat transfer from the condensing steam and reduction of the thermal resistance of the cylinder shell can lead to significant improvement in the heat transfer from steam to paper.

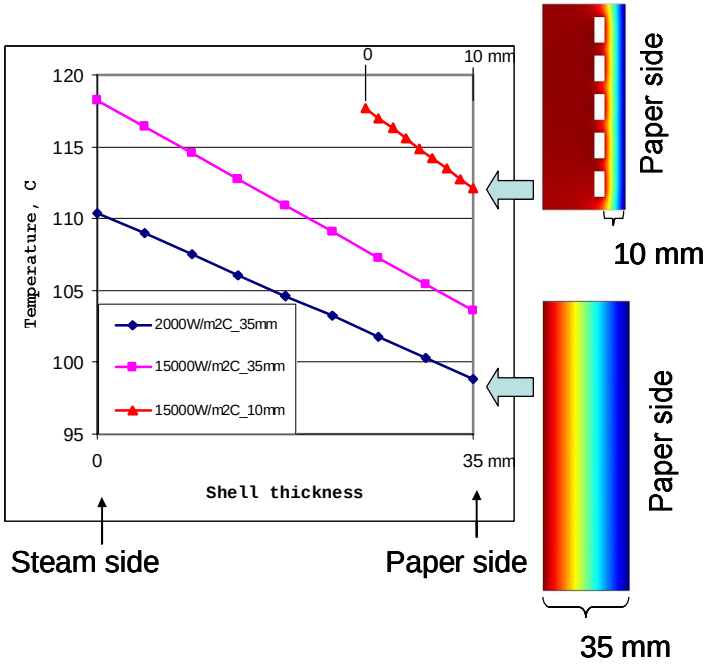


*Figure 40. Temperature of the cylinder shell as a function of shell thickness [170]. Thin cylinder shells were made with holes (channels) for steam, the temperature distribution in such an arrangement is shown in the top right corner, whereas the typical temperature distribution is shown in the bottom right corner. Typical heat transfer coefficient from steam to paper was 2000* W/m²°C *and its temperature distribution through a 35* mm *shell is the lowest curve (blue), increased heat transfer coefficient of 15000* W/m²°C *using a 35* mm *cylinder shell is given in the middle (pink) and the highest heat transfer coefficient through a 10* mm *cylinder shell is the highest curve (red).*

### 4.2.5. Temperature and moisture gradients

Measured and simulated results for the time evolution of moisture and temperature during drying are shown in Figure 41. These results show that the

difference in moisture between the top and bottom surfaces can be almost 30 %-units, when the drying temperature in impingement drying is 160 °C and the drying jet velocity is 50 m/s. Using an impingement velocity of 100 m/s this moisture difference increased to over 35 %-units. An increase in temperature was seen when the paper was almost dry.

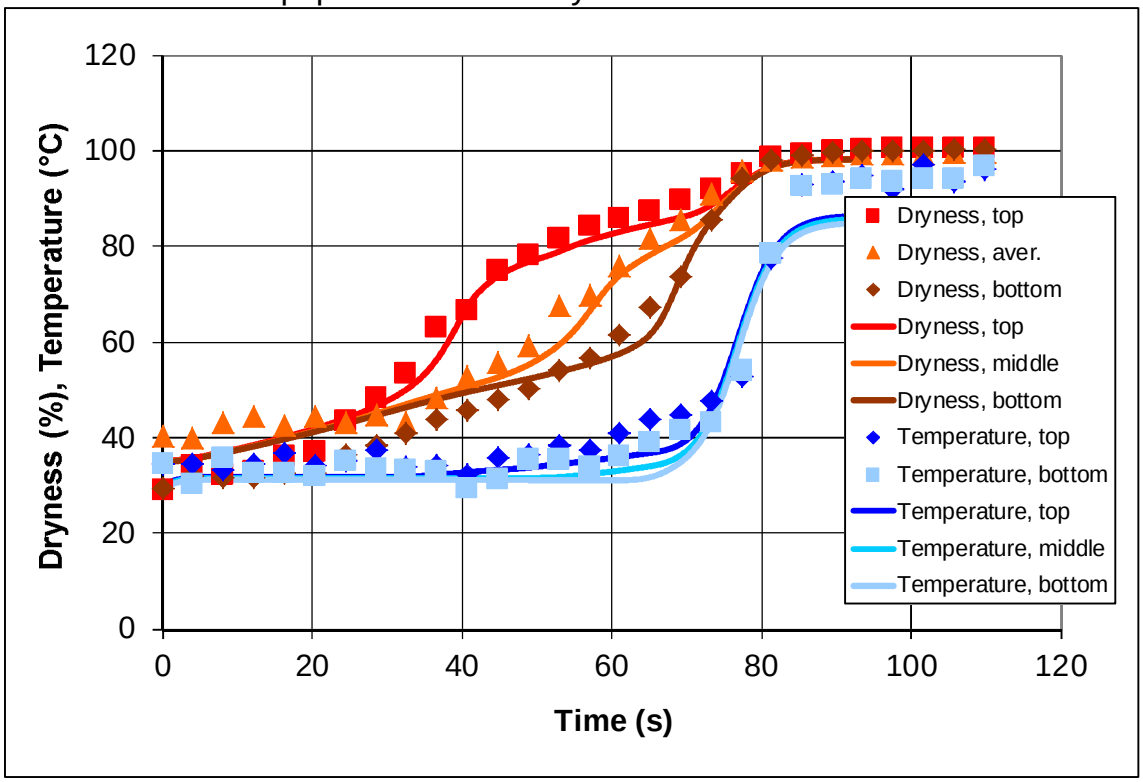


*Figure 41. The time evolution of moisture and temperature during drying as given by simulations with the model described in [166]. Lines are simulated values and points are measured values.*

## 4.3. Up-scaled simulations: paper machine

In publication [42] simulations were done to increase our understanding of impingement drying through a fabric. The combined air-cylinder drying process was studied with the drying simulation model described above. The efficiency of the process was considered as a function of dryness. A combined process means impingement drying on a cylinder covered with a permeable fabric. Paper was dried in a single drying cylinder covered with an impingement box. The focus of the study was on improvement of the drying rate. Differences in the temperature profiles during drying were also compared and discussed. In combined drying the drying rate was on the average three times that in cylinder drying. Results also show more than a 50% improvement in the drying rate in the combined drying compared to the sum of separate processes, for drynesses above 80%. Next an example of a machine-scale simulation with impingement on each cylinder is shown (Figure 42 – 45). It is

based on the model explained in Section 3, and conditions of combined air-cylinder drying process are the same as in publication [81], with a machine speed of 1200 m/min. This simulation showed that the moisture difference between the top and bottom sides of paper was greatly reduced. Figure 43 shows that the related moisture gradient can be reduced to a level of 7%. For cylinder drying this gradient can be as high as 25%, as shown in publication [43].

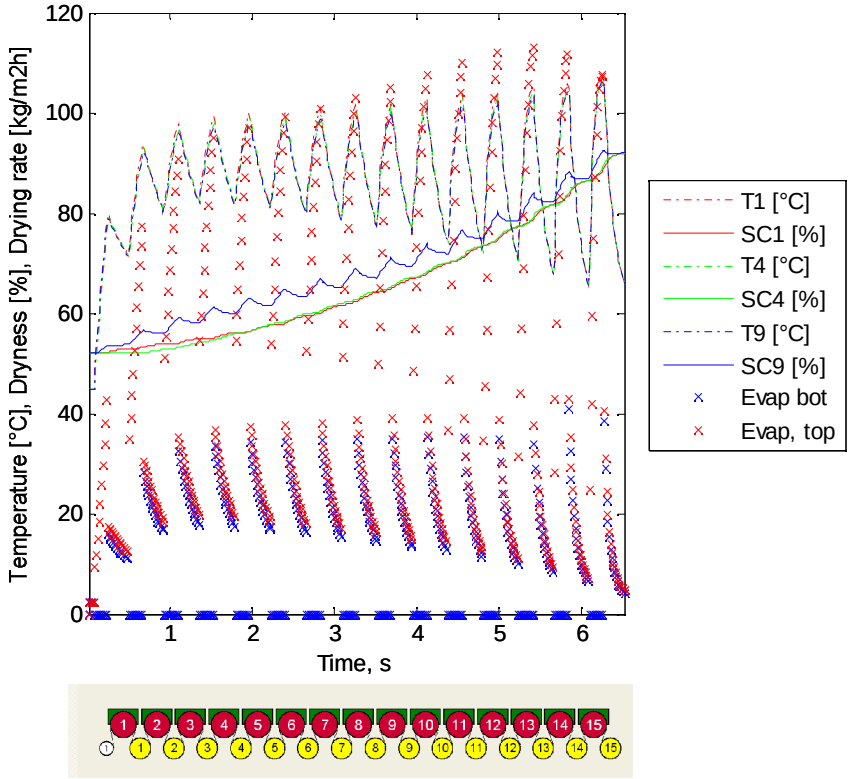


*Figure 42. The time evolution of the temperature, dryness and drying rate of the paper web in a drying section with impingement in each cylinder.*

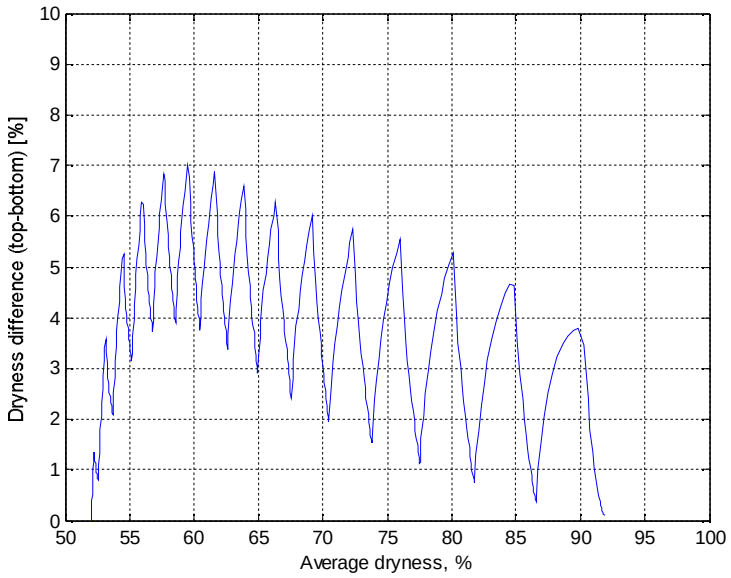


*Figure 43. The difference of dryness between the top and bottom layers of a paper web as a function of average dryness based on numerical simulation.*

The distributions of temperature and moisture in the thickness direction of paper are shown in Figure 44 as a function of time. The values of both quantities are shown with respect to their average values.

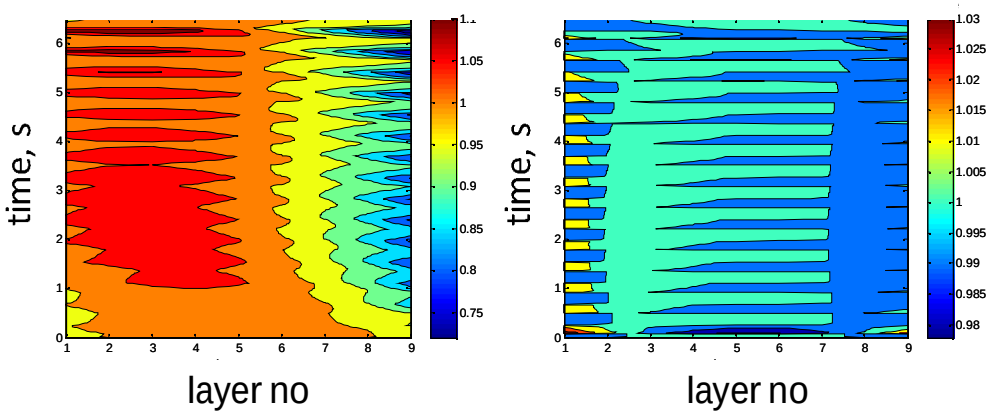


*Figure 44. The distribution of moisture (left) and temperature (right) in the thickness direction of paper during drying as a function of time. The colour coding illustrates the relative differences of these quantities from their average values.*

It is evident from Figure 44 that temperature gradients inside the paper are considerably smaller than moisture gradients. This fact shows the importance of the movement of moisture inside the paper, for its quality aspects in particular, while the surface temperature of paper already gives reasonable information of the heat transfer (see Figure 45). This is also true during cylinder drying, where the heating time is short, about 0.2 seconds. The overall temperature changes during drying are large, but the temperature is quite evenly distributed in the thickness direction of paper.

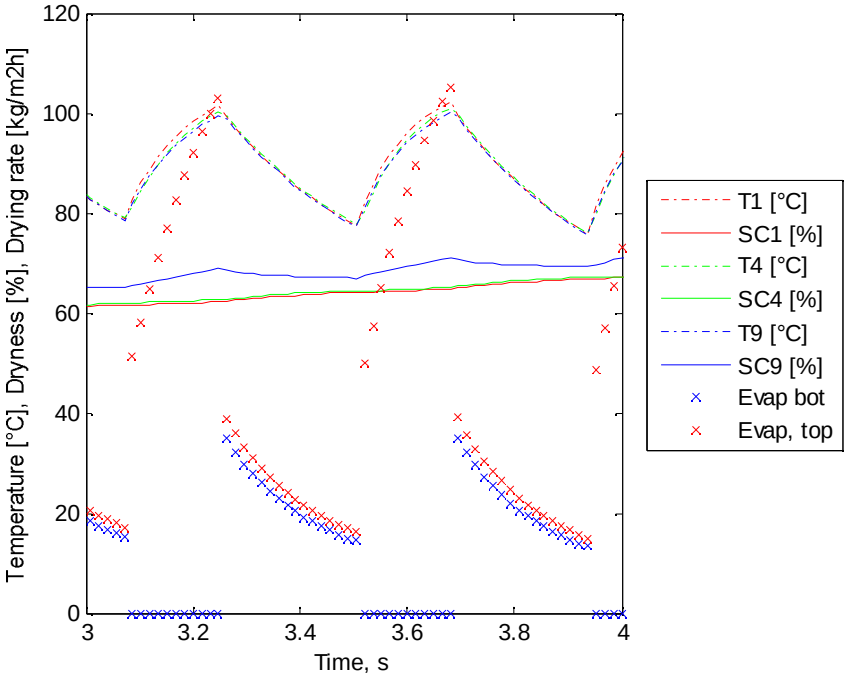


*Figure 45. The evolution of (average) temperature, dryness and drying rate of paper from 3 to 4 s during its drying as given by a numerical simulation.*

# 5. CONCLUSIONS

The results represented here on impingement drying through a fabric on a cylinder show that great improvement in the drying rate can be obtained that way. Energy issues were not considered in this work, although they are very important at the scale of the whole paper machine. As drying is responsible for most of the energy consumption in the paper machine, favourable effects on energy consumption are expected as well. Usually in paper machine the primary energy source is steam that results from power generation. New impingement technologies make it possible to use e.g. natural gas for production of hot air, and there are some possibilities to use high pressure steam to heat air in the temperature range of less than 200 °C. This applies to drying through a fabric on a cylinder. Some changes are definitely needed in the dryer section to achieve the efficiency improvement related to drying paper faster and in a smaller space (shorter dryer section). Cheap energy will not be available in large scale in the future.

The main part of the research was experimental, but it also included a number of numerical simulations. Such combination of methods improved our understanding of the relevant physical phenomena involved in the process, whereby a better control of the process could be obtained, so that products of improved quality can eventually be manufactured. Simulation results also need verification, and this was achieved by comparing them with measured results. Measurements were done in the thickness direction of paper on the development of moisture and temperature during drying. Comparison of results showed that the models developed work very well also in situations for which they were not originally designed, with only small changes.

In the first phase of the research, a drying unit was constructed. The aim was that it should be of small scale, flexible and versatile. Since a continuous web is difficult to have in such an equipment, small sheets of a size equivalent to A4 sheets (or smaller) were chosen for paper samples. Methods for continuous runs with A4 sheets were also planned, but it would have been very costly to build

such a unit, and therefore a semi-static rig was built. Static in the sense that paper was not moving on the cylinder, but it was placed on a curved hot surface and covered with fabric for good contact. The impingement unit was dynamic, although paper was moving through the impingement region. Various drying methods were possible to realize with such systems: a typical cylinder drying, normal impingement drying on a fabric (with or without suction from the other side) and combination of these two methods, *i.e.* drying through a fabric on a cylinder, the main topic of this work. Yet another possibility would have been a two-sided impingement between fabrics or with one fabric only.

During the work some interesting findings were made. One of these was the lower paper temperature in combined drying compared to cylinder drying. A measurement system to evaluate this effect was tested in Metso Research Center in Turku, Finland. Changes in paper temperature were found to be responsible for the big differences observed in separate sub-process measurements. In cylinder drying the temperature is always close to that of the cylinder surface, but in the combined process the paper temperature is decreased. Heat flux to paper is greatly affected by its temperature, and therefore this temperature has a significant effect on drying.

Drying shrinkage was also reduced in combined drying, and some effects of shrinkage prevention were indicated. In normal cylinder drying a large part of drying takes place after the web has passed the cylinder, *i.e.* during cooling of the paper. Wood fibres shrink during drying, which has a big effect on paper properties. If the shrinkage of paper is allowed, its elastic moduli will decrease. In impingement drying shrinkage can be controlled using vacuum on the other side of the paper. For low shrinkage and curl the vacuum has to be quite high (few kPa). Cooling of the paper during drying will also improve its elastic properties as shown in publication [45]. Curl and possibly cockling tendencies are reduced as well.

In conclusion, possibilities to control paper quality during drying are available, at least on the laboratory level. Methods developed here could already be used in the existing paper machines to improve the quality of paper and to save production costs.

Further studies should however be done to increase the heat transfer from the cylinder, which would be important for bringing the proposed drying method to use in a production scale.

# 6. REFERENCES


[1] Holik, H., (Ed.), Handbook of Paper and Board, 2006 Wiley, ISBN: 3-527-30997-7

[2] Kononov, A. and Paulapuro, H., Air dynamic forming as an alternative for conventional papermaking, Paperi ja Puu Vol. 86 No. 4/2004 pp. 243-248

[3] Kilpeläinen, J. Suomen paperiteollisuuden tulevaisuus, maailman metsäteollisuus ja Suomen metsäteollisuuden tulevaisuus- seminaari Joensuu 25.11.2005

[4] World fibre outlook 2020, Know How Wire 1/2007, ISSN 0780-7880, pp.4-8.

[5] Suhonen, T., Pöyry World Paper Markets up to 2025 (2008 edition).

[6] FAO (Food and Agriculture organisation of the United Nations) statistics. Retrieved 30-12-2009 from http://www.fao.org/

[7] Forsström, J.; Keränen, J.; Hytönen, E.; Soria, A.; Szabó, L., Development of a Model of the World Pulp and Paper Industry, 2006, Retrieved 30-12-2009 from http://www.jrc.es/. Institute for Prospective Technological Studies (IPTS), Luxembourg: Office for Official Publications of the European Communities. 76 p. IPTS Publications : EUR 22544 EN

[8] Szabó L., Soria A., Forsström, J., Keränen J., Hytönen, E., A world model of the pulp and paper industry: Demand, energy consumption and emission scenarios to 2030, 2009, Environ. Sci. Policy, doi:10.1016/j.envsci.2009.01.011

[9] Hetemäki, L., Hänninen, R., Metlan työraportteja 122, 2009, Retrieved from (16.3.2010) http://www.metla.fi/julkaisut/workingpapers/2009/mwp122.htm ISBN 978-951-40-2165-7 (PDF), ISSN 1795-150X

[10] Oinonen, H. and Wahlström, B. Innovations are the cornerstone for developing P&B technologies, Paper and Timber, Vol.83, No.6, 2001, pp.448-451.

[11] Pikulik, I., Poirier, N., Leger, F. Papermaking in the third millennium, 1999, Pulp and Paper Canada, 100:10 III, pp. 23-27

[12] Johansson, T., Paperin ominaisuuksien kehittyminen kuivatuksessa ja menetelmät haihdutusnopeuskäyrien karakteroimiseksi, 1998, Licenciate work, HUT

[13] Page, D.H., Tydeman, P.A. and Hunt, M., A study of Fibre-to-fibre bonding by direct observation, 1961, FRC symposium, Oxford, p. 171-193

[14] Karlsson. M., (ed.) Papermaking book series: Papermaking Part 2, 2000, Drying, Fapet, ISBN 952-5216-09-8

[15] Grön, J., Karlsson, M., Korpela, M. S. and Gliese, T., Mechanical Coated Paper Structures Challenged by New Technology, Helsinki, 5-7.6.2007 Pulpaper conference

[16] Lievonen, M., Production Inputs. June 2, 2008 Nordland, http://w3.upm-kymmene.com/upm/internet/cms/upmmma.nsf/lupgraphics/Matti_Lievonen_Production_Inputs.pdf/$file/Matti_Lievonen_Production_Inputs.pdf (checked 22.10.2008)

[17] Foex Indexes of pulp, paper and recovered paper price indexes. Retrieved 30-12-2009 from http: / /www.foex.fi
[18] Perrault, R. D., Tappi Practical Aspects of Pressing & Drying Short Course, Tappi Press, Atlanta, 1995, p. 274
[19] Waananen, K.M., Litchfield, J.B. and Okos, M.R., Classification of drying models for porous solids, 1993, Drying technology 11(1), 1-40
[20] Timofeev, O. Effect of Convective Heat / Mass Exchange and Pressing Material Influence on the Efficiency of Contact Paper Drying, PhD Thesis, 1987, Leningrad Technological Institute for the Pulp and. Paper Industry, Leningrad, USSR
[21] Edelmann, K., Kaijaluoto, S., Timofeev, O., Saarenko, T., Kiiskinen, H. and Karlsson, M. The impact of new paper drying technologies on energy consumption. Progress'96, International Papermaking Conference, Poland, Lodz, 17-19.6.1996
[22] Kuhasalo, A., Solutions for the three phases of paper drying, 1998, XI Valmet Paper Technology Days, pp. 73-79
[23] Kuhasalo, A., Challenges set by high speed on dryer section, 1994, Feature
[24] Ylikauppila, J. and Ilvespää, H., Neue Trockenpartiekonzepte für Papiermaschinen, Das Papier vol. 49, no. 10A, Oct. 1995, pp V115-V121
[25] Tolonen, T., Developments of the dryer section. Valmet PM Days94, 15-16 June 1994, Jyväskylä, Finland, pp. 33-37.
[26] Hahn, G.E. Get the most out of steam, Chemical engineering, Jan. 1994. p. 80-85
[27] Kays, W., London, A. Compact heat exchangers. The National Press, Palo Alto, California, 1955, pp.156
[28] Mujumdar, A.S. Impingement Drying, Handbook of Industrial Drying, Marcel Dekker, Inc.: New York, 1987, 461-474
[29] Paltakari, J., Effect of blow boxes on evaporation during cylinder contact in a paper machine dryer section, 1996, IDS'96, Krakow, Poland, Vol.B, pp.1173-1180
[30] Crotogino, R. The growing significance of air drying. Paper Technology and Industry, Aug.1975, pp.247-257
[31] Elbert, U., Sundqvist, H., Johansson, B., Juppi, K. First OptiDry started up at the Nordland Papier AG mill. Paper and Timber, Vol.82, No.3, 2000, pp.179-181.
[32] Burgess, B., Chapman, S., Seto, W. The Papridryer Process part 1 - The basic concept and laboratory results. Pulp and Paper Mag. of Canada, 73, N11, Nov. 1972, T314-T331
[33] Lehtinen, J. 1995, Condebelt drying of paper and paperboard for optimizing quality and production for many grades. Drying Technology, Vol. 13, no. 8&9, pp. 2049-2068
[34] Orloff, D. I., Impulse drying of recycled multi-ply linerboard: Laboratory scale studies, 1993, Tappi journal, vol 77, no. 2. pp. 169-179
[35] Orloff, D.I. Phelan, P.M. Crouse, J.W., Linerboard drying on a sheet fed pilot impulse drying shoe press, 1994, Tappi journal, vol 78, no. 1. pp. 129-141
[36] Pikulik, I. High Intensity drying of paper, 80th annual meeting, CPPA 1994, A11-A23
[37] Poirier, N. Sadeghi, M. and Pikulik, I. Papridry™ System: The Future Of Paper Drying? Drying 2004 – Proceedings of the 14th International Drying Symposium (IDS 2004), São Paulo, Brazil, 22-25 August 2004, vol. B, pp. 1271-1278
[38] Karlsson, M. Drying of paper – an overview, The state of paper drying knowledge, 12th Fundamental Research Symposium, Oxford, September 2001
[39] Ionides, G. N., Jackson, M., Smith, M. K. and Forgacs, O. L Factors influencing the strength properties of wet webs, 1977, FRC symposium, Oxford, p. 357-381
[40] Robertson, A.A., The physical properties of wet webs, Part 2, fibre properties and wet web behaviour, 1963, Svensk papperstidning, vol. 66. no.12
[41] Tarnawski, W.Z., Drying and shrinking of the paper, 1978, Proceedings 1st International Drying, Symposium, Montreal, Canada, pp. 201-207
[42] Keränen, J.; Timofeev, O.; Talja, R., Simulated combined air-cylinder drying process, 3rd Nordic Drying Conference - 2005. Karlstad, 15. - 17.6.2005. SINTEF. Karlstad, P-33

[43] Talja, R.; Timofeev, O.; Keränen, J.; Manninen, J., Impingement drying in papermaking, 12th International Drying Symposium, IDS2000. Noordwijkerhout, 28 - 31 Aug. 2000 . Dutch Working Party on Drying. Noordwijkerhout, 9 p.

[44] Talja, R.; Timofeev, O.; Keränen, J.; Milosavljevic, N., Some aspects of the combined contact-impingement drying of paper, International State-of-the-Art Conference, Resource- and energy Saving in the Pulp and Paper Industry and Municipal Economy (Process, Equipment, Automation). St. Petersburg, Oct. 27 - 28, 2005. Saint Petersburg State Technological University of Plant Polymers. St. Petersburg, 237 – 242

[45] Timofeev, O.; Keränen, J.; Kiiskinen, H., Paper curl induced by drying: 88th Paptac Annual Meeting. Montreal, 28 - 31 Jan 2001. Paptac. Montreal, 4 p.

[46] Timofeev, O.; Keränen, J.; Kiiskinen, H.; Kiuru, J.; Tanaka, A., Temperature measurements and simulations inside a paper in a fuser nip: Proc. of the 14th International Drying Symposium (IDS 2004), Vol B. Sao Paulo, Brazil, 22 - 25 Aug. 2004, 1249 – 1254

[47] Timofeev, O.; Keränen, J.; Milosavljevic, N.; Talja, R., Experimental research on the combined contact-impingement drying of paper on the dryer cylinder, IDS 2002. 13th International Drying Symposium. Beijing, 27 - 30 Aug. 2002. Beijing University of Chemical Technology. Beijing, 8 p.

[48] Lampinen, M., Mechanics and thermodynamics of drying, 1979, Doctoral thesis, Helsinki University of Technology.

[49] Lampinen, M., Ojala, K., Mathematical modeling of web drying, 1993, Advances in Transport Processes IX, pp. 271-347, Elsevier.

[50] Rajala, P. and Karlsson, M. "A drying model for coated paper, for improved printing properties", HTD-Vol. 317-2, 1995 IMECE, Proceedings of the ASME Heat transfer division Vol. 317-2, pp.445-450.

[51] Rajala, P., Karlsson, M., A drying model for coated paper, for improved printing properties. Proceedings of the ASME Heat Transfer Division, Vol. 317-2, 1995, pp.445-450.

[52] Reardon, S.A., Davis, M.R. and Doe, P. E., Computational Modelling Of Paper Drying Machines, 2000 Tappi Journal (September)

[53] Timofeev, O., Karlsson, M., and Kiiskinen, H. Identification of Mass Transfer coefficients for Single-tier Dryer Section, 1995, Proceedings of the ASME Heat Transfer Division, HTD-Vol. 317-2, 413-420

[54] Asensio, M. C., Seyed-Yagoobi, J., Lehtinen, Karlsson, M. A., J. A., Timofeev, O. N., Juppi, K., Comparison of several multi-cylinder paper drying simulation models, IDS 1994, Gold Coast, Australia, p. 1171-1178,

[55] Wilhelmsson, B. An experimental and theoretical study of multi-cylinder paper drying, 1995, Ph.D. thesis, Lund University, Department of Chemical Engineering I.

[56] Keränen, J.; Paaso, J.; Timofeev, O.; Kiiskinen, H., Moisture and Temperature Measurement of Paper in Thickness Direction (Supported by Simulations), Progress in Paper Physics Seminar PPPS 2008. Espoo, 2 - 5 June 2008. Helsinki University of Technology. Espoo, 207 - 210

[57] Paaso, J., Moisture depth profiling in paper using near-infrared spectroscopy, Doctoral dissertation, (2007)

[58] Dreshfield Jr., A. C., A study of transverse moisture distribution and movement during hot-surface drying of paper, 1956, Doctoral thesis, IPST, Atlanta

[59] Batchelor, W.J., Wu, Z. and Johnston, R.E. Measurement of z-direction moisture transport and shrinkage in the drying of paper, 2004, Appita Journal Vol. 57(2) 107-111, 127

[60] Paltakari, J., Internal and External Factors affecting the paper drying process, 2000, Doctoral Thesis, Helsinki University of technology, Reports, series A12, Espoo

[61] Tiitta, M. and Olkkonen H. Electrical impedance spectroscopy device for measurement of moisture gradients in wood, 2002, Review of scientific instruments, vol 73. no. 8. pp. 3093-3100

[62] Wessman, D., Harding, S. and Stenström, S. Moisture Profiles Measured By NMR Imaging During The Convective Drying Of Cardboard, IDS 2000, Netherlands

[63] Hytönen, E., Heat Transfer Coefficients in Through Fabric Drying of Paper (in Finnish), 2004, MSc. thesis, Physics department of Jyväskylä University

[64] Lewyta, J. and DeCrosta, E. F., The effect of dryer fabric characteristics on paper drying - a laboratory study, 1980, Tappi, Vol. 63, No. 5

[65] Kiiskinen, H., The drying rate and quality effects in impingement drying of newsprint, (in Finnish) 1995, Licentiate thesis, Tampere University of Technology, Tampere, Finland.

[66] Kiiskinen, H., Juppi, K., Timofeev, O., Karlsson, M. and Edelmann, K., Impingement drying of multi-ply linerboard, 1999, Pulp & Paper Canada, pp. 43-45

[67] Lang, I., Poirier, N. Evaluation of high velocity impingement hoods applied to conventional drying cylinders, 1998, Proceedings of 84th CPPA Conference, Montreal, pp. B307-B310

[68] Rounds, D.A. and Wedel, G.L., Drying Rate and Energy Consumption for an Air Cap Dryer System, Beloit Corporation, Beloit, Wisconsin, U.S.A. Proceedings of The First International Symposium on Drying McGill University, Montreal, Canada, August 3-5, 1978, A.S. Mujumdar Editor Published by Science press, Princeton

[69] Zhang, G.; Keränen, J.; Niskanen, K., Effect of drying conditions on the mechanical properties of paper, 2005, Paperi ja Puu / Pulp and Timber. Vol. 86 No: 3, 164 – 168

[70] Keränen, J. Myllys, M., Kiiskinen, H., Some insight on paper structure and properties with different drying characteristics, 2009, Appita Journal, Vol 62 No 2, pp. 146-151

[71] Van Den Akker, J.A., Latherop, A.L., Voelker, M.H., And Dearth, L.R., Importance of Fiber Strength to Sheet Strength, 1958, Tappi J. 41(8): 416-425.

[72] Cao, B., Tschirner, U., Ramaswamy, S., Impact of pulp chemical composition on recycling, 1998, Tappi Journal, Vol. 81, No.12 pp.119-127

[73] Van Der Akker, J. A., Jentzen, C. A. and Spiegelberg, H. L., Effects on individual fibres of drying under tension, 1965, FRC symposium, Cambridge, p. 477-506

[74] Kärkkäinen, M., Puutieteen Perusteet, 2003, Metsäkustannus Oy, ISBN-952-5118-51-7

[75] Steenberg, B., Beating and the mechanical properties of paper, 1957, FRC symposium, Oxford, p. 241-262

[76] Corte, H., The porous structure of paper - Its measurement, its importance and its modification by beating, 1957, FRC symposium, Oxford, p. 301-332

[77] Corte, H., Kallmes, O. J., Statistical geometry of a fibrous network, 1961, FRC symposium, Oxford, p. 13-46

[78] Gallay, W., Some aspects of the theory of beating process, Fundamentals of papermaking fibres, 1957, 1st fundamental research symposium, Cambridge, pp. 377-387

[79] Braaten, K.R., Fibre and fibril properties versus light scattering and surface smoothbness for mechanical pulps, 2000, Pulp and Paper Canada, vol. 101, no.5. T122-126

[80] Reme, P.A., Helle, T., Quantitative assessment of mechanical fibre dimensions during defibration and fibre developement, 2001, JPPS, Vol 27. No. 1

[81] Niskanen, K., (ed.) Papermaking book series: Paper Physics, 1998, KCL, The Finnish Pulp and Paper Research Institute, ISBN 952-5216-16-0

[82] Nanko, H. and Wu, J.: Mechanisms of Paper Shrinkage During Drying, 1995 International Paper Physics Conference (CPPA and Tappi) Proc., 103-113.

[83] Nanko, H., Ohsawa, J., Mechanism of fibre bond formation-Editor C.F. Baker, 1989, Fundamentals of papermaking vol2, Transactions of the ninth fundamental research symposium, Cambridge

[84] Weise, U., Characterization and mechanisms of changes in wood pulp fibres caused by water removal , 1997 Doctoral thesis, Helsinki University of Technology, Espoo.

[85] Constantino, R. P. A., I'Anson, S. J. and Sampson, W. W., The Effect Of Machine Conditions And Furnish Properties On Paper Cd Shrinkage Profile, September 2005, 13th Fundamental Research Symposium, Cambridge (pp.283-306)

[86] Glynn, P., Jones, H.W.H, and Gallay, W. Drying Stresses and Curl in Paper, 1961, Pulp Paper Mag. Can. 62(1):T39-T48

[87] Gärd, J., The influence of fibre curl on the shrinkage and strength properties of paper, 2002, Masters Thesis, LTU:257, ISSN 1402-1617, ISRN: LTU-EX –02/257—SE

[88] I'Anson, S. J., Constantino, R. P. A., Hoole, S. M. and Sampson, W. W., Estimation of the profile of cross-machine shrinkage of paper, 2008. Meas. Sci. Technol. 19 015701 (11pp)

[89] Kajanto, I., Niskanen, K. Dimensional Stability. Paper Physics, 1998, Vol 16 (K. Niskanen ed). Papermaking Science and Technology, Fapet Oy, Helsinki, Finland

[90] Ketoja, J.; Tanaka, A.; Kiuru, J.; Timofeev, O., Keränen, J.; Kiiskinen, H., Stress Oscillation in Drying Euromech Colloquium 486, 2006, Deformation and Fracture Processes in Paper and Wood Materials. Sundsvall, Sweden. FSCN - Fibre Science and Communication Network at the Mid Sweden University. Sundsvall

[91] Kuno H., Hasuike M., Suzuki S., Sanada A., Ohira K., Improvement of Dimensional Stability of Paper in a Drying Process. (Fourth Report). Shrinkage Prevention of Sheet Edge and Curl Control, 2001, Japan Tappi Journal, ISSN:0022-815X, vol.55;no.6;pp.828-837

[92] Kuno H., Hasuike M., Suzuki S., Sanada A., Ohira K., Improvement of Dimensional Stability of Paper in a Drying Process. (Second Report). Experimental Verification by Static Paper Drying under Restraint, 2000, Japan Tappi Journal, ISSN:0022-815X vol.54;no.6;pp.827-836

[93] Nonomura, F., Abe, Y., Takeuchi, N., 1999, A study on the curling behavior of paper resulting from heatroller heating. Proceedings of the 1999 Tappi Int. Paper Physics Conf., p.83-95

[94] Olsson, A.M., Salmén, L., Molecular Mechanisms Involved in Creep Phenomena of Paper, 1999 Tappi International Paper Physics Conference, Sept.26-30, 1999, San Diego, California, Catamaran Hotel, pp.67-73.

[95] Pye, I. T., Washburn, O. V. and Buchanan, J. G., Structural changes in paper on pressing and drying, 1965, FRC symposium, Cambridge, p. 353-367

[96] Rutland, D.F. Dimensional Stability and Curl. In Pulp and Paper manufacture (M. Kouris ed.), 1992, vol. 9, Tappi Press, Atlanta, Chap. V.

[97] Selin S., Paperin käyristymän yksinkertainen malli, 2001, M. Sc. thesis, Jyväskylä University, Physics department

[98] Uesaka, T. Dimensional Stability of Paper: Upgrading Paper Performance in End Use. JPPS Vol. 17 No 2, 1991, pp. J39-J46

[99] Wahlström, T., Influence of shrinkage and stretch during drying on paper properties, 1999, Licentiate thesis, Royal Institute of Technology, Stockholm, Sweden

[100] Xinshu W., Improving The Papermaking Properties Of Kraft Pulp By Controlling Hornification And Internal Fibrillation, 2006, Doctoral Thesis, HUT

[101] Boerner, J. and Orloff, D., Effects of Basis weight and freeness on sheet permeability and critical impulse-drying temperature, 1993, Tappi Journal, vol 77, no. 2. pp. 163-168)

[102] Kiiskinen, H., The drying rate and quality effects in impingement drying of printing papers. 10th Anniversary Int. Symp., Oct. 20-21, 1998, Kangwon National Univ., Chunchon, Korea, pp.172-180

[103] Nissan, A.H., The effect of water on Youngs modulus on paper. Tappi 60 (1977) No 10, pp 98-101.

[104] Sanborn, I.B., A Study Of Irreversible, Stress-Inducedchanges In The Macrostructure Of Paper, 1962, Tappi J. 45(6): 465-474.

[105] Park S., Venditti R.A., Jameel H., Pawlak J.J., 2006, Changes in pore size distribution during drying of cellulose fibers as measured by differential scanning calorimetry. Carbohydr Polym 66(1):97–103
[106] Maloney, T. C., Paulapuro H. and Stenius P.: Hydration and Swelling of pulp fibers measured with differential scanning calorimetry, 1998, Nord. Pulp and Pap. Res. J. 13:1, 31-36.
[107] Back, E., Salmen, L. Glass Transition of Wood Components Hold Implications for Moulding and Pulping Processes, 1982, Tappi Journal Vol. 65 No. 7
[108] Salmén, L., Olsson, A.-M., Interaction between hemicelluloses, lignin and cellolose: structure-property relationships, 1998, JPPS, vol. 24. No. 3. pp.99-103
[109] Salmén, L., The Cell Wall as Composite Structure, Paper Structure and Properties, Ed. Bristow, J.A. and Kolseth, P. , 1986, Marcel Dekker, Inc., New York, pp.51-73.
[110] Brezinski, J. P, A Study of the Viscoelastic Properties of Paper by Means of Tensile Creep Tests, 1955, Doctor's Dissertation, Institute of Paper Chemistry, Wisconsin, USA
[111] Brezinski, J.P., The Creep Properties of Paper, 1956, Tappi J. 39(2): 116-128.
[112] Craven, B.D., An Analysis of the Stress / Strain Curve for Paper, 1962, Appita J. 16(2): 59-67.
[113] Htun, M., The influence of drying strategies on mechanical properties of paper, 1980, Doctoral Thesis, Kunglika Tekniska Högskolan
[114] Hansson, T., Fellers, C., Htun, M. Drying strategies and a new restraint technique to improve cross-directional properties of paper, 1989, Fundamental research symposium, Cambridge
[115] Page, D.H., Tydeman, P.A. And Htun, M., The Behavior of Fiber-to-fiber Bonds in Sheets under Dynamic Conditions, The formation and structure of paper, Ed. Bolam, F., 1962, Vol.1, pp.269-243, London, Tech. Assoc. Brit. Paper Board Makers' Assoc.
[116] Parker, J.L., The Effects of Ethylamine Decrystallization of Cellulose Fibers on the Viscoelastic Properties of Paper, 1962, Tappi J.45(12): 936-943.
[117] Schulz, J.H., The Effect Of Straining During Drying On The Mechanical And Viscoelastic Behavior Of Paper., 1961, Tappi J. 44(10): 736-744.
[118] Zhang, G.; Niskanen, K.; Tanaka, A.; Keränen, J..; Timofeev, O., Effect of drying and fibre chemical composition on the creep strain of paper, 1962, Journal of Pulp and Paper Science. Vol. 29, No: 7, 213-219
[119] Zhang, G.; Tanaka, A.; Timofeev, O.; Keränen, J.; Kiiskinen, H., Effect of drying method on the creep behaviour of paper, 2002, 88th PAPTAC Annual Meeting. Book A. Montreal, 28 - 31 Jan. 2002. PAPTAC. Montreal, 219 – 2
[120] Nordman, L., Bonding in paper sheets, 1957, FRC symposium, Oxford, p. 333-348
[121] Seth, R. S., The difference between never-dried and dried chemical pulps, 2001, Tappi Solutions, Vol. 1. No. 1.
[122] Benson. R.E., Effects of Relative Humidity and Temperature on Tensile Stress-Strain Properties of Kraft Linerboard, 1971, Tappi 54, No 5, pp 699-703.
[123] Byrd, V.L., Effect of Relative Humidity Changes during Creep on Handsheet Paper Properties, 1972, Tappi J. 55(2): 247-252.
[124] Considine, J.M., Gunderson, D.E., Thrlin, P. and Fellers, C., Compressive Creep Behavior of Paperboard in a Cyclic Humidity Environment-exploratory Experiment, 1989, Tappi J. 72(11): 131-136.
[125] Haslach, H.W. Jr., The Mechanics of Moisture Accelerated Tensile Creep in Paper, Tappi Journal. 77(10): 179-186.
[126] Jayme, G. and Hunger, G., The rearrangement of microfibrils in dried cellulose and the implication of this structure alteration on pulp properties, 1957, FRC symposium, Oxford, p. p. 263-270
[127] Nanri, Y., Uesaka, T., Dimensional stability of mechanical pulps-drying shrinkage and hygroexpansivity, 1993, Tappi Journal, pp.62-66
[128] van Liev, G. P., The deformation of paper in z-direction, 1973, Doctoral dissertation,

IPST, Atlanta

[129] Retulainen, E., Moss, P. and Nieminen, K., Effect of fines on the properties of fibre networks. Baker, C.F. (editor), Products of papermaking, Vol. 2. Transactions of the 10th Fundamental Research Symposium held at Oxford: September 1993. Pira International. 727-769

[130] Viitaharju, P, Niskanen, K.: Dried-in shrinkage profiles of paper webs, 1993, Tappi Journal vol 76, No. 8 p. 129-134

[131] Juppi, K., Experimental and theoretical study of the effect of a new dryer construction on paper machine runnability, 2001, Doctoral Thesis, HUT

[132] Salmén, L., Fellers, C. and Htun, M., The in-plane and out-of-plane hygroexpansional prosperties of paper, 1985, VIIIth Fund., Oxford, Manchester, pp.511-528

[133] Green, C., Relationship of dimesional stability to rheology of paper structures, 1983, International paper physics conference, pp.165-170

[134] Htun, M. and de Ruvo, A., Relation between drying stresses and internal stresses and the mechanical properties of paper, 1977, FRC symposium, Oxford, p. 357-381

[135] Glynn, P., Jones, H.W.H., Gallay, W., The fundamentals of curl in paper, October, 1959, Pulp and paper magazine of Canada, pp.316-323

[136] Stenström, S: Product Engineering by the Paper Dryer, 2004, 14th International Drying Symposium (IDS 2004) São Paulo, Brazil, 22-25 August, A, 89-98

[137] Retulainen, E., Hämäläinen, A., Three years of Condebelt drying at Stora Enso's Pankakoski Mill, 2000, Tappi Journal, Vol. 83, No. 5

[138] Asensio, M. C.. Transport phenomena during drying of deformable, hygroscopic porous media: Fundamentals and applications, 1999, Ph.D. dissertation, Texas A&M University, College Station, TX.

[139] Baggerud, E. and Stenström, S., Modeling Of Moisture Gradients For Convective Drying Of Industrial Pulp Sheets, IDS 2000, Netherlands

[140] Baggerud, E., Modelling of mass and heat transport in paper – Evaluation of mechanisms and shrinkage, 2004, PhD-thesis, Lund University, LUTKDH / (TKKA-1001) / 1-228, Lund, Sweden

[141] Bond, J.F Gomes, V.G. and Douglas, W.J.M. Computer Simulation of Drying Paper by Multiple Techniques, 1996, Pulp and Paper Canada, 97:12, T433-435.

[142] Han, S. T. Drying of paper, 1970, Tappi 53(6):1034-46.

[143] Karlsson, M. Stenström, S., comparison of two modeling approaches for a multi-cylinder paper dryer Drying 2004 – Proceedings of the 14th International Drying Symposium (IDS 2004) São Paulo, Brazil

[144] Nissan, A.H., W.G. Kaye. An analytical approach to the problem of drying of thin fibrous sheets on multicylinder machines, July 1955, Tappi Journal, vol 38, no.7 (pp. 385-398)

[145] Weineisen, H., modeling through drying of tissue – effect of pore size distribution on drying characteristics Drying 2004 – Proceedings of the 14th International Drying Symposium (IDS 2004) São Paulo, Brazil, vol. A, pp. 397-404

[146] Guérin, D., Morin, V., Chaussy, D. and Auriault, J-L, Thermal Conductivity of Handsheets, Papers and Model Coating Layers, September 2001, 12th Fundamental Research Symposium, Oxford, 927-945

[147] Kartovaara, I. Rajala, R., Luukkala, M. and Sipi, K., Conduction of Heat in Paper, Papermaking Raw Materials, 1985, VIIIth Fund., Oxford, Manchester, pp.381-412

[148] Yaws, C. L., Narasimhan, P., K., Gabbula, C., Yaws' Handbook of Antoine Coefficients for Vapor Pressure (2nd Electronic Edition). Knovel. Online version available at: http://knovel.com

[149] Robert C. W., CRC Handbook of Chemistry and Physics, 1969, 50th Ed.

[150] Berg, C-G, Heat and mass transfer in turbulant moist air drying processes, 1999, Doctoral Thesis, Åbo Akademi

[151] Heikkilä, P, A study on the drying process of pigment coated paper webs, 1993,

Academic dissertation, Åbo Akademi, ISBN 951-650-208-3

[152] Incropera, F. P. De Witt, D. P. Fundamentals of Heat and Mass Transfer, 1996, Fourth Edition, John Wiley & Sons, Inc., p.320

[153] Hall, C.W., Laws and Models, science, engineering and technology, 2000, CRC Press, London, p.424, ISBN 0-8493-2018-6

[154] Martin, H. Heat and Mass Transfer between Impinging Gas Jets and Solid Surfaces, in J.P. Hartnett and T.F. Irvine Jr. (Ed.) Advances in Heat Transfer, 1977, Academic Press: New York, San Francisco, London, 1-60

[155] Heikkilä, P. and Milosavljevic, N. Influences of Impingement Temperature and Nozzle Geometry on Heat Transfer – Experimental and Theoretical Analysis, 2003, Drying Technology, 21(10), Marcel Dekker, Inc., 1957-1968

[156] Heikkilä, P. and Milosavljevic, N., Influence of Thermal Radiation on the Total Heat Transfer Coefficient at High Impingement Temperatures, June 27-29, 2001, Proceedings of the 1st Nordic Drying Conference, NDC'01, Trondheim, Norway

[157] Heikkilä, P., Milosavljevic, N. 1998, Study of high temperature tissue drying. Proceedings of the 11th International Drying Simposium (IDS'98), Halkidiki, Greece, vol. B, pp. 1513-1520

[158] Heikkilä, P. and Milosavljevic, n. Investigation of Impingement Heat Transfer Coefficient at High Temperatures, 2002, Drying Technology, 20(1), Marcel Dekker, Inc., 211-222

[159] Huber, A.M. Viskanta, R. Effect of jet-jet spacing on convective heat transfer to confined, impingement arrays of axisymmetric air jets, Dec. 1994, International Journal of Heat and Mass Transfer, v 37, n 18, p 2859-69

[160] Poirier, D., Guadagano, J. and Tourigny, C., Methods for evaluating hood drying rates

[161] Milosavljevic, N. and Heikkilä, P. The Wall Jet –to Surface Heat Transfer in Impingement Drying, 2004, Proceedings of the 14th International Drying Symposium (IDS2004) São Paulo, vol. B, 1287-1294

[162] Krizek, F., Impinging Flows - Research and Application in Drying Technique Source: Coating, v 28, n 411995, p 106

[163] Simula S., Electrical and thermal properties of paper, 1999, PhD thesis, KCL.

[164] Bernada, P., Stenström, S., Månsson, S., Experimental study of the moisture distribution inside a pulp sheet using MRI, Part I; Principles of the MRI technique, 1998, JPPS, Vol. 24, No. 12, pp. 373-379

[165] Bernada, P., Stenström, S., Månsson, S., Experimental study of the moisture distribution inside a pulp sheet using MRI, Part II; Drying experiments, 1998, JPPS, Vol. 24, No. 12, pp. 380-387

[166] Keränen, J.; Paaso, J.; Timofeev, O.; Kiiskinen, H., Moisture and Temperature Measurement of Paper in Thickness Direction, 2009, Appita Journal, Vol 62 No 4, pp. 308-313

[167] Gallay W., Interdependence of paper properties, 1961, FRC symposium, Oxford, p. 491-532,

[168] Stone, J. E. and Scallan, A. M.., Influence of drying on the pore structures of the cell wall, 1965, FRC symposium, Cambridge, p. 145-166

[169] Wikstöm, M., Mäkelä, P. and Rigdahl, M., Influence of temperature and type of coating latex on the out-of-plane compression behaviour of coating layers, 2000, Tappi Journal, Vol. 83, No. 8

[170] Timofeev, O.; Keränen, J.; Kiiskinen, H., Paper curl induced by drying, 2002, Pulp and Paper Canada, Vol. 103 No: 8, 25 - 28.

[171] Malashenko, A., Timofeev, O., Karlsson, M., Heikkilä, P., Edelmann, K., Further advances in paper drying, IDS'98, Halkidiki, Greece, vol. B. pp.1554-1562

[172] Wedel, G., Breiten, J., Deshpande, R., Air impingement on single-tier dryers, May 2000, Tappi Journal.

[173] IUPAC. Compendium of Chemical Terminology, 2nd ed. (the "Gold Book"), 1997, Compiled by A. D. McNaught and A. Wilkinson. Blackwell Scientific Publications, Oxford. XML on-line corrected version: http://goldbook.iupac.org (2006-) created by M. Nic, J. Jirat, B. Kosata; updates compiled by A. Jenkins. ISBN 0-9678550-9-8. doi:10.1351/goldbook. http://www.iupac.org/goldbook/B00626.pdf

[174] Timofeev, O., Milosavljevic, N., Keränen, J., Kiiskinen, H., Analysis of the cylinder dryer with improved heat transfer rate, 2008, 16th International Drying Symposium (IDS 2008), Hyderabad, India

[175] Atchison, J.E. Data on Non-wood Plant Fibers; Pulp and Paper Manufacture, 1993, vol. 3, Secondary Fibrers and Non-Wood Pulping. Tappi.

[176] Atchison, J.E.. The Future of Non-wood Plant Fibers in Pulp and Papermaking; Pulp and Paper Manufacture, 1993, vol. 3, Secondary Fibrers and Non-Wood Pulping. Tappi.

[177] Dhamodaran, T.K., Gnanaharan, R., and Sankara, K., Bamboo for Pulp and Paper, From Kerala Forest Research Institute India, Retrieved 30-12-2009 from http://www.inbar.int/

[178] Diesen, M.. Papermaking Science and Technology – Book 2, Economics of The Pulp and Paper Industry, 1998, Finland: Fapet Oy.

[179] Honey Nampak, Effect Of Chip Thickness On Kraft Cooking Bleach Ability Of Acacia Mangium And Eucalyptus, 2003, Camalduensis

[180] Castleman, T., Hemp Biomass for Energy. Retrieved 30-12-2009 from http://fuelandfiber.com

[181] Kultikova, E. V., Structure and Properties Relationships of Densified Wood M.Sc. Thesis, (1999). Retrieved 30-12-2009 from http://scholar.lib.vt.edu

[182] Technology in Australia, p.797, Bagasse. Retrieved 30-12-2009 from http://www.austehc.unimelb.edu.au

[183] Webber, C.L. III and R.E. Bledsoe. 1993. Kenaf: Production, harvesting, processing, and products. p. 416-421. In: J. Janick and J.E. Simon (eds.), New crops. Wiley, New York. Retrieved 30-12-2009 from http://www.hort.purdue.edu

[184] Kundu, S. ; Ghose, T.K. ; Mukhopadhyay, S.N., Bioconversion of cellulose into ethanol by Clostridium thermocellum--product inhibition, Biotechnol. Bioeng.; (United States); Journal Volume: XXV:4 (1983). Retrieved 30-12-2009 from http://www.osti.gov

[185] Klaavu, A. Handling Acacia Mangium, 1999, Paper Asia, 15, 1: 35.

[186] Law, K. High Yield Pulping of Fast Growing Tropical Species – Acacia Mangium, 1998, Tappi Proceeding Pulping Conference, 625-629.

[187] Paavilainen, L. Quality-competitiveness of Asian Short-fibre Raw Materials in Different Paper Grades. Paper and Timber, 82: 3/2000.

[188] Malinen, R. Lecture Notes, 2004, Pulp Manufacture

[189] Malinen, Raimo. Lecture Notes of Advanced pulp mill, 2003 – AIT

[190] Mohlin, U.B. Pulp Evaluation for Modern Papermaking. 6th International Conference on New Available Technologies. 1999, p. 343-350.

[191] Nguyen Hong Minh. Comparison of Eucalyptus urophylla, Eucalyptus camaldulensis and Acacias from Vietnam as Fibre Raw Material for Paper, 2000, Master Thesis Thailand: Asian Institute of Technology.

[192] Yang, H. Sakai, N. Watanabe, M., Drying model with non-isotropic shrinkage deformation undergoing simultaneous heat and mass transfer, 2001, Drying technology 19, 1441-1460

[193] Peter, J., Nelson, Charles, W.J., Chin, Susan, G., Grover, and Ryyanent, H. Elemental Chlorine-free (ECF) and Totally Chlorine-free (TCF) Bleaching of Eucalyptus Kraft Pulps, 1995. 49th Appita Annual General Conference Proceedings. Australia: Appita Press.

[194] Ramadorai, T.S., Trikannad, P.M., and Ravindranathan, N. Bamboo - A Potential Raw Material for Papermaking in Tropical Countries. 1981 Pulping Conference Proceeding of the Technical Association of the Pulp and Paper Industry. Atlanta, Tappi Press, 207-

215.

[195] Sundholm, J. Papermaking Science and Technology – Book 5, Mechanical Pulp, 1999, Finland: Fapet Oy.

[196] Wood handbook, Gen. Tech. Rep. FPL–GTR–113. Madison, WI: U.S. Forest Products Laboratory. 1999. 463 p.